ISTANBUL TECHNICAL UNIVERSITY ★ INSTITUTE OF SCIENCE AND TECHNOLOGY

POSITION CONTROL OF PERMANENT MAGNET SYNCHRONOUS MOTORS (PMSM) FOR DIRECT DRIVE ROBOTICS APPLICATIONS

MASTER THESIS

Ali AHMADI, B.Sc.

Department : Electrical Engineering

Programme: Control and Automation Engineering

JULY 2005

ISTANBUL TECHNICAL UNIVERSITY ★ INSTITUTE OF SCIENCE AND TECHNOLOGY

POSITION CONTROL OF PERMANENT MAGNET SYNCHRONOUS MOTORS (PMSM) FOR DIRECT DRIVE ROBOTICS APPLICATIONS

MASTER THESIS

Ali AHMADI, B.Sc.

(504021136)

Date of submission : 9 May 2005

Date of defence examination: 29 June 2005

Supervisor (Chairman): **Assoc. Prof. Dr. Seta BOĞOSYAN (İ.T.Ü)**

Members of the Examining Committee **Assoc. Prof. Dr. Hakan TEMELTAŞ (İ.T.Ü)**

Asst. Prof. Dr. Ata MUGAN (İ.T.Ü)

JULY 2005

ACKNOWLEDGEMENT

I would like to thank my prior thesis supervisor Assoc. Prof. Dr. Metin GÖKAŞAN and my thesis supervisor Assoc. Prof. Dr. Seta BOĞOSYAN for both their help and guidance in the preparation of this thesis and encouragement of my research efforts. I wish to thank also Prof. Dr. Leyla GÖREN, Assoc. Prof. Dr. Hakan TEMELTAŞ, Asst. Prof. Dr. Mohammad-R. AKBARZADEH-TOTONCHI and also some asistants like Tolga HASDEMİR, Engin YEŞİL and Saffet ALTAY.

July, 2005 Ali AHMADI

CONTENTS

ABBREVIATIONS

CNC	: Computer numerical control
DSP	: Digital signal processor
DOF	: Degree of freedom
IGBT	: Insulated gate bipolar transistor
FA	: Factory automation
NC	: Numerical control
PMSM	: Permanent megnet synchromous motor
PM	: Permanent magnet
PWM	: Pulse width modulation
ROM	: Read only memory
SM	: Synchronous motor
2DOF	: Two degree of freedom
DDR	: Direct drive robot
IJC	: Independent joint control
MBC	: Model based control

LIST OF TABLES

LIST OF FIGURES

LIST OF SYMBOLS

Θ_r^*	: Reference position of rotor
Θ_r	: Position of rotor
I*	: Motor torque current demand reference
R	: Resistance
L	: Inductance
q	: Quadrature axis
d	: Direct axis
I	: Current
V	: Voltage
ω_r	: Angular velocity of rotor
K^r_{qdo} (Θr)	: Prak's transformation matrix
$(K^r_{qd0})^{-1}$ (Θr)	: Inverse Prak's transformation matrix
Φ	: Magnetic flux
V_{abcs}	: Stator vlotages
I_{abcs}	: Stator currents
e_{abcs}	: The back-electromotor force voltages
T_e	: Electromagnetic torque
T_L	: Load
K_t	: Torque constant
J	: Rotor inertia
B	: Viscous friction factor
B_r	: Residual magnetic flux density
H_c	: Holding power
K_p	: Proportional coefficient
K_i	: Integral coefficient
K_d	: Differential coefficient
I	: Link inertia
$g(q)$	: Gravitational torque
$f(\dot{q})$	: Friction torque
$B(q)$	: Inertia matrix
$C(q,\dot{q})$	: Coriolis torque
q	: Position trajectory
$\dot{q}$	: Velocity trajectory
$\ddot{q}$	: Acceleration trajectory

DOĞRUDAN TAHRİKLİ ROBOTİC UYGULAMALARI İÇİN SABİT MIKNATISLI SENKRON MOTORLARIN (SMSM) KONUM DENETİMİ

ÖZET

Sabit mıknatıslı senkron motorlar (SMSM) hızlı moment cevab ve yüksek performans kriterleri gerektiren robot kolu, CNC tezgahları, asansör, elektrikli otomobil ve birçok başka mekatronik uygulamalarında kullanılırlar.

Bu tezde, SMSM motorların konum kontrolları Matlab/Simulink yazılım paketi kullanılarak incelenmiş ve zorlu bir uygulama olarak 2 serbestlik dereceli doğrudan tahrikli bir düzlemsel robot kolu üzerinde simüle edilmiştir. İlken, SMSM'nin alan oryantasyonlu kontrolu uygulanmış ve sonra da, tüm sistemin dinamik modeline uygulanmiştir. 2 serbestlik dereceli robotun herbir eklemini bir SMSM sürmektedir.

Sonraki adımda, değişken yük etkileri altında istenen konum yörüngelerinin izlenmesi için lineer ve lineer olmayan kontrolörler geliştrilmiştir. Amaç, istenen konum yörüngelerinin gerek geçici, gerekse sürekli rejimde minimum hata ile izlenmesidir. Lineer kontrolörler PD ve PID tipi olarak seçilmiş, lineer olmayan kontrolör olarak ise modele dayalı bir yöntem olan PD+ geliştrilmiştir. Bu kontrolörlerin performansı farklı yük ve parametreler için karşılaştırılmış, PID ve PD+'ı üstün kılan çalışma tartışılmıştır.

POSITION CONTROL OF PERMANENT MAGNET SYNCHRONOUS MOTORS (PMSM) FOR DIRECT DRIVE ROBOTICS APPLICATIONS

ABSTRACT

Permanent magnet synchronous motors (PMSM) are widely used in many applications that require rapid torque response and high-performance criteria such as robotic manipulators, CNC machine tools, elevators, electric vehicle and many other applications in the area of mechatronics.

In this thesis, the position control of a PMSM based on Matlab/Simulink software package is studied and as a challenging application, the developed controls are simulated for a 2-DOF direct-drive (DD) planar robotic arm. First, the field-oriented PMSM servo drive is implemented and the dynamic model of the system at nominal conditions is simulated. Then a 2-DOF direct drive robot is taken into consideration with two PMSMs as an example driving each link.

Linear and nonlinear controllers are designed to track any given position trajectory under varying load effects. The aim of the controllers is to track the desired position trajectory with minimum error in both transient and steady state. The linear controllers are PD and PID type while the nonlinear controller is, a nonlinear model based controller, known as proportional-derivative-plus (PD+) controller. The performance of these controllers is tested under different load and reference conditions and compared for tracking performance. The superiority of PID and PD+ controllers is discussed based on the system operating conditions.

CHAPTER 1. INTRODUCTION

1.1 Introduction

Servomotors are used as key components of automated systems by performing accurate positioning, accurate speed regulation, and precise force control (motion control) in response to commands from computers and sensors. [2]

In the field of factory automation (FA), numerical control (NC) machin tools, industrial robots, etc.., are used to save energy and promote automation, which gives high productivity and produces high quality products. They are becoming more and more intelligent. Servomotors and motion control technologies that based on machatronics engineering are being applied to this new equipment. [2]

Servomotors are also improved in industrial drive systems, robots, military fields, the aerospace industry, manufacturing systems, computer and communication equipment, and the automobile and construction machine industry to enable factory automation, office automation, agriculture automation, and other automated systems. [1]

One of the examples of applications of servomotors and the charactetristics and performance required for servomotors used in those applications is application to industrial robots. The fields of application of industrial robots are increasing because robots can repeat simple tasks, improve quality and productivity, and work even under unfavourable conditions. Servomotors used for industrial robots should be of low inertia, high responsiveness, small size, and light weight. Low inertia and high responsiveness are indispensable factors for improving operational speed. Small size and light weight are the factors contributing directly to reduction of the weight of the robot arm.

In order to optimize the transfer of mechanical power from the motor (P_m) to the joint (P_u) of the robot arm, it is necessary to interpose a transmission (geared type robots) or allow direct connection of the motor to the joint without the use of any transmission element (direct drive type robots).

In this study, we address the experimental evaluation of robot controllers on direct drive arms. A direct drive arm is a mechanical arm in which the shafts of articulated joints are directly coupled to the rotors of motors with high torque.

Since the arm does not contain transmission mechanisms between the motors and their loads, the drive system has no backlash and has high mechanical stiffness, all of which are desirable for fast and accurate robots.

In the literature, a variety of control techniques have been developed to address the problem. Linear controllers are mostly based on PD and PID controllers, which is the widely used approach with industrial robots. Even through linear methods provide ease-of-application, for more sophisticated applications and high performance goals, the nonlinear dynamics of the system has to be taken into account when designing control algorithms.

Extensive research has been conducted developing nonlinear control methods for robots. Nonlinear methods can be model-based, (i.e. computed torque control, PD control with computed feedforward, PD control and PD+) for which an accurate model of the system is required. Thus, they are often combined with on-line parameter estimation techniques [Bogosyan, 1995].

In this thesis, PD+ is taken as one of these nonlinear methods of the model-based.

A key feature of this thesis that distinguishes it from the other robot control studies is considering the whole effect dynamics of the direct drive robot and also actuator dynamics that PMSMs are used as the purpose but in other robot control studies you can see only the link dynamics.

1.2 Purpose of the thesis

The main contribution of this thesis is to develop and apply nonmodel and model based controllers for the position control of servomotors, namely, permanent magnet synchronous motors (PMSM).

For this purpose, the control of PMSMs driven the direct-drive 2 degree of freedom (2DOF) planar arm robot will be taken into consideration.

The system performance is tested with the Matlab/Simulink based simulation package. To take into account the real system behavior, the power system block-set is used. The motors are controlled by some controllers and match the time-domain

command tracking specification under the motor parameters. The performance is tested under different load and reference conditions.

Three controllers are developed for the position and trajectory control of the arm; namely, PID and PD controllers as standard linear controllers and PD+ as a nonlinear model based controller.

For this purpose, each rotary joint of the manipulator is considered as an individual system and the control is applied to each joint on a motor-load basis. Various linear control strategies, such as PD and PID are developed first in chapter 4 and then applied to each joint of the manipulator. As a second method, a nonlinear model based controller, known as proportional-derivative plus (PD+) controller is designed in chapter 5.

Simulation results are taken for both accurately known and uncertain dynamics.

At the last the performance of these controllers was compared and better tracking accuracy with less errors will observe.

1.3 Layout of the thesis

This thesis is consisted of seven chapters. In chapter 1 general information, purpose of the thesis and layout of the thesis is placed as an introduction chapter.

In chapter 2 brushless servomotors, their structure, materials of PM technologies, components and operational principles of brushless servomotors are described.

In chapter 3 drive system of brushless servomotors are placed and a position servo control system for a PMSM is described in details.

In chapter 4 the mathematical model of the PMSM is explained and the linear controllers of PD and PID are designed.

In chapter 5 a two-link planar arm of a robot and its mathematical equations is described and two PMSMs are used for controlling this arm by using a PD+ controller as a nonlinear model based controller.

In chapter 6 the whole system, two-link planar arm, is simulated by Matlab/simulink software package.

In the last chapter conclusion are listed.

CHAPTER 2. BRUSHLESS SERVOMOTORS AND THEIR OPERATIONAL PRINCIPLES

2.1 Introduction

The servomotor is an important component of actuators for FA and NC equipment. Brushless servomotors are lightweight, small, easily integrated, efficient, controllable, and maintenance is free. Easy servomotor maintenance is desirable, especially in such places as unmanned factories where a great number of servomotors are employed; brushless servomotors offer a great advantage in such applications.

The current passing through the armature coil of a motor will be one of the alternative sine, square, trapezoidal, or other waveformas.

Commutator switches (brushes) are usually mechanically installed on motors to generate those alternative currents. But in brushless servomotors alternative currents can be generated by external semiconductor switching circuits.

2.2 Brushless servomotor

Brushless servomotors have been developed in industrial field requiring large capacities alongside the developement of (Insulated gate bipolar transistor) IGBT technology. Brushless servomotors have been replacing brush type motors in machine tool and robotics applications over the last number of years. The first electronically controlled dc brush motor systems used analog control circuits and thyristor power switches. The present day brushless drive now use IGBT switches and a high speed microcontroller or a digital signal processor (DSP) which implements digital control loops for the motor position, velocity and current.

Figure 2.1 : An example of a brushless servomotor

Figure 2.1 shows the appearance of a brushless servomotor. A rotor position detector and a speed detector are mounted on the motor shaft. A thermal detector is installed on the stator to detect overload operation. As most of the loss in the motor takes place in the stator, overload is easily detected there. Furthermore the stator housing can be designed for easy cooling. Ferrit is chosen for the rotor pole because of its low price, relatively high performance, and particularly low sensitivity to demagnetization.

The application of brushless servomotors became attractive for several reasons: reduction of the price of power transistors, establishment of the technique of current control of PWM invertors, developement of permanet magnet materials, developement of highly accurate detectors, and manufacture of these components in a compact form. In this way, brushless servomotors were able to be equipped with the delicacy of dc motors and the strength of structure of ac motors. It is no exaggeration to say that brushless servomotors created a new phase in the developement of control motors.

2.2.1 Structure of brushless servomotors

Brushless servomotors rectify current by means of a transistor, instead of a commutator used in dc servomotors. On the other hand, brushless servomotors are also called ac servomotors because brushless servomotors of synchronous type with a permanent magnet rotor detect the position of the rotational magnetic field to control the three-phase current of the armature. Then they obtain the same torque characteristic dc motors by making the field and the current meet at right angles.

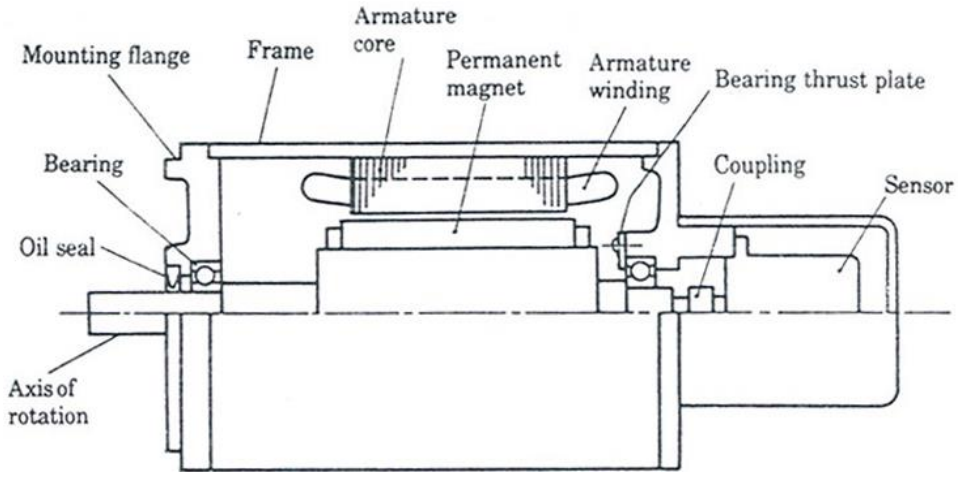

Figure 2.2 : Structure of brushless servomotor

The structure of a brushless servomotor is shown in figure 2.2.

They are of the rotational-magnetic-field type, in which the permanent magnet for providing magnetic flux is placed in the rotor. The windings are in the static armature which is part of the stator. Therefore, the magnetic field for generating torque is stationary in dc servomotors, while it rotates in brushless servomotors. In other words, the armature revolves in dc servomotors, while that is stationary as a stator in brushless servomotors.

As servomotors are accelerated or decelerated very fast, the maximum has to be several times larger than the rated torque. In contrast, dc servomotors have a limit of rectification. As brushless servomotors do not have such a limit of rectification, they can be operated up into the boundary of high-speed rotation without decreasing the maximum torque.

In brushless servomotors, in addition, heat diffusion occurs not on the rotating part but only on the armature of the stator,since the permanent magnet is mounted on the axis of rotation. The heat generated on the armature of the stator diffuses into the air through the frame. Therefore, it is easier to cool brushless servomotors than to cool dc servomotors, which have heat generation on the rotor. Moreover, brushless servomotors provide sure overload protection, because the temperature of the heat generation part can be detected directly.

2.2.2 Materials of permanent magnets in brushless servomotors

Materials that produce magnetic field in the lack of electromotor force (e.m.f) are called permanent magnet. Generally permanent magnets are made by some elements like iron, nickel and cobalt. Permanent magnets are roughly determined by residual magnetic flux density B_r , holding power H_c and maximum energy product $(BH)_{max}$.

The energy stored in the in the gap of a magnetic circuit including permanent magnets is proportional to the product of the magnetic flux density and holding power. Therefore, the better the magnetic material is, the more magnetic energy it possesses.

Al-Ni-Co magnts are the first improved commercial magnets. They were produced in about 1935. Ferrite magnets were produced in about 1960 and SmCo magnets in about 1975. The last improved magnets are Neodyum-Iron-Boron (NdFeB). This magnet has a marvellous performance with its maximum energy poduct among the other magnets and consequently it has been applied to industrial use. For lowest cost, ferrite or ceramic magnets are the universal choice.

The magnetic characteristics of permanent magnets are shown accurately by a demagnetization curve in figure 2.3.

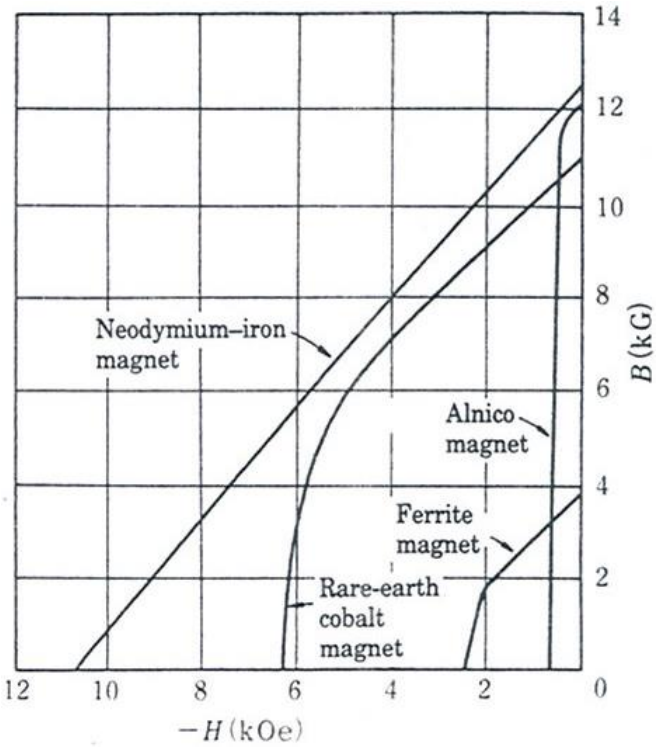

Figure 2.3 : Demagnetization curves of several types of PM

A ‘hard’ PM material is one in which the hysteresis loop is straight throughout the second quadrant, such as ceramic, rare-earth/cobalt, and NdFeb magnets.

A ‘Soft’ PM material is one with a ‘knee’ in the second quadrant, such as Alnico.

Figure 2.4 is the B-H loop or ‘hysteresis loop’ of a hard PM material.

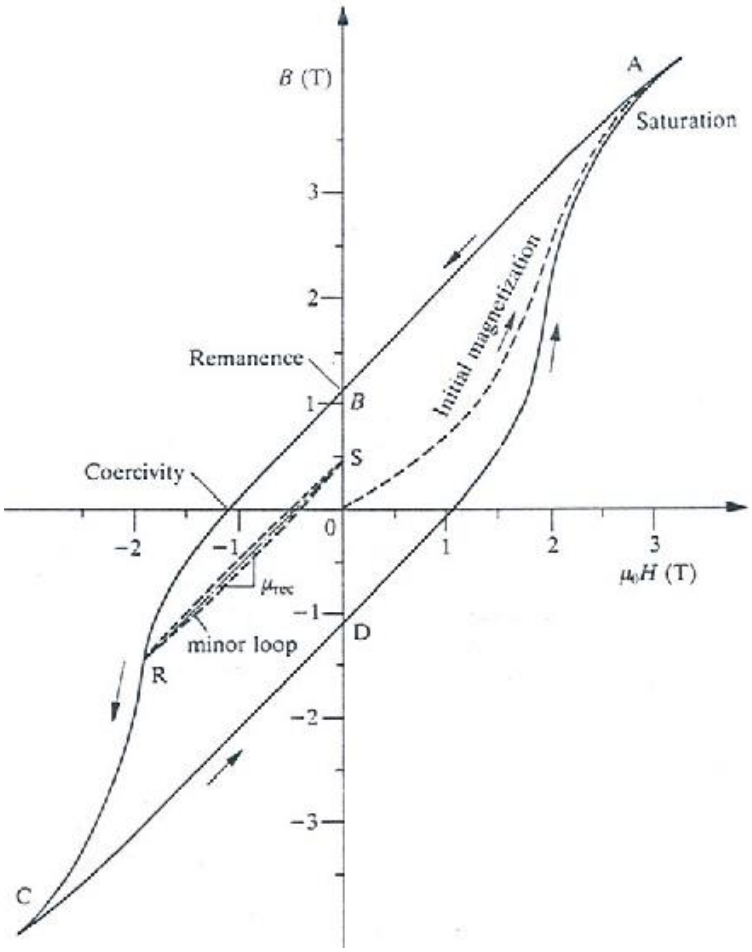

Figure 2.4 : B-H hysteresis loop of a hard PM material

2.2.3 Brushless servomotor components

A brushless servomotor comprises a rotor, a stator, a sensor, a frame, bearing and a coupling. Some brushless servomotors have a brake.

Rotor : The structure of the rotor is of the rotational-magnetic-field type, with permanent magnets fixed on the axis of rotation.

Stator : A stator consists of an armature core and armature windings. The armature core is made by laminating punched silicon steel sheet of 0.35-0.5 mm thickness.

Sensor : The sensor of a brushless servomotor is required to have two functions. One is detection of rotor position. The other is detection of rotational speed. Rotary encoders, brushless resolvers, and so on, are generally used as sensors.

Frame : A frame not only fixes the stator but also constitutes a part of the magnetic pathas a yoke.

Bearing : Ball bearings are used for bruhless servomotors because they are subject to little mechanical loss. The outer rings of the ball bearing are fixed with bearing holders to avoid creep, because of the repeated sharp acceleration and thermal expansion of the axis of rotation.

Coupling : A coupling combines a rotor and a sensor, which are mounted on the same axis. The coupling used for servomotors should correctly transmit the rotor position and the speed to the sensor without being distorted even when the motor is accelerated or decelerated sharply.

2.2.4 Advantage and disadvantages of brushless servomotors

Advantages : The well known advantages of brushless over brush motors include improved reliability, higher power to weight ratios, and an overall better dynamic performance.

- They have higher maximum speed and greater capasity
- Brushless system causes easy maintenance and produce less noise.
- In spite of their light weight and small volume they produce high moment and represent high performance.
- Because of the stator housing design cooling the motor is easy.
- Sine wave output current control to reduce torque ripple.

Disadvantages:

- Control circuits are usually difficult.
- The sensors should be used because of rotor position detector and this makes it expensive.
- Brushless permanent magnet current control servomotors are expensive.

- In spite of using suitable magnetic materials for keeping permanent magnet into the motor, during the time they will lose their magnetization.

2.3 Operational principles

In this section operational principles of dc motors, ac motors and then brushless servomotors are described.

2.3.1 Operational principles of dc motors

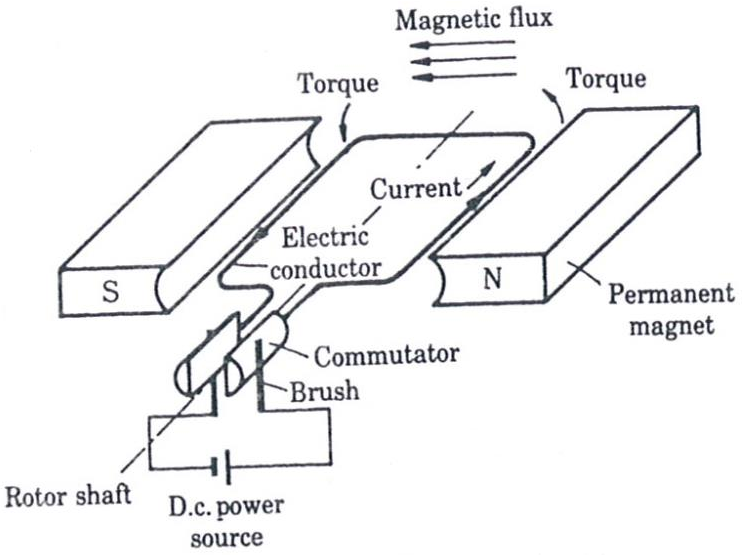

Figure 2.5 : Basic principle of dc motors

The principles of the dc motor are shown schematically in figure 2.5. When the current flows in the electrical conductor after passing through the brushes and the commutator in the magnetic field that produced by permanent magnets N and S, torque is generated in the direction of the arrow shown in figure 2.6 by helping of Fleming's Left Hand Rule. Then rotor is going to rotate and the torque decreases and will be zero when the rotor comes near 90 degree. In 90 degree current and torque becomes zero. But the rotor can't stop because of the rotor's inertia. A little degree after 90 commutation takes place and the torque is going to increase again and makes the rotor to rotate continousely.

Motors for practical use have dozens of commutators. Therefore, a little degree creats commutation and makes them to rotate at their maximum torque. Thus, in dc motors torque variation is reduced by increasing the number of commutators.

2.3.2 Operational principles of ac motors

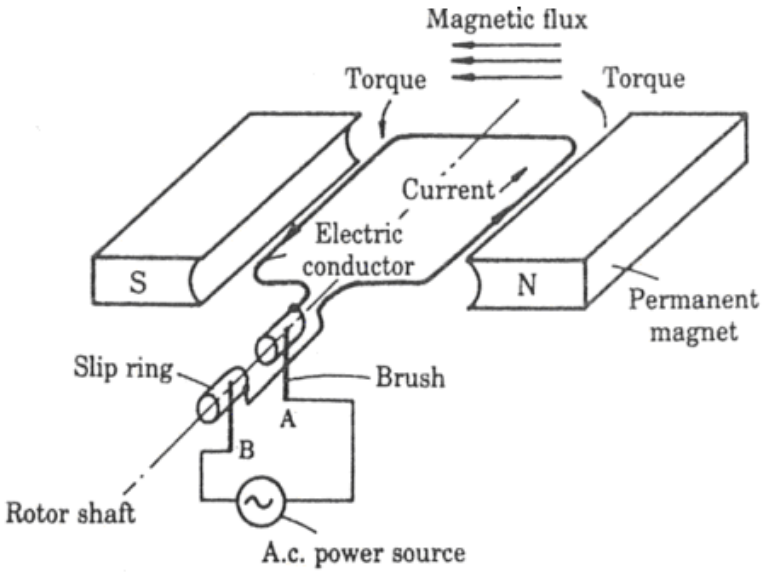

Figure 2.6 : Basic principle of ac motors

The principles of the ac motor are shown schematically in figure 2.6. Here a slip ring is used instead of a commutator. After energizing the motor so as to make brushe A positive and brush B negative, torque is generated and rotor rotates like the same as dc motors. As a result, alternative currents of ac power source makes the rotor rotate continousely at the rotational speed corresponding to the applied frequency. Therefore, by changing the frequency rotational speed can variate.

These motors are called revolving-armature type.

2.3.3 Operational principles of brushless servomotors

The brushless motor is rotated by reversing the polarity of the power source according to the changing rotor position. Figure 2.7 shows a kind of brushless ac motor.

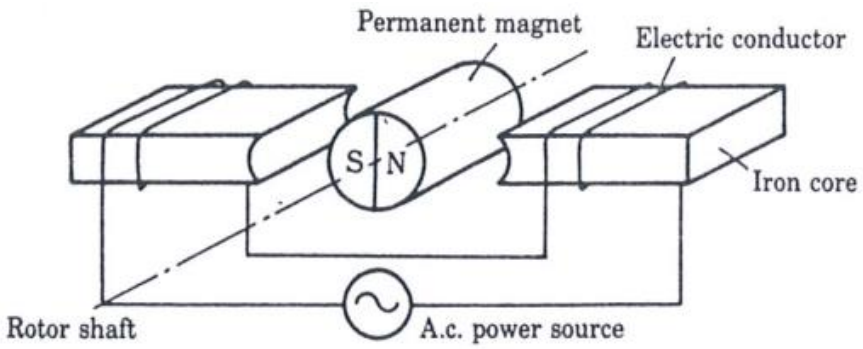

Figure 2.7 : Basic principle of brushless ac motor

The torque produced by the motor is directly proportional to the current fed to the armature windings and that the generated voltage at the armature terminals is directly proportional to the motor velocity.

The basic principle of operation of a brushless drive is that the motor winding voltages and currents are synchronized to the rotor position to ensure constant torque production at a constant speed.

In brushless servomotors, torque variation is reduced by making the coil of the armature in three-phase and by sending the current of each phase into a sine wave.

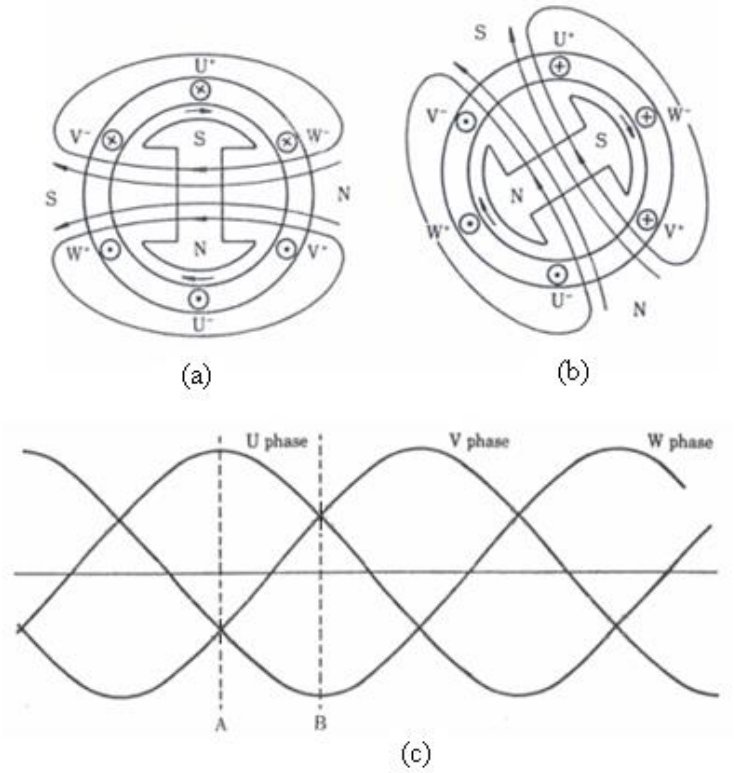

Figure 2.8 : Principle of a brushless servomotor

Cross-sectional views of a three-phase PMSM are shown in figure 2.8 (a) and (b).

U^+, U^-, V^+, V^-, W^+ and W^- illustrate the begining or the end of the coil of each phase.

When the motor is energized by three-phase alternative currents as shown in figure 2.8 (c), at point A of the alternative currents in the figure 2.8 (c), only phase U is positive and phase V and W are both negative.

In this condition, the direction of the current of each coil is as shown in figure 2.8 (a) and the vector of the magnetic flux induced by the current is generated in the direction from N to S. Therefore, torque is generated to rotate the rotor clockwise

due to attractive forces between the magnets. At point B magnetic flux is generated 60 degree further clockwise.

As a result from the above, a continuously rotating field can be obtained by making three-phase currents flow in the stator coil.

Thus, most of the brushless servomotors are of the revolving-field type.

CHAPTER 3. PMSM CONTROL DRIVE CIRCUITS FOR POSITION CONTROL

3.1 Introduction

The basic principle of operation of a brushless drive is that the motor winding voltages and currents are synchronized to the rotor position to ensure constant torque production at a constant speed. The mechanical commutator of the brush dc motor is replaced by electronic switches which supply current to the motor windings as a function of the rotor position.

3.2 Necessary components for controlling a servomotor

The components necessary for the control of a servomotor are a main frame, sensors for angle, angular velocity, current, voltage, magnetic flux, and temperature, and a semiconductor power converter (power amplifier), including various analog or digital ICs for triggering control. In addition to these, a small motor-driven gear having a position and speed sensors also mounted on the motor shaft. A dijital controller (DSP) is included too. The whole system is shown in figure 3.1.

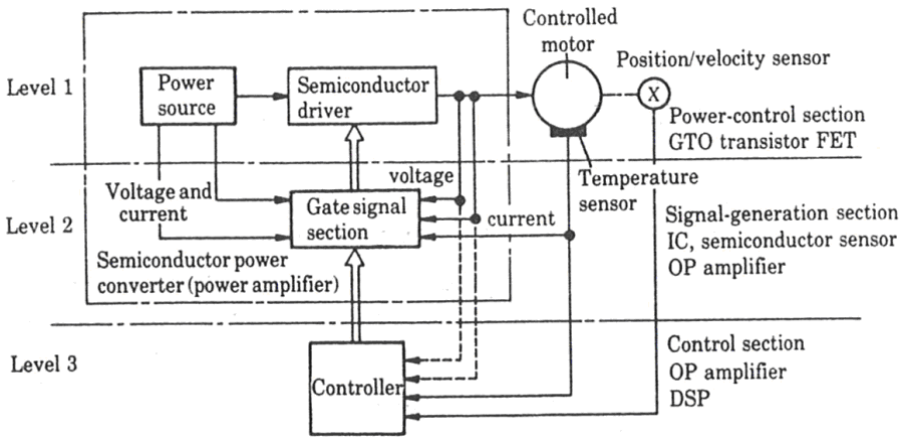

Figure 3.1 : Driving system of brushless servomotors

The power-control section consists of a motor, sensors and semicoducor switching circuits including some IGBT that triggered by PWM.

In the signal generation part, motor voltage, current, flux, and frequency are controlled so as to obtain accurate and maximum torque response. Three-phase alternative currents are generated in this section.

Motion control (position, speed and force control) is obtained in the control section by some controllers like DSP or microcontrollers.

In evaluating a servomotor driving system, detectors need to be able to detect rotational position for position control. The position / speed signal is calculated from the position encoder signal. An encoder is used for the purpose, and the encoder and small-sized motor are sometimes united into a single unit, the ‘encoder motor’ in order to make the system smaller.

The controller shown at the bottom of figure 3.1 is usually used for regulation and tracking with respect to position and speed. The whole purpose requires great computational effort, so they are performed by high-speed digital signal processors (DSP) combined with personal computers. DSPs will be used increasingly not only as digital controllers and signal processors but also as analyzer and design equipment.

Figure 3.2 shows the schematic diagram of overall system.

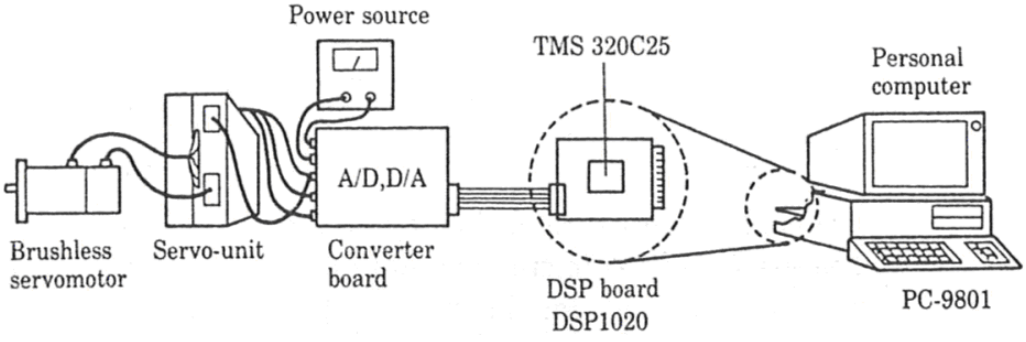

Figure 3.2 : Schematic diagram of overall system

3.3 Drive configuration

A typical brushless drive system consists of a three phase brushless motor fed from a three phase PWM controlled power inverter. The drive control system has an outer motion loop, as in a brush dc servo system, which calculates the required torque to

maintain the target position / velocity. The inner current control loop forces the appropriate winding currents, based on the machine model, so that the machine generates the desired torque.

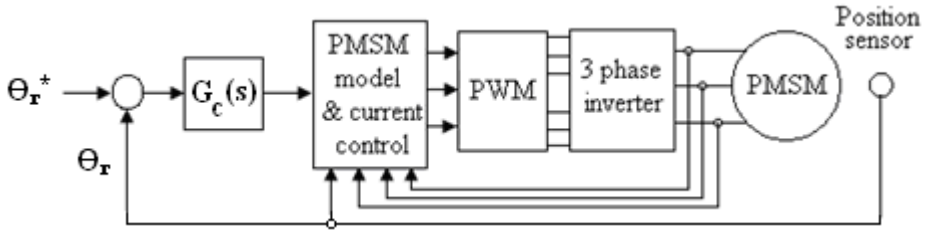

Figure 3.3 : Generic brushless drive system

Generic brushless drive system of a brushless servomotor is shown in figure 3.3.

The phase to be controlled is single-phase in the dc motor and three-phase in the brushless motor. Furthermore the brushless motor has a rotor position detector, a sine wave generation circuit, a speed detector, and so on, but the dc motor has none of these.

3.3.1 Brushless control drive evolution

The first brushless drives introduced were of the brushless dc type because of the simplicity of the position sensor and the ease of adoption from the dc motor control systems [4].

These are still used in low applications such as in fans but the brushless ac system is the preferred system in high servo systems. The development of brushless ac systems was enabled by the availability of encoders or integrated resolver to digital (R/D) converters which allowed the implementation of a brushless ac drive with mixed signal components [5].

3.3.1.1 Brushless dc drive

The brushless dc drive is so called because the windings are commutated (switched) based on inputs from a low resolution position sensor. Typically the sensor consists of a set of hall devices driven by the rotor field magnet. There are six commutation points per electrical cycle, two per phase, based on digital signals from three hall devices. In between switching points the windings are controlled in a similar way to a brush type dc motor. The position / velocity control, current control and PWM circuits are almost exactly the same as in a commutator dc motor controller. The

information from the hall sensors is decoded to select the appropriate current feedback signal and power inverter switches for each commutation segment. The control hardware for a brushless dc drive is described in figure 3.4 below.

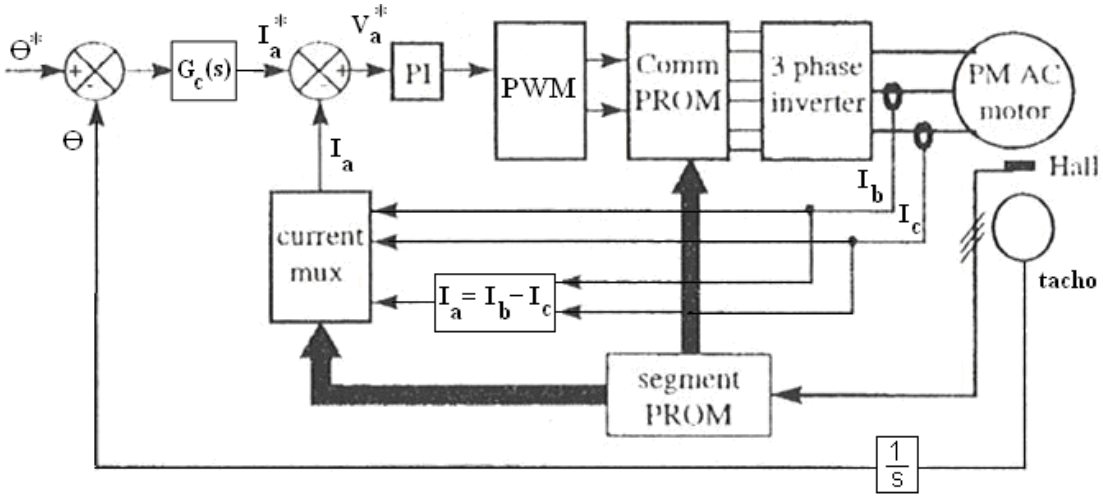

Figure 3.4 : Brushless dc drive controller

3.3.1.2 Brushless ac drive

The brushless ac drive is so called because the motor is driven with sinusoidal shaped ac currents. This has the advantages of much smoother torque production but requires much higher resolution position information. A constant torque is produced when the three phase windings carry three phase sinusoidal currents synchronized to the rotor field position. The control hardware for a brushless ac drive is described in figure 3.5 below.

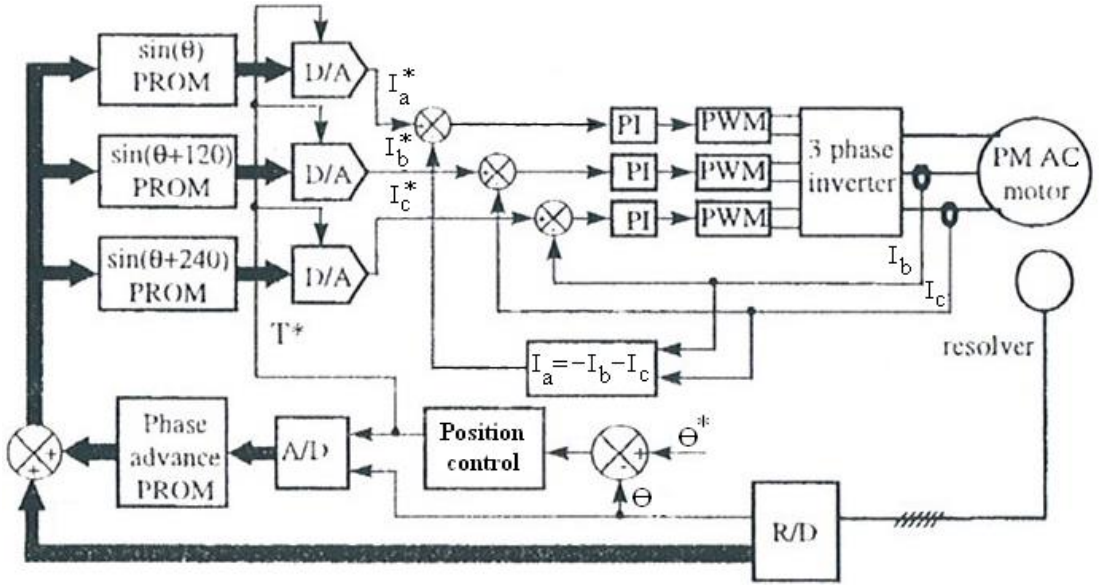

Figure 3.5 : Brushless ac drive control using mixed signal components

3.4 The PMSM position servo control system and circuit description

In the PMSM position servo control system shown in figure 3.6 the key component in this control system is encoder and the rotor position detector circuit.

The rotor position detector circuit is used for receiving a rotor position signal θ_r from the encoder and converting it to a form that can be read by the sine wave generation circuit that follows the rotor position detector.

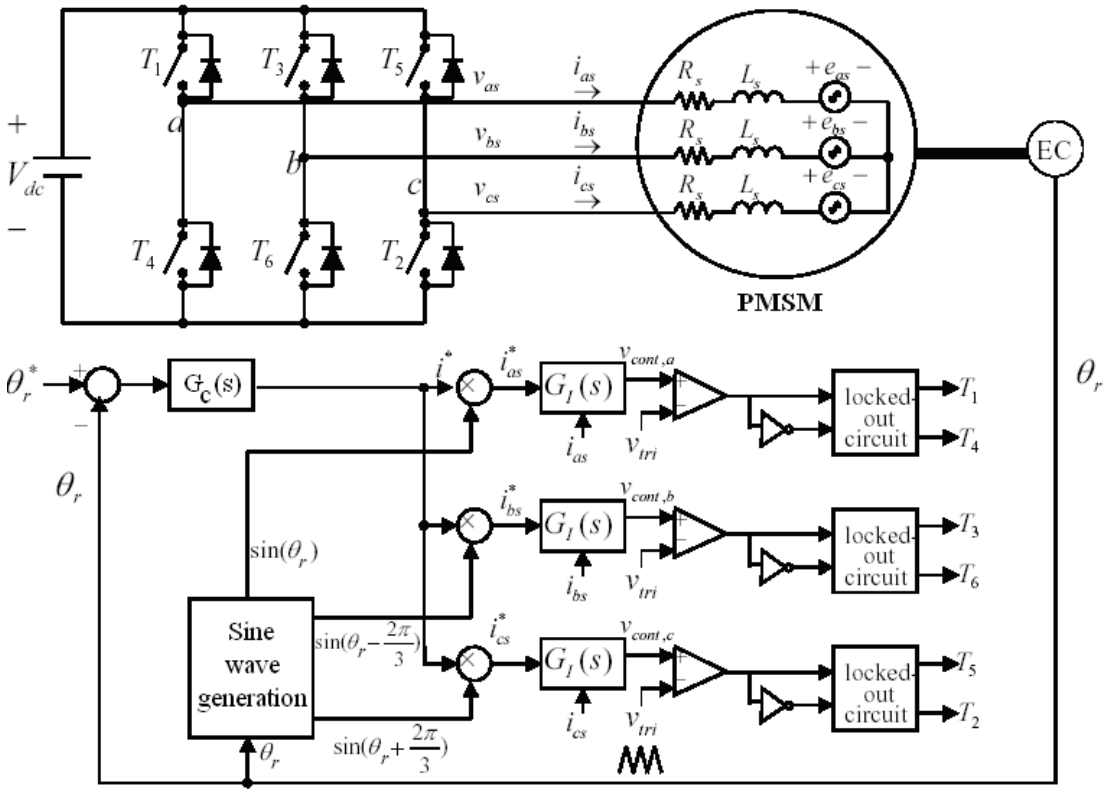

Figure 3.6 : The PMSM position servo control system

The position signal Θ_r is the feedback input for the position loop which produces the motor torque current demand reference i* by a position controller like PID.

In sine wave generation, the necessary data, each item of which corresponds to an address, are written on a ROM. The rotor position word is used to address ROM with the look up tables for the reference sinusoidal profiles.

The three multiplying digital to analog converters combine the torque current reference i* and the sinusoidal profiles to produce three sinusoidal winding profiles for the motor. Three individual current loops, i_{as}, i_{bs}, i_{cs}, then force the winding

currents to follow these profiles and produce a constant torque proportional to the torque current reference i*.

The aim of the brushless servomotor is to make sine wave currents flow in the motor, so it is ideal for a brushless servomotor to have the output of the current amplifier of the sine waves applied directly to the motor after amplifying the power. However, amplification of the sine waves is not practical, because that means using a power transistor in the proportional region. This makes it difficult to solve the problem of high temperature due to power loss. Therefore, the power loss is reduced by switching the power transistor. This method is called PWM (pulse width modulation). In this method, the current of a motor is converted into a controlled pulse of width proportional to the amplitude of the sine wave so that it may become a sine wave on the average. Figure 3.7 shows the principles of the method.

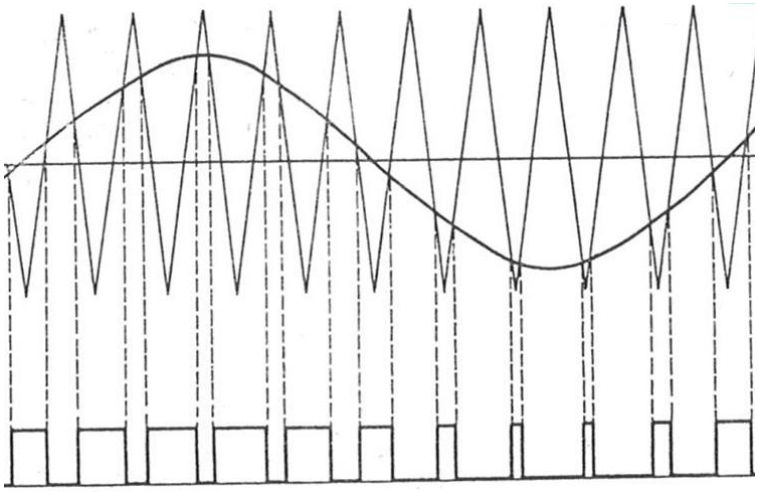

Figure 3.7 : Principle of sine wave PWM

A triangular carrier wave oscillating with constant frequency and amplitude, and the sine wave output from the current amplifier are compared by a comparator. It is important to decide the method of selecting the oscillating frequency of the chopping wave. As the carrier frequency equals the switching frequency of the power transistor, it increases the switching loss proportionally as it is made higher, and it reduces the speed of response of the servomotor as it is made lower.

Generally speaking, a carrier frequency of 10-20 kHz, is selected when the inverter consisted of IGBTs.

Thus, in the PMSM position servo control system, if the motor current is larger than the command value, the inverter switches itself in the direction that limits the current.

If the motor current is smaller than the command value, the inverter switches itself in the direction that increases the current.

3.5 Digital Controller

A digital controller has a high speed computing engine with instructions which make it ideal for implementing control laws. The power converter used digital signals for driving. Therefore a number of unnecessary analog to digital and digital to analog conversions take place between the output of the motion loop and the power converter interface. It is now possible to implement of all current loops digitally enabling an all digital drive controller. Microcontrollers and digital signal processors are increasingly being used to implement algorithms for the control purpose.

CHAPTER 4. MATHEMATICAL MODEL FOR PMSM DRIVE SYSTEM

4.1 Introduction

In this chapter, by using the block diagram of the PMSM position servo control system, the mathematical model of abc and dqo is constituted. Then by using Park's transformation, stator equations are transformed to rotor qdo equations and q,d,o axis system is defined. This model is called phase transformation model.

4.2 Equivalent circuits of q and d and the Park's transformation.

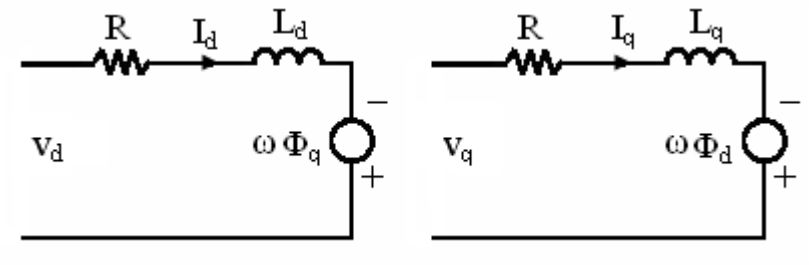

(a) **(b)**

Figure 4.1 : Equivalent circuits of d and q of PMSM

In order to transform stator variables to rotor qdo axis, $K^{r}{}_{qdo}(\theta_r)$ that called Park's trasformation matrix is used.

$$V_{qdos} = K^{r}{}_{qdo}(\theta_r) * V_{abcs} \tag{4.1}$$

$$I_{qdos} = K^{r}{}_{qdo}(\theta_r) * I_{abcs} \tag{4.2}$$

$$K^{r}{}_{qdo}(\theta_r) = \frac{2}{3}\begin{bmatrix} \cos\theta & \cos(\theta-120) & \cos(\theta+120) \\ \sin\theta & \sin(\theta-120) & \sin(\theta+120) \\ 0.5 & 0.5 & 0.5 \end{bmatrix} \tag{4.3}$$

$$V_{abcs} = \begin{bmatrix} v_{as} & v_{bs} & v_{cs} \end{bmatrix}^T \quad , \quad I_{abcs} = \begin{bmatrix} i_{as} & i_{bs} & i_{cs} \end{bmatrix}^T \tag{4.4}$$

Voltage and current of the stator can be obtained by inverse Park's transformation.

$$V_{abcs} = (K^r{}_{qdo})^{-1}(\theta_r) * V_{qdos} \tag{4.5}$$

$$I_{abcs} = (K^r{}_{qdo})^{-1}(\theta_r) * I_{qdos} \tag{4.6}$$

$$(K^r{}_{qdo})^{-1}(\theta_r) = \begin{bmatrix} \cos\theta & \sin\theta & 1 \\ \cos(\theta-120) & \sin(\theta-120) & 1 \\ \cos(\theta+120) & \sin(\theta+120) & 1 \end{bmatrix} \tag{4.7}$$

Thus,

$$\begin{bmatrix} V_{as} \\ V_{bs} \\ V_{cs} \end{bmatrix} = \begin{bmatrix} \cos\theta & \sin\theta & 1 \\ \cos(\theta-120) & \sin(\theta-120) & 1 \\ \cos(\theta+120) & \sin(\theta+120) & 1 \end{bmatrix} \begin{bmatrix} V_q \\ V_d \\ V_o \end{bmatrix} \tag{4.8}$$

$$\begin{bmatrix} i_{as} \\ i_{bs} \\ i_{cs} \end{bmatrix} = \begin{bmatrix} \cos\theta & \sin\theta & 1 \\ \cos(\theta-120) & \sin(\theta-120) & 1 \\ \cos(\theta+120) & \sin(\theta+120) & 1 \end{bmatrix} \begin{bmatrix} i_q \\ i_d \\ i_o \end{bmatrix} \tag{4.9}$$

4.2.1 Electromagnetic torque and the relationship with qdo axis

In permanent magnet synchronous motor, for existing torque two terms affect in the equation. One of them is a torque that existed by permanent magnet. The other one is a torque that existed by inductances L_q and L_d of q and d axises. You can see the related equation in the following.

$$T_e = \frac{3}{2} p\left[I_q \phi_m + (L_d - L_q) I_q I_d\right] \tag{4.10}$$

ϕ_m : Magnetic flux existed by PM

L_d, L_q : Inductances of d and q axises

I_d, I_q : Currents of d and q axises in permanent state

p : Pole number pairs

In the torque equation of (4.10) the term $I_q\phi_m$ shows a torque that existed by permanent magnet and current I_q of q axis. The second term shows a torque that existed by the difference of inductances L_d and L_q and multiplying by I_q and I_d.

4.3 Mathematical model and block diagram of PMSM (Three-phase)

Block diagram of the PMSM position servo control system is shown in figure 4.2. The brushless servomotor is shown in the block diagram consists of a three-phase PMSM fed from a three-phase PWM controlled power inverter. In the block diagram there are two loops. The outer motion loop which calculates the required torque to keep the desired position. The inner current control loop which regulate suitable winding currents so that the machine generates the desired torque.

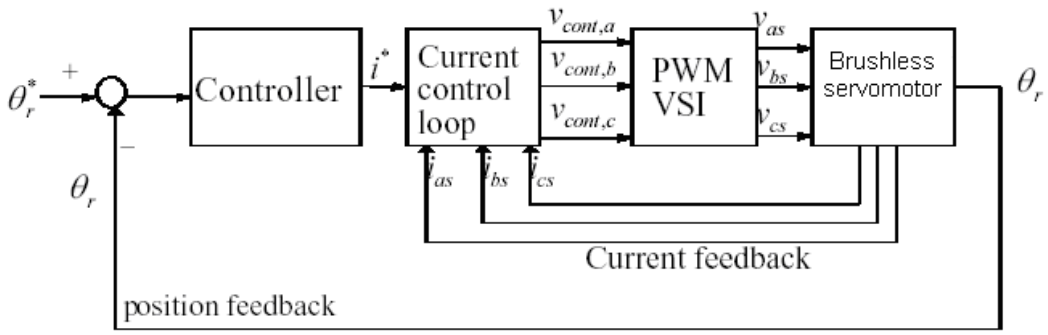

Figure 4.2 : Block diagram of the PMSM position servo control system

The voltage equations in machine variables are

$$\begin{bmatrix} V_{as} \\ V_{bs} \\ V_{cs} \end{bmatrix} = R_s \begin{bmatrix} i_{as} \\ i_{bs} \\ i_{cs} \end{bmatrix} + L_s \frac{d}{dt} \begin{bmatrix} i_{as} \\ i_{bs} \\ i_{cs} \end{bmatrix} + \begin{bmatrix} e_{as} \\ e_{bs} \\ e_{cs} \end{bmatrix} \tag{4.11}$$

$$= R_s \begin{bmatrix} i_{as} \\ i_{bs} \\ i_{cs} \end{bmatrix} + L_s \frac{d}{dt} \begin{bmatrix} i_{as} \\ i_{bs} \\ i_{cs} \end{bmatrix} + \omega_r K_e \begin{bmatrix} \sin\theta_r \\ \sin(\theta_r - 2\frac{\pi}{3}) \\ \sin(\theta_r + 2\frac{\pi}{3}) \end{bmatrix} \tag{4.12}$$

v_{as}, v_{bs}, v_{cs} the applied stator voltage,

i_{as}, i_{bs}, i_{cs} the applied stator current,

R_s, L_s the resistance and inductance of each stator winding,

e_{as}, e_{bs}, e_{cs} the back-EMF voltage,

ω_r, θ_r the electrical rotor angular velocity and displacement,

K_e the voltage constant

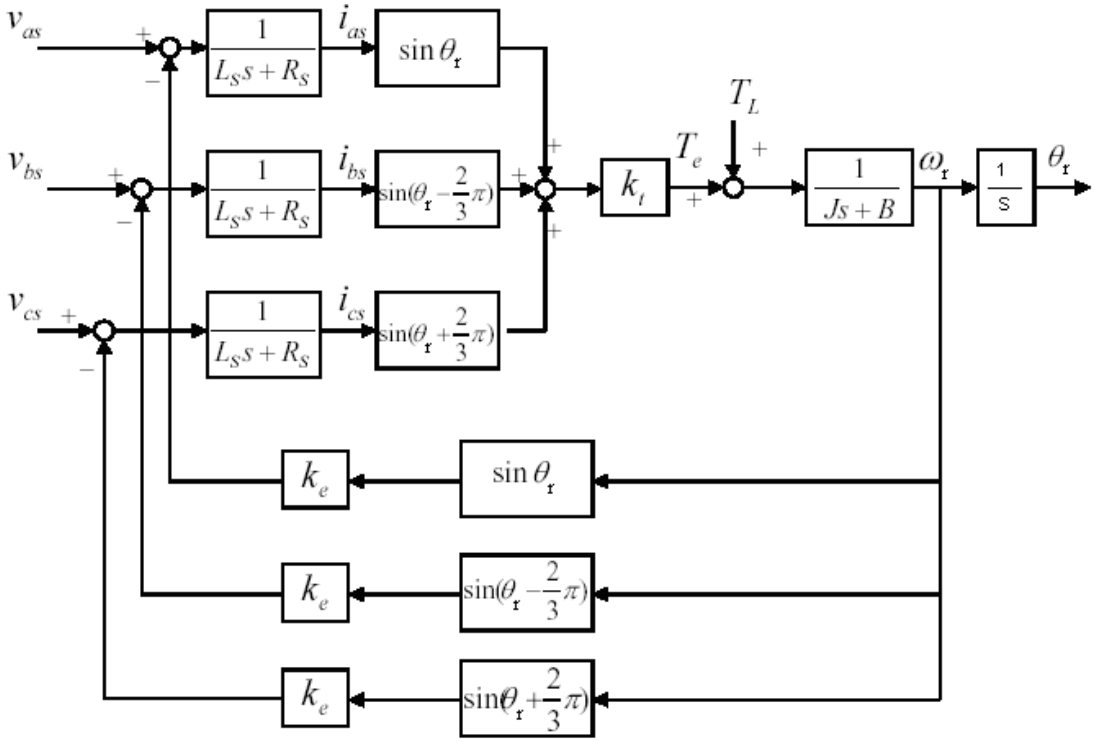

Figure 4.3 : Mathematical diagram of the PMSM

Mathematical diagram of the PMSM is shown in figure 4.3. The electromagnetic torque, position and velocity equations can be related as

$$T_e = K_t \left[i_{as} \sin\theta_r + i_{bs} \sin(\theta_r - 2\frac{\pi}{3}) + i_{cs} \sin(\theta_r + 2\frac{\pi}{3}) \right] \quad (4.13)$$

$$T_e + T_L = J\frac{d\omega_r}{dt} + B\omega_r \quad (4.14)$$

$$\theta_r = \int \omega_r dt \quad (4.15)$$

4.3.1 Closed loop transfer function of the model with the effect of load as a disturbance signal using PID controller

In order to find the closed-loop transfer function of the model with the effective of load T_L, the load T_L is considered as a disturbance input and the reference input θ_r* should be supposed to zero. The diagram is shown in figure 4.4.

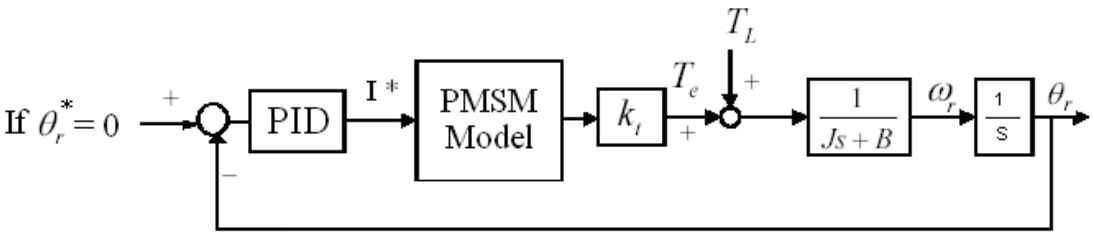

Figure 4.4 : Closed loop system with PID control (T_L = disturbance input)

From the figure 4.3 the electromagnetic torque can be expressed as

$$T_e = K_t\left[i_{as}\sin\theta_r + i_{bs}\sin(\theta_r - 2\frac{\pi}{3}) + i_{cs}\sin(\theta_r + 2\frac{\pi}{3}) \right] \quad (4.16)$$

If the phrase in the parenthesis be I_x (4.17)

$$I_x = i_{as}\sin\theta_r + i_{bs}\sin(\theta_r - 2\frac{\pi}{3}) + i_{cs}\sin(\theta_r + 2\frac{\pi}{3}) \quad (4.18)$$

$$T_e = K_t I_x \Rightarrow T_e(s) = K_t I_x(s) \quad (4.19)$$

$$T_e + T_L = J\frac{d\omega_r}{dt} + B\omega_r \quad , \quad \theta_r = \int \omega_r dt \quad (4.20)$$

$$T_e = J\frac{d\omega_r}{dt} + B\omega_r - T_L \Rightarrow T_e(s) = s(sJ+B)\theta_r(s) - T_L(s) \quad (4.21)$$

As in figure 4.4 Current I* can be expressed as

$$\mathrm{I}^*(\mathrm{s}) = \left[K_p + K_d s + \frac{K_i}{s} \right]\left[0 - \theta_r(s)\right] \quad (4.22)$$

$$\mathrm{I}^*(\mathrm{s}) = -\left[K_p + K_d s + \frac{K_i}{s} \right]\theta_r(s) \quad (4.23)$$

From the equations of (4.19) , (4.21)

$$K_t I_x(s) = s(sJ+B)\theta_r(s) - T_L(s) \quad (4.24)$$

Assume that the system is ideal. Then in figure 4.2 i_{as}, i_{bs}, i_{cs} currents should be equal to I* approximately.

Therefore,

$$I_x(s) = I^*(s) \tag{4.25}$$

By putting the value of $I^*(s)$ from equation (4.23) in equation (4.24)

$$-K_t\left[K_p + K_d s + \frac{K_i}{s}\right]\theta_r(s) = s(sJ+B)\theta_r(s) - T_L(s) \tag{4.26}$$

Closed loop transfer function of the model by considering T_L as disturbance input will be as follows

$$\frac{\theta_r(s)}{T_L(s)} = \frac{\frac{s}{J}}{s^3 + \frac{B + K_t K_d}{J}s^2 + \frac{K_t K_p}{J}s + \frac{K_t K_i}{J}} \tag{4.27}$$

4.3.2 Closed loop transfer function of the model with the effect of load as a disturbance signal using PD controller

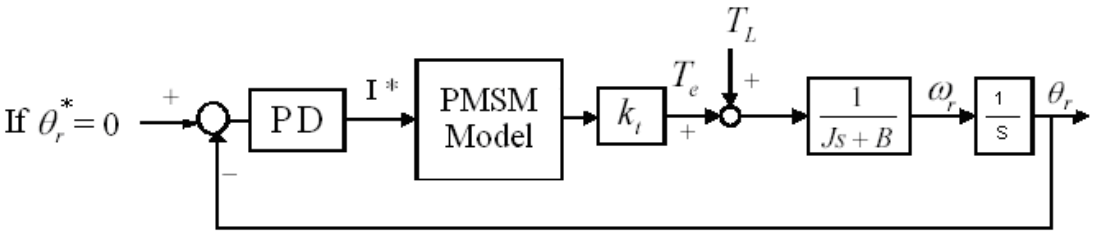

Figure 4.5 : Closed loop system with PD control (T_L = disturbance input)

As in figure 4.4 Current I* can be expressed as

$$I^*(s) = [K_p + K_d s][0 - \theta_r] \tag{4.28}$$

$$I^*(s) = -[K_p + K_d s]\,\theta_r \tag{4.29}$$

Again from (4.25) and by putting the value of $I^*(s)$ from equation (4.29) in equation (4.24) ;

$$-K_t[K_p + K_d s]\,\theta_r(s) = s(sJ+B)\theta_r(s) - T_L(s) \tag{4.30}$$

Closed loop transfer function of the model by considering T_L as disturbance input will be as follows

$$\frac{\theta_r(s)}{T_L(s)} = \frac{\frac{1}{J}}{s^2 + \frac{B + K_t K_d}{J} s + \frac{K_t K_p}{J}} \tag{4.31}$$

4.3.3 Permanent magnet synchronous motor parameters in closed loop transfer function of the model

Table 4.1 : Parameters of PMSMs

Parameters of PMSM 1	**Notation**	**Values**	**Unit**
Resistance	R_1	1	Ω
Inductance	L_1	0.01	H
Torque constant	K_{t1}	4.5	Nm/A
Viscous friction factor	B_{m1}	2.288	Nm.s/rad
Inertia of motor	I_{m1}	0.522	$kg.m^2$
Inertia link 1	I_1	1.266	$kg.m^2$
Total inertia	J_1	2.351	$kg.m^2$
Parameters of PMSM 2	**Notation**	**Values**	**Unit**
Resistance	R_2	1	Ω
Inductance	L_2	0.01	H
Torque constant	K_{t2}	1.5	Nm/A
Viscous friction factor	B_{m2}	0.006	Nm.s/rad
Inertia of motor	I_{m2}	0.012	$kg.m^2$
Inertia link 2	I_2	0.093	$kg.m^2$
Total inertia	J_2	0.1119	$kg.m^2$

Thus,

For the two PMSMs with PID controller we have the following transfer functions

$$\frac{\theta_{r1}(s)}{T_{L1}(s)} = \frac{\frac{s}{J_1}}{s^3 + \frac{B_{m1} + K_{t1}K_{d1}}{J_1} s^2 + \frac{K_{t1}K_{p1}}{J_1} s + \frac{K_{t1}K_{i1}}{J_1}} \tag{4.32}$$

$$\frac{\theta_{r2}(s)}{T_{L2}(s)} = \frac{\frac{s}{J_2}}{s^3 + \frac{B_{m2} + K_{t2}K_{d2}}{J_2} s^2 + \frac{K_{t2}K_{p2}}{J_2} s + \frac{K_{t2}K_{i2}}{J_2}} \tag{4.33}$$

$$\frac{\theta_{r1}(s)}{T_{L1}(s)} = \frac{\frac{s}{2.351}}{s^3 + \frac{2.288 + 4.5K_{d1}}{2.351}s^2 + \frac{4.5K_{p1}}{2.351}s + \frac{4.5K_{i1}}{2.351}} \tag{4.34}$$

$$\frac{\theta_{r2}(s)}{T_{L2}(s)} = \frac{\frac{s}{0.1119}}{s^3 + \frac{0.006 + 1.5K_{d2}}{0.1119}s^2 + \frac{1.5K_{p2}}{0.1119}s + \frac{1.5K_{i2}}{0.1119}} \tag{4.35}$$

Characteristic equations of the two PMSMs with PID controller will be

$$s^3 + \frac{2.288 + 4.5K_{d1}}{2.351}s^2 + \frac{4.5K_{p1}}{2.351}s + \frac{4.5K_{i1}}{2.351} \tag{4.36}$$

$$s^3 + \frac{0.006 + 1.5K_{d2}}{0.1119}s^2 + \frac{1.5K_{p2}}{0.1119}s + \frac{1.5K_{i2}}{0.1119} \tag{4.37}$$

For PD controller the design is the same as in PID controller but the characteristic equations are in the second order and the integral coefficient is zero. Therefore, characteristic equations of the two PMSMs with PD controller will be

$$s^2 + \frac{2.288 + 4.5K_{d1}}{2.351}s + \frac{4.5K_{p1}}{2.351} \tag{4.38}$$

$$s^2 + \frac{0.006 + 1.5K_{d2}}{0.1119}s + \frac{1.5K_{p2}}{0.1119} \tag{4.39}$$

4.3.4 Design and specifying the system parameters for the model

The position-control system reveals important properties of the time response of typical second and third order closed loop systems. Particularly, the effects on the transient response relative to the location of the roots of the characteristic equation. However, in practice, successful design of a control system cannot depend only on choosing values of the system parameters so that the characteristic equation roots are properly placed.

We shall show that although the roots of the characteristic equation, which are the poles of the closed loop transfer function, affect the transient response of linear time-invarient control systems, particularly the stability, the zeros of the transfer function, if there are any, are also important.

By looking at the closed loop transfer function of the model, it will be seen that it is a third-order system.

Closed loop transfer function of a second-order control system with unity feedback is represented here :

$$\frac{Y(s)}{R(s)} = \frac{\omega_n^2}{s^2 + 2\xi\omega_n s + \omega_n^2} \tag{4.40}$$

The second-order control system of (4.40) can be designed for the model with PD controller, but in order to design the system for the model with PID controller, a pole should be added to a closed loop transfer function of the second-order control system to convert it to a third-order control system.

Since the poles of the transfer function are roots of the characteristic equation, they control the transient response of the system directly. Consider the closed loop transfer function

$$\frac{Y(s)}{R(s)} = \frac{\omega_n^2}{(s^2 + 2\xi\omega_n s + \omega_n^2)(1 + T_p s)} \tag{4.41}$$

Where the term $(1+T_p s)$ is added to a second-order transfer function. As we said before the zeros of transfer function are also important. If we look at the closed loop transfer function of the PMSM model we can see that there is a zero at origin and this zero will be an undesirable zero for the system. Thus, in achieving satisfactory time-domain performance of control system we should place the pole $s = \frac{-1}{T_p}$ near origin in order to cancel these undesirable pole and zero. As this pole is moved toward the origin in the s-plane, the rise time increase and the maximum overshoot decreases.

Thus, it is important to choose system parameters properly to make a sensible response for the model.

Figure 4.6 shows the unit-step responses of a second-order system for various values of ζ. As seen, the response becomes more ascillatory with larger overshoot as ζ decreases. When $\zeta \geq 1$, the step response does not exhibit any overshoot; that is, y (t) never exceeds its final value during the transient. The responses also show that ω_n has a direct effect on the rise time, delay time and settling time, but does not affect the overshoot. In ideal systems ζ is chosen between 0.5 and 0.7

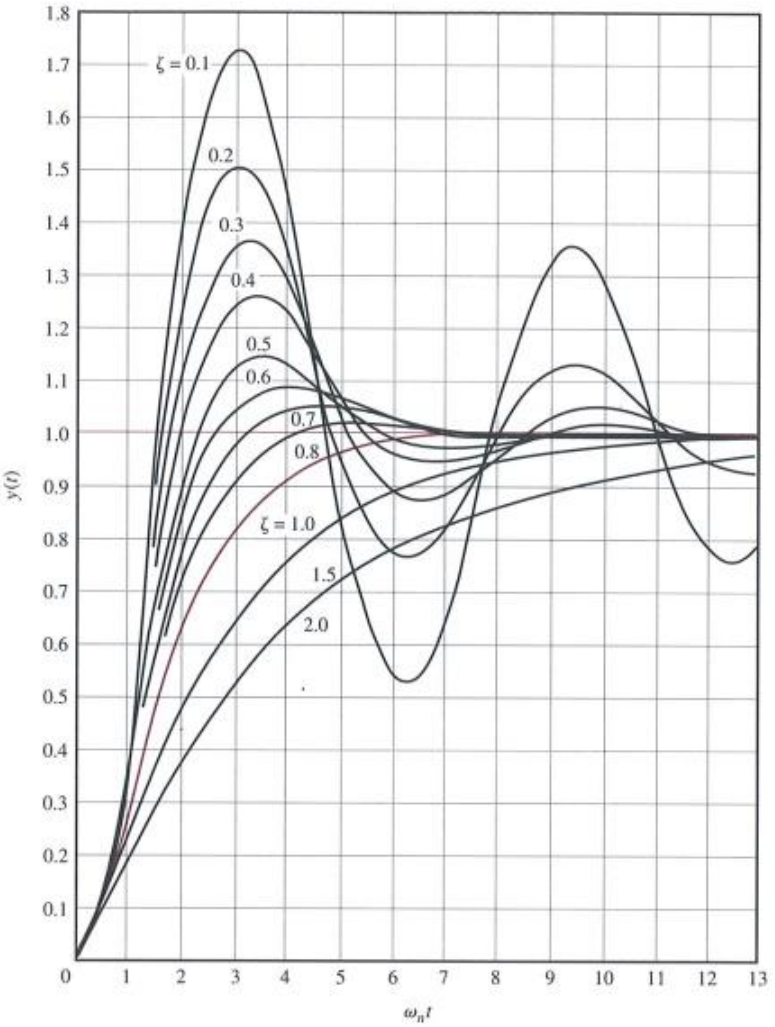

Figure 4.6 : Unit-step responses of a second order system with various damping ratio

The closed loop transfer function in equation (4.41) is written

$$\frac{Y(s)}{R(s)} = \frac{\omega_n^2}{T_p s^3 + (1 + 2T_p \xi\omega_n)s^2 + (2\xi\omega_n + T_p\omega_n^2)s + \omega_n^2} \tag{4.42}$$

$$\frac{Y(s)}{R(s)} = \frac{\frac{\omega_n^2}{T_p}}{s^3 + \frac{1 + 2T_p\xi\omega_n}{T_p}s^2 + \frac{2\xi\omega_n + T_p\omega_n^2}{T_p}s + \frac{\omega_n^2}{T_p}} \tag{4.43}$$

Characteristic equation of the closed loop transfer function in equation (4.43) will be as follow

$$s^3 + \frac{1 + 2T_p\xi\omega_n}{T_p}s^2 + \frac{2\xi\omega_n + T_p\omega_n^2}{T_p}s + \frac{\omega_n^2}{T_p} \tag{4.44}$$

For the position servo control system we should specify the system parameters for the model. In ideal systems ζ is chosen between 0.5 and 0.7

Here the system is designed by choosing $\xi = 0.5$ and a settling time about $t_s = 0.64(s)$.

Also T_p should be chosen too. The system has a pole at $s = \frac{-1}{T_p}$. As the value of T_p increases, this pole moves closer to the origin beside the zero in the s-plane and cancel each other. By choosing $T_p = 5$ the system behaves properly.

Threfore, the following parameters is chosen for the system.

Table 4.2 : Parameteres of the system

System parameteres	Symbols	Values
Damping factor	ζ	0.5
Settling time	t_s	0.64 s
Adding a pole	$s = -1 / T_p$	-0.2

$\zeta = 0.5 \Rightarrow \Phi = \cos^{-1}(0.5) = 60$

We can approximate the settling time for the prototype second-order system as

$$t_s \cong \frac{3.2}{\xi\omega_n} \; ; \; 0 < \zeta < 0.69 \tag{4.45}$$

$$\omega_n \cong \frac{3.2}{t_s\xi} = 10 \tag{4.46}$$

by putting the values of ω_n = 10, ζ = 0.5, t_s = 0.64 (s), T_p = 5 in the charactetristic equation of (4.44), the characteristic equation of the system will be as follow

$$s^3 + 10.2s^2 + 102s + 20 \tag{4.47}$$

$$s^3 + 10.2s^2 + 102s + 20 = (s^2 + 10s + 100)(s + 0.2) \tag{4.48}$$

Poles of the system : $s_{1,2} = -5 \pm 8.66\,j$, $s_3 = -0.2$ (4.49)

Undesired pole of $s_3 = -0.2$ will be cancelled by the zero of the closed loop transfer function of PMSM model. Thus, only desired dominant poles will remain.

4.3.5 Design of gains for PID and PD controllers

In this section, the PID and PD controllers that produce a maximum current i* as the torque current reference are designed.

In order to find the coefficients of K_p, K_i and K_d of the PID controllers, the characteristic equations of the designed system, (4.47), and the two PMSM models, (4.36),(4.37) should be considered equal.

$$s^3 + \frac{2.288 + 4.5K_{d1}}{2.351}s^2 + \frac{4.5K_{p1}}{2.351}s + \frac{4.5K_{i1}}{2.351} = s^3 + 10.2s^2 + 102s + 20 \tag{4.50}$$

$$s^3 + \frac{0.006 + 1.5K_{d2}}{0.1119}s^2 + \frac{1.5K_{p2}}{0.1119}s + \frac{1.5K_{i2}}{0.1119} = s^3 + 10.2s^2 + 102s + 20 \tag{4.51}$$

Thus, the coefficients of PID controllers for PMSMs is calculated as

PMSM 1
$$\begin{aligned} K_{p1} &= 53.29 \\ K_{i1} &= 10.45 \\ K_{d1} &= 4.82 \end{aligned} \tag{4.52}$$

PMSM 2
$$\begin{aligned} K_{p2} &= 7.61 \\ K_{i2} &= 1.49 \\ K_{d2} &= 0.76 \end{aligned} \tag{4.53}$$

In order to find the coefficients of K_p and K_d of the PD controllers, the characteristic equations of the second-order system and the two PMSM models, (4.38) and (4.39) should be considered equal.

$$s^2 + \frac{2.288 + 4.5K_{d1}}{2.351}s + \frac{4.5K_{p1}}{2.351} = s^2 + 2\xi\omega_n s + \omega_n^2 = s^2 + 10s + 100 \tag{4.54}$$

$$s^2 + \frac{0.006 + 1.5K_{d2}}{0.1119}s + \frac{1.5K_{p2}}{0.1119} = s^2 + 2\xi\omega_n s + \omega_n^2 = s^2 + 10s + 100 \tag{4.55}$$

PMSM 1
$$\begin{aligned} K_{p1} &= 52.24 \\ K_{d1} &= 4.72 \end{aligned} \tag{4.56}$$

PMSM 2
$$\begin{aligned} K_{p2} &= 7.46 \\ K_{d2} &= 0.74 \end{aligned} \tag{4.57}$$

CHAPTER 5. TWO DEGREE OF FREEDOM (2DOF) DIRECT DRIVE ROBOT (DDR) DRIVEN BY PMSM

5.1 Introduction

Actuation of joint motions is entrusted to motors which allow realizing a desired motion for the mechanical system. The most employed motors in robotic applications are the electric servomotors. Among them, the most popular are the permanent magnet direct current (dc) servomotors and the brushless dc servomotors, in view of their good control flexibility.

As an challenging example of robotic configurations exposed to load uncertainties, a two degree of freedom (2DOF) direct drive robot is considered. Three controllers are developed for the position and trajectory control of the arm; namely, PID and PD controllers as standard linear controllers that are designed in chapter four, PD+ as a nonlinear model based controller that is designed in this chapter.

5.2 Industrial robot

The term automation denotes a technology aimed at replacing human beings with machines in a manufacturing process.

The industrial robot is a machine with significant characteristics of versatility and flexibility. According to the widely accepted definition of the Robot Institute of America, a robot is a reprogrammable multifunctional manipulator designed to move materials, parts, tools or specialized devices through variable programmed motions for the performance of a variety of tasks.

Industrial robots present three fundamental capacities that make them useful for a manufacturing process : material handling, manipulation, and measurement.

Material handling : The robot’s capacity to pick up an object, move it in space on predefined paths and release it.

Manipulation : The robot's capacity to manipulate both objects and tools make it suitable to be employed for manufacturing.

Measurement : The robot's capacity to explorethe three-dimensional space together with the availability of measurements on the manipulator's status allow using a robot as a measuring device.

5.2.1 Components of an industrial robot

An industrial robot is constituted by :

- Manipulator that consists of a sequence of rigid bodies (links) connected by means of articulations (joints); a manipulator is characterized by an arm that ensures mobility, a wrist that confers dexterity, and an end effector that performs the task required of the robot.
- Actuators that set the manipulator in motion through actuation of the joints; the motors employed are typically electric and hydraulic, and occasioally pneumatic.
- Sensors that measure the status of the manipulator.
- A control system (computer) that enables control and supervision of manipulator motion.

5.2.2 Manipulator structure

Manipulator's mobility is ensured by the presence of joints. The articulation between two consecutive links can be realized by means of either a prismatic or a revolute joint.

A prismatic joint realizes a relative translational motion between the two links, whereas a revolute joint realizes a relative rotational motion between the two links. Revolute joints are usually preferred to prismatic joints in view of of their compactness and reliability.

The degrees of mobility shall be properly distributed along the mechanical structure in order to provide the degrees of freedom required for the excecution of a given task. In the most general case of a task consisting of arbitrarily positioning and orienting an object in the three-dimensional space, six are the required degrees of

freedom, three for positioning a point on the object and three for orienting the object with respect to a reference coordinate frame.

As an example of a six degree of freedom robot manipulator, PUMA 560 manipulator is shown in figure 5.1, which is a popular robot manipulator used in industries.

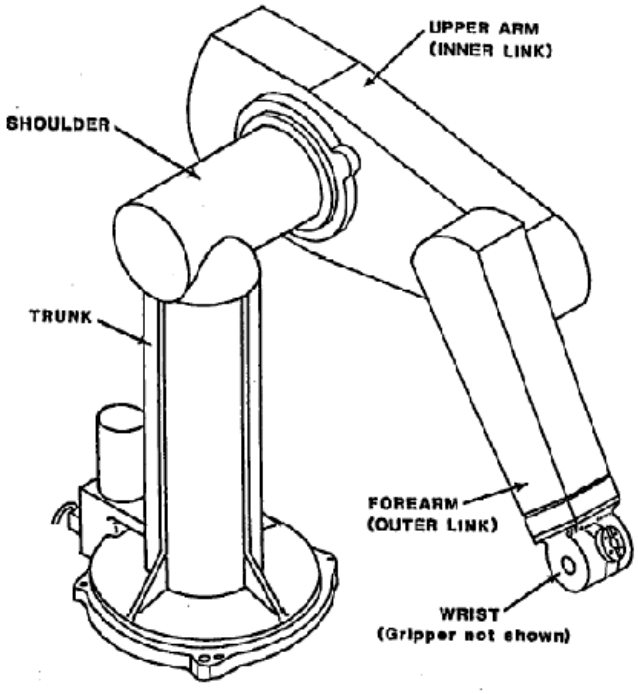

Figure 5.1 : A six degrees of freedom PUMA 560 manipulator.

(Source:http://www.seas.upenn.edu)

5.3 Control problem of robot manipulators and a brief literature review

The position and tracking control problem of robot manipulators involves development of algorithms to make the end-effector track a desired trajectory with minimum error in spite of structured and unstructured uncertainties and external disturbances. In the literature, a variety of control techniques have been developed to address the problem. Linear controllers are mostly based on PD and PID controllers, which is the widely used approach with industrial robots.

For more sophisticated applications and high performance goals, the nonlinear dynamics of the system has to be taken into account when designing control algorithms. Nonlinear control methods can be achieved by model-based control algorithms on a direct-drive robotic arm. Various model-based control algorithms

can be used for the purpose like computed torque control, PD+ control, PD control with computed feedforward and PD control.

The first comparison of control algorithms on a direct-drive arm was reported in 1983 by Asada et al. [12].

The linear PD controller and its combination with feedforward compensation were implemented on the Direct-Drive Arm I. Further experiments conducted on the Direct-Drive Arm I were described in the book by Asada and Youcef-Toumi [13].

In studies taking the dynamics model of the system into consideration, such as [Reyes and Kelly, 2000] in [11], it has been demonstrated through experiments that model-based methods achieved better performance than the PID control.

A closed-chain direct-drive arm was used by Lu et al. [16] to implement four control algorithms including the PD control, computed torque control and the PD control plus feedforward. The model-based control methods appeared to be the best as compared to the independent joint PD and PID controllers.

5.4 Control of 2DOF planar arm manipulator

Control methods in robotics can be classified by two basic approaches; independent joint control (IJC) and model based control (MBC).

The independent joint control approach considers each joint independently as a single-input/single-output system but the model based control takes the full arm dynamic model into consideration in the design of the control input.

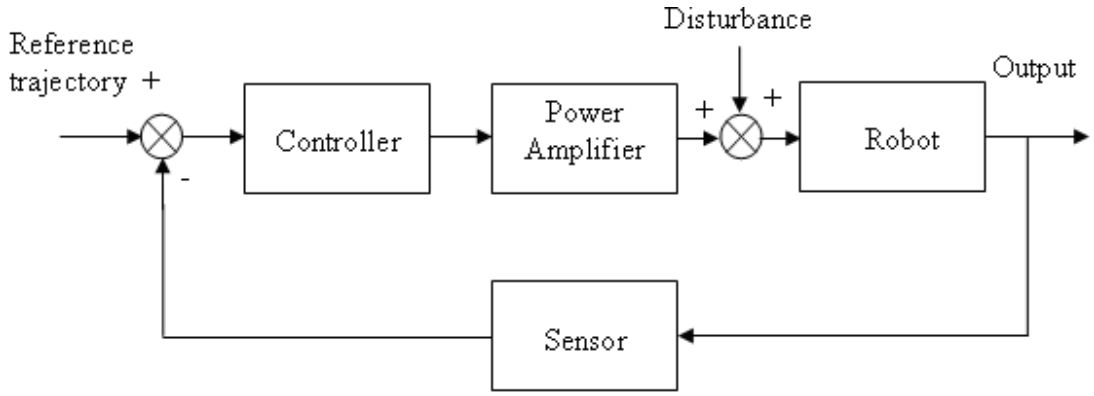

Figure 5.2 : Single-input/single-output feedback control system.

The block diagram of the single-input/single-output system under consideration is shown in the figure 5.2.

With this approach, the robot control problem is converted to the problem of joint actuator control with arm dynamics taken into consideration as a disturbance.

The basic aim of the control input is to make the plant follow a desired output for a given reference signal. However, the disturbance effects influencing the system performance should also be taken into consideration. Therefore, a controller must be designed in such a way that the reference trajectory tracking is achieved, while also compensating for the effect of the disturbances acting on the system.

Figure. 5.3 demonstrate the schematic diagrams of the 2DOF closed loop control system.

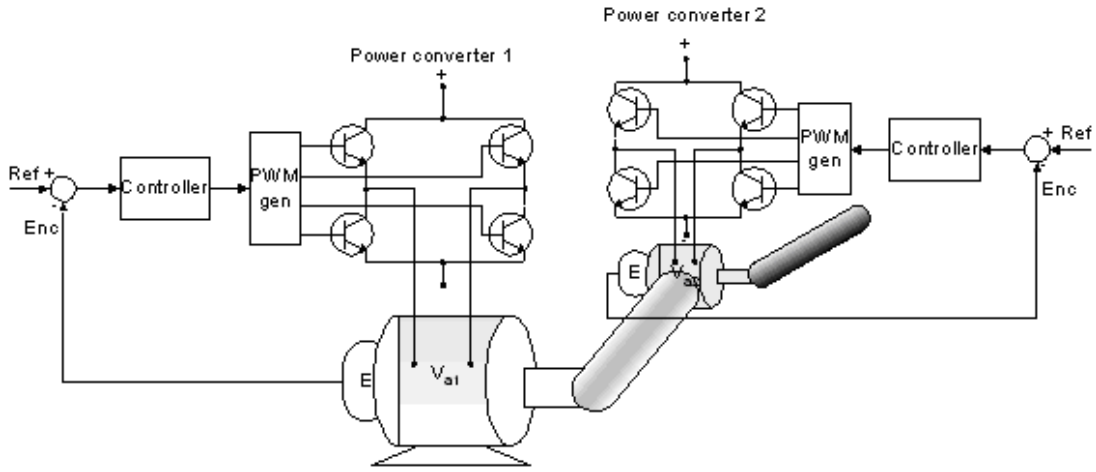

Figure 5.3 : Schematic of 2DOF system with closed loop control

5.4.1 Independent Joint Control with PID and PD controllers

The simplest control strategy that can be thought of is one that regards the manipulator as formed by n independent systems (the n joints) and controls each joint axis as a single-input/single-output system. Coupling effects between joints due to varying configuration during motion are treated as disturbance inputs.

Figure 5.4 gives the simplified block diagram used in the control design.
We used this simplified block diagram in 4.3.1 and 4.3.2 of chapter four for PID and PD controller and obtained the closed loop transfer functions of the two joints.

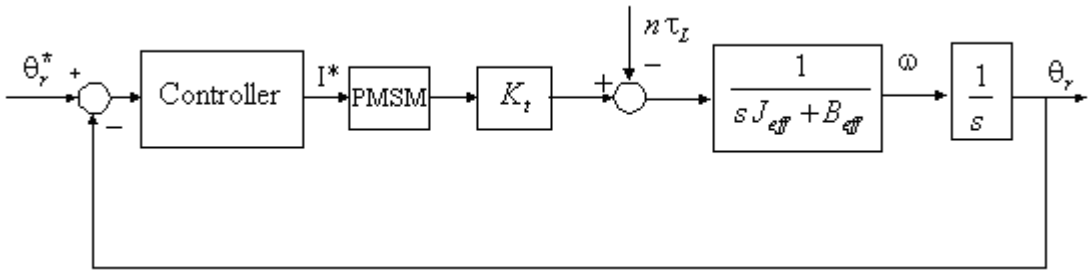

Figure 5.4 : Simplified version of closed loop control

After analyzing the system in terms of ζ (damping ratio) and ω_n (undamped natural frequency), we found the PID and PD controller gains by root locus analysis.

In order to have accurate position we should regulate the model with suitable K_p, K_i and K_d coefficients of the controllers. The boundary values on K_p and K_d can help us to play with the gains to regulate the controllers for accurate position.

K_p is chosen such that it ensures: $\omega_n \leq 0.5\omega_r$

ω_r : lowest structural frequency in the system

The boundary values on K_p and K_d are determined as follows [Bogosyan, Robot Control, lecture notes, 2004]:

$$0 < K_p \leq \frac{\omega_r^2 \, J_{eff}}{4 K_t} \tag{5.1}$$

$$K_d \geq \frac{2\sqrt{K_t \, K_p \, J_{eff}} - B_{eff}}{K_t} \tag{5.2}$$

Here, J_{eff} is the effective inertia, which includes the motor inertia and relation of that to the two links. B_{eff} is the effective friction, which is the sum of motor viscous friction and linear frictional terms of the load.

In this study the following gains of PID and PD controllers were regulated by helping boundary values.

$$\text{PID :} \quad \begin{matrix} K_{p1} = 35 \\ K_{i1} = 30 \\ K_{d1} = 5 \end{matrix} \quad , \quad \begin{matrix} K_{p2} = 15 \\ K_{i2} = 1.05 \\ K_{d2} = 0.4 \end{matrix} \tag{5.3}$$

$$\text{PD :} \quad \begin{matrix} K_{p1} = 35 \\ K_{d1} = 5 \end{matrix} \quad , \quad \begin{matrix} K_{p2} = 15 \\ K_{d2} = 0.4 \end{matrix} \tag{5.4}$$

As it is well-known, the PD control gives rise to a zero steady-state error for a step-type input, with Type 1 systems. Consequently, considering the fact that the position control of the joint actuator gives rise to a Type 1 system, the steady-state error would be zero for set-point position control. However, when the effect of link dynamics is also taken into account, a steady-state

$$e_{\infty} \approx \frac{T_L}{K_p} \tag{5.5}$$

will occur. Thus, in the best case of constant disturbance (which is true in our set-point position control), the PD control will give rise to a constant steady-state error. As a solution, an integral term is added to the PD controller and thus, a PID (proportional-integral-derivative) controller is obtained. With integral control, the steady-state error due to step-type disturbances will be made zero.

5.4.2 Model-based controller (PD+)

A PD+ controller consists of a standard PD controller combined with the robot dynamics, which is assumed to be known.

In this study, a PD+ controller is used and K_p , K_d are $n \times n$ matrices (Proportional and Derivative gain matrices, respectively). The control algorithm against which all controllers are measured is the Proportional-Drivetive controller. This controller labled τ_{pd+} , is given by [11,14,15] : $\tilde{q} = q_r * - q_r$, $\dot{\tilde{q}} = \dot{q}_r * - \dot{q}_r$

$$\tau_{pd+} = K_p \tilde{q} + K_d \dot{\tilde{q}} + B(q_r)\ddot{q}_r + C(q_r, \dot{q}_r)\dot{q}_r + g(q_r) + f(\dot{q}_r) \tag{5.6}$$

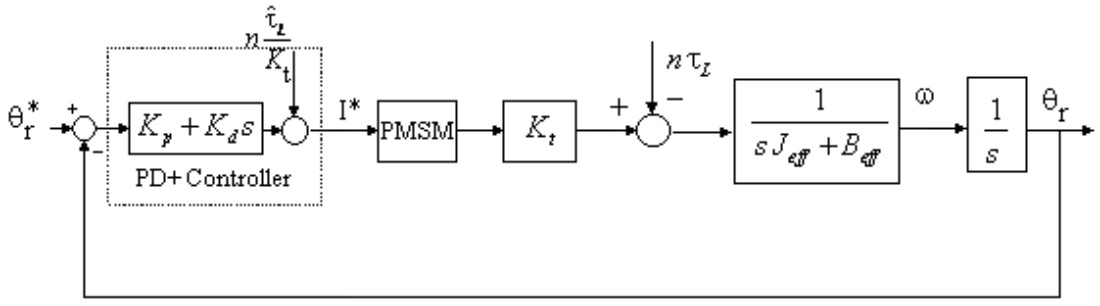

Figure 5.5 : Closed loop system with PD+ controller

The first two terms on the right-hand side of (5.6) represent a PD controller, while the remaining deponds on the robot dynamics. It has been proven in the literature that

under exact robot and friction models, and symmetric positive definite matrices K_p and K_d, the PD+ controller provides asymptotically exact tracking without exact linearization. [Whitcomb, 1993].

This controller is perhaps the simplest and popular control scheme used to solve the point-to-point robot control.

5.5 Experimental arm system description

The experimental set-up built at CICESE Research Center consists of a direct-drive vertical robot arm with 2 dof whose rigid links are joined with revolute joints as shown in figure 5.6, [11].

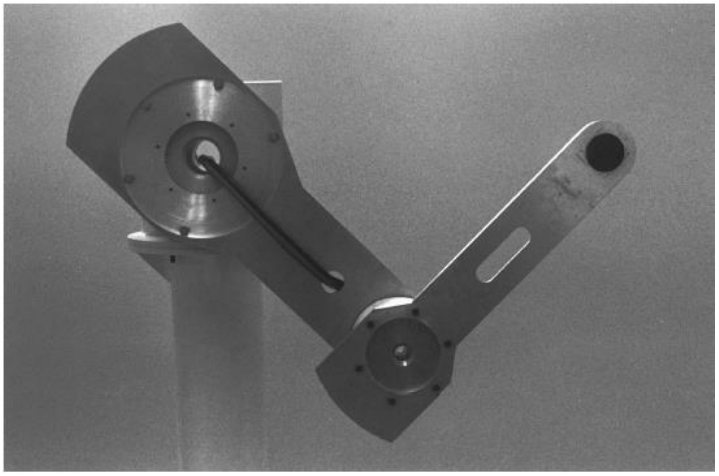

Figure 5.6 : Experimental arm

Both links made of 6061 aluminum are 0.45 long, and they are actuated by brushless direct-drive servo actuator to drive the joints without gear reduction. Position information is obtained from incremental encoders located on the motors [11].

Table 5.1 : Parameters of robot arm

Parameters of robot arm	Notation	Values	Unit
Length link 1	l_1	0.45	m
Length link 2	l_2	0.45	m
Mass link 1	m_1	23.902	kg
Mass link 2	m_2	1.285	kg
Link (1) center of mass	l_{c1}	0.522	$kg.m^2$
Link (2) center of mass	l_{c2}	1.266	$kg.m^2$
Gravity acceleration	g	9.81	m/s^2

5.6 Dynamic model of a two-link planar arm

Robot dynamics deals with the calculation of forces/torques, which are required to cause motion. Robot manipulators are basically positioning devices. In order to move or place an object by the end-effector, the joint actuators of a manipulator should be given a set of torque/force functions. This set of torque/force functions can be obtained by formulating dynamic equations of the manipulator.

Consider the two-link planar arm in figure 5.7. Let l_1, l_2 be the lengthes of the two links, and l_{c1}, l_{c2} be the distances of the centres of mass of the two links from the respective joint axes. Let also m_1, m_2 be the masses of two links. Finally, let I_1, I_2 be the moments of inertia relative to the centres of mass of the two links.

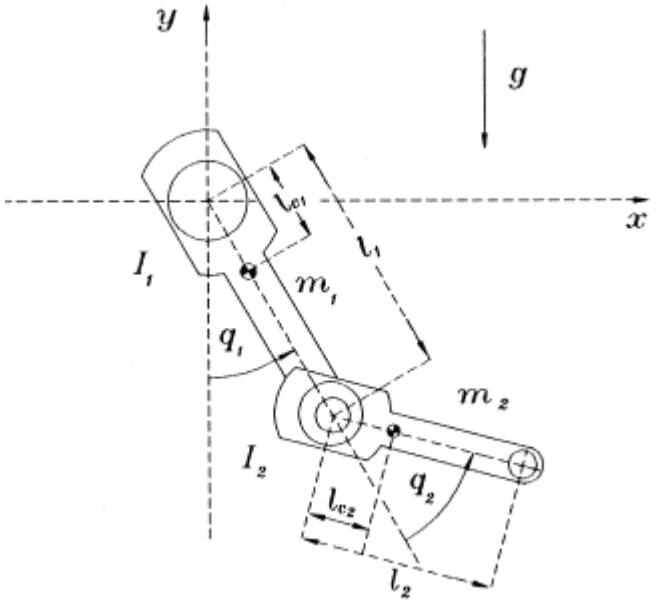

Figure 5.7 : 2-DOF planar arm

The dynamics of a serial n-link rigid robot can be written as :

$$B(q)\ddot{q} + C(q,\dot{q})\dot{q} + g(q) + f(\dot{q}) = \tau \tag{5.7}$$

Where q is the $n \times 1$ vector of joint displacements, $\dot{q}$ is the $n \times 1$ vector of joint velocities, τ is the $n \times 1$ vector of applied torque inputs, $B(q)$ is the $n \times n$ symmetric positive definite manipulator inertia matrix, $C(q,\dot{q})$ is the $n \times n$ matrix of centripetal and Coriolis torques, $g(q)$ is the $n \times 1$ vector of gravitational torques, and $f(\dot{q})$ stands for the $n \times 1$ vector of friction torques.

For two-link planar arm, n = 2;

$$\begin{bmatrix}\tau_1\\ \tau_2\end{bmatrix}_{2\times1} = [B(q)]_{2\times2}\begin{bmatrix}\ddot{q}_1\\ \ddot{q}_2\end{bmatrix}_{2\times1} + [C(q,\dot{q})]_{2\times2}\begin{bmatrix}\dot{q}_1\\ \dot{q}_2\end{bmatrix}_{2\times1} + [g(q)]_{2\times1} + [f(\dot{q})]_{2\times1} \tag{5.8}$$

We can obtain the following equations for the robot dynamics [10].

$$B(q) = \begin{bmatrix} b_{11} & b_{12} \\ b_{21} & b_{22} \end{bmatrix} \tag{5.9}$$

$$b_{11} = \{ I_1 + m_1 l_{c1}{}^2 + I_2 + m_2 [(l_1 + l_{c2})^2 + l_{c2}{}^2 + 2(l_1 + l_{c2}) l_{c2} \cos(q_2)]\} \tag{5.10}$$

$$b_{12} = b_{21} = \{ I_2 + m_2 [l_{c2}{}^2 + (l_1 + l_{c2}) l_{c2} \cos(q_2)]\} \tag{5.11}$$

$$b_{22} = I_2 + m_2 l_{c2}{}^2 \tag{5.12}$$

$$C(q,\dot{q}) = \begin{bmatrix} c_{11} & c_{12} \\ c_{21} & c_{22} \end{bmatrix} \tag{5.13}$$

$$c_{11} = -m_2 (l_1 + l_{c2}) l_{c2} \sin(q_2) \dot{q}_2 \tag{5.14}$$

$$c_{12} = -m_2 (l_1 + l_{c2}) l_{c2} \sin(q_2) (\dot{q}_1 + \dot{q}_2) \tag{5.15}$$

$$c_{21} = m_2 (l_1 + l_{c2}) l_{c2} \sin(q_2) \dot{q}_1 \tag{5.16}$$

$$c_{22} = 0 \tag{5.17}$$

$$N(q,\dot{q}) = \dot{B}(q) - 2C(q,\dot{q}) = \begin{bmatrix} n_{11} & n_{12} \\ n_{21} & n_{22} \end{bmatrix} : \text{Skew-symmetry of Matrix } \dot{B} - 2C \tag{5.18}$$

$$n_{11} = 0 \ , \quad n_{22} = 0 \tag{5.19}$$

$$n_{12} = 2m_2 (l_1 + l_{c2}) l_{c2} \sin(q_2) \dot{q}_1 + m_2 (l_1 + l_{c2}) l_{c2} \sin(q_2) \dot{q}_2 \tag{5.20}$$

$$n_{21} = -2m_2 (l_1 + l_{c2}) l_{c2} \sin(q_2) \dot{q}_1 - m_2 (l_1 + l_{c2}) l_{c2} \sin(q_2) \dot{q}_2 \tag{5.21}$$

$$g(q) = \begin{bmatrix} G_1 \\ G_2 \end{bmatrix} \tag{5.22}$$

$$G_1 = [\, m_1 l_{c1} + m_2 (l_1 + l_{c2}) \,]\, g \sin(q_1) + m_2 l_{c2} g \sin(q_1 + q_2) \tag{5.23}$$

$$G_2 = m_2 l_{c2} g \sin(q_1 + q_2) \tag{5.24}$$

$$f(\dot{q}) = \begin{bmatrix} b_1 \dot{q}_1 + f_{c1} sign(\dot{q}_1) \\ b_2 \dot{q}_2 + f_{c2} sign(\dot{q}_2) \end{bmatrix} \tag{5.25}$$

In the absence of friction and tip contact forces, the resulting equations of motion are

$$\begin{aligned} \tau_1 = {} & \{ I_1 + m_1 l_{c1}^{\,2} + I_2 + m_2 [\, (l_1 + l_{c2})^2 + l_{c2}^{\,2} + 2(l_1 + l_{c2}) l_{c2} \cos(q_2) \,] \} \ddot{q}_1 \\ & + \{ I_2 + m_2 [\, l_{c2}^{\,2} + (l_1 + l_{c2}) l_{c2} \cos(q_2) \,] \} \ddot{q}_2 \\ & - 2 m_2 (l_1 + l_{c2}) l_{c2} \sin(q_2) \dot{q}_1 \dot{q}_2 - m_2 (l_1 + l_{c2}) l_{c2} \sin(q_2) \dot{q}_2^{\,2} \\ & + [\, m_1 l_{c1} + m_2 (l_1 + l_{c2}) \,]\, g \sin(q_1) + m_2 l_{c2} g \sin(q_1 + q_2) \end{aligned} \tag{5.26}$$

$$\begin{aligned} \tau_2 = {} & \{ I_2 + m_2 [\, l_{c2}^{\,2} + (l_1 + l_{c2}) l_{c2} \cos(q_2) \,] \} \ddot{q}_1 + [\, I_2 + m_2 l_{c2}^{\,2} \,] \ddot{q}_2 \\ & + m_2 (l_1 + l_{c2}) l_{c2} \sin(q_2) \dot{q}_1^{\,2} + m_2 l_{c2} g \sin(q_1 + q_2) \end{aligned} \tag{5.27}$$

Regarding the nonconservative forces doing work at the manipulator joints, these are given by the actuation tores τ minus the viscous friction torques $F_v . \dot{q}$ and the static friction torques $f_s(q, \dot{q})$.

$$B(q)\ddot{q} + C(q, \dot{q})\dot{q} + g(q) = \tau - F_v . \dot{q} - F_s . sign(\dot{q}) \tag{5.28}$$

In this study the static friction torques is considered zero.

We can write the system model in the matrix form as below;

$$\begin{bmatrix} B_{11}+B_{11}(q_2) & B_{12}(q_2) \\ B_{12}(q_2) & B_{22} \end{bmatrix}\begin{bmatrix} \ddot{q}_1 \\ \ddot{q}_2 \end{bmatrix}+\begin{bmatrix} C_{11}(q_2)\dot{q}_2 & C_{12}(q_2)\dot{q}_2 \\ C_{21}(q_2)\dot{q}_1 & 0 \end{bmatrix}\begin{bmatrix} \dot{q}_1 \\ \dot{q}_2 \end{bmatrix}+\begin{bmatrix} G_1(q_1,q_2) \\ G_2(q_1,q_2) \end{bmatrix}+$$

$$\begin{bmatrix} B_{m1} & 0 \\ 0 & B_{m2} \end{bmatrix}\begin{bmatrix} \ddot{q}_1 \\ \ddot{q}_2 \end{bmatrix}=\begin{bmatrix} \tau_1 \\ \tau_2 \end{bmatrix} \tag{5.29}$$

Separating the linear and nonlinear terms of inertia, the equation (3.15) can be written as;

$$\begin{bmatrix} B_{11} & 0 \\ 0 & B_{22} \end{bmatrix}\begin{bmatrix} \ddot{q}_1 \\ \ddot{q}_2 \end{bmatrix}+\begin{bmatrix} B_{m1} & 0 \\ 0 & B_{m2} \end{bmatrix}\begin{bmatrix} \ddot{q}_1 \\ \ddot{q}_2 \end{bmatrix}=\begin{bmatrix} \tau_1 \\ \tau_2 \end{bmatrix}-$$

$$\left\{\begin{bmatrix} B_{11}(q_2) & B_{12}(q_2) \\ B_{12}(q_2) & 0 \end{bmatrix}\begin{bmatrix} \ddot{q}_1 \\ \ddot{q}_2 \end{bmatrix}+\begin{bmatrix} C_{11}(q_2)\dot{q}_2 & C_{12}(q_2)\dot{q}_2 \\ C_{21}(q_2)\dot{q}_1 & 0 \end{bmatrix}\begin{bmatrix} \dot{q}_1 \\ \dot{q}_2 \end{bmatrix}+\begin{bmatrix} G_1(q_1,q_2) \\ G_2(q_1,q_2) \end{bmatrix}\right\} \tag{5.30}$$
$$\tau_L$$

As you can see in figure 5.5 the PD+ current control input can be represented as;

$$u = K_p(q_r{}^* - q_r) + K_d(\dot{q}_r{}^* - \dot{q}_r) + \frac{n\hat{\tau}_L}{K_t} \tag{5.31}$$

where *u* is the control current input; $\hat{\tau}_L$ is the load torque; the symbol '^' represents the calculated value of the load torque and K_t is motor torque constant and n is the gear ratio. In direct-drive robot arm model the gear ratio is considered one. Now, we can write the control current inputs for each joint actuator;

$$u_1 = K_{p1}(q_{r1}{}^* - q_{r1}) + K_{d1}(\dot{q}_{r1}{}^* - \dot{q}_{r1}) +$$
$$n\left[\frac{\hat{B}_{11}(q_2)\ddot{q}_1 + \hat{B}_{12}(q_2)\ddot{q}_2 + \hat{C}_{11}(q_2)\dot{q}_2\dot{q}_1 + \hat{C}_{12}(q_2)\dot{q}_2^2 + \hat{G}_1(q_1,q_2)}{K_{t1}}\right] \tag{5.32}$$

$$u_2 = K_{p2}(q_{r2}{}^* - q_{r2}) + K_{d2}(\dot{q}_{r2}{}^* - \dot{q}_{r2}) + n\left[\frac{\hat{B}_{12}(q_2)\ddot{q}_1 + \hat{C}_{21}(q_2)\dot{q}_1^2 + \hat{G}_2(q_1,q_2)}{K_{t2}}\right] \tag{5.33}$$

CHAPTER 6. SIMULATION OF 2DOF DIRECT DRIVE ROBOT BY USING MATLAB/SIMULINK SOFTWARE PACKAGE

6.1 Modeling the system in Matlab with version 6.5

Figure 6.1 shows the main model of position control system of the two-link planar arm. This model is simulated in Matlab of version 6.5. This version consists of a great and powerful tool boxes in simulink library browser. Required tool boxes can be choosed from this window.

After finishing the design, we will have a model like figure 6.1.

6.2 Circuit description

By looking at the model we can see that two PMSM models are used as a shoulder and an elbow of the two-link planar arm. These PMSMs are actuating the joints and the torques of these two PMSMs are the torques that we calculated in chapter 5 as τ_1 and τ_2 of our two-link planar arm.

By double-clicking on function blocks of gravity, acceleration and Coriolis of two PMSMs model we can define the equations (5.22) and (5.23) for the function blocks.

These two PMSMs models are designed and simulated by us at Matlab/Simulink programme.

Some tool boxes like PMSM block, machines measurement, IGBT and PWM generator are ready tool boxes that we can get them directly from the simulink library browser window especially “simpowersystems” block-sets and some of the blocks is designed by us.

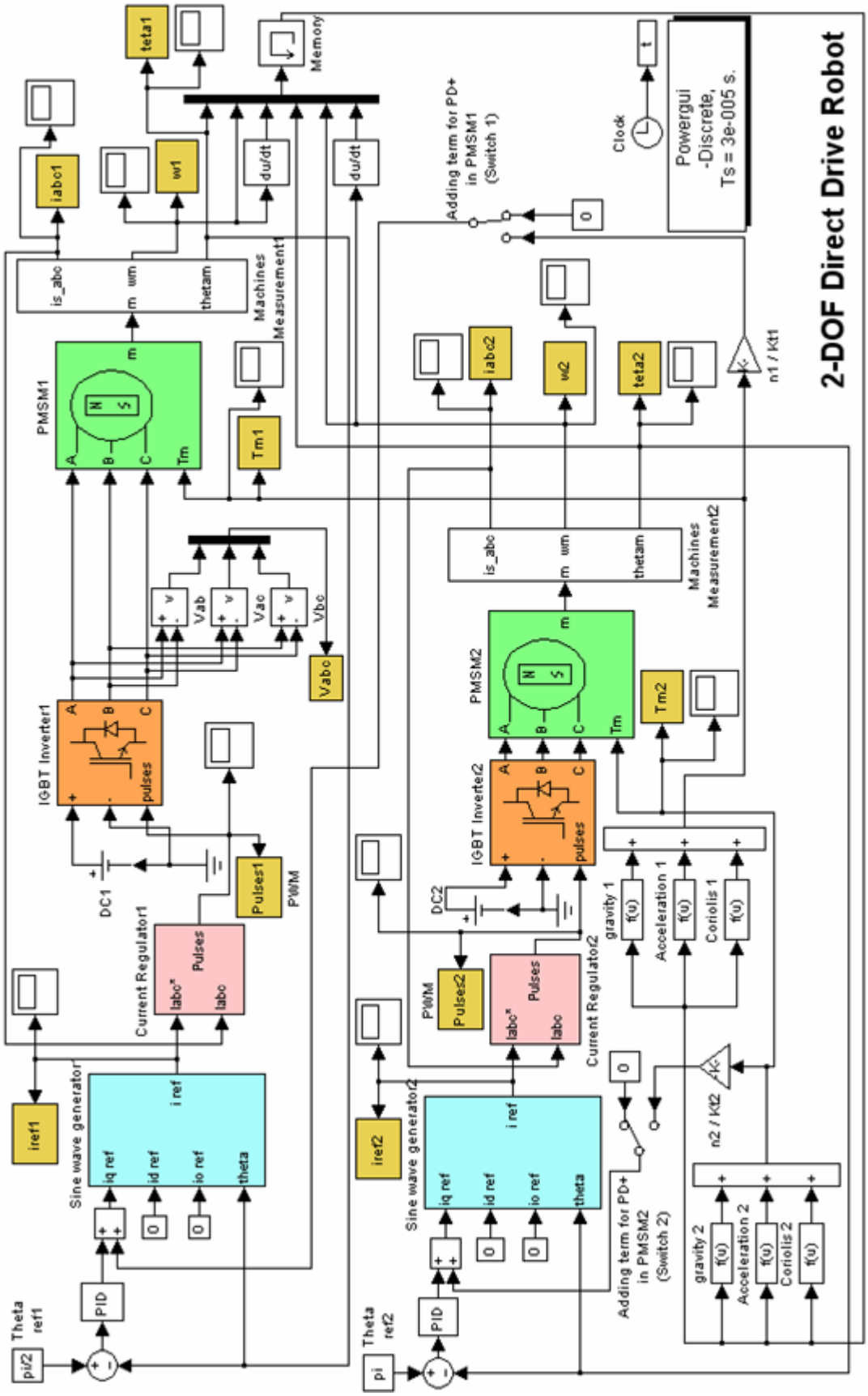

Figure 6.1 : 2-DOF direct drive robot model

Three-phase PMSMs with the parameteres of Table 4.1 is fed by an IGBT inverter. By double-clicking on the two PMSMs blocks we can enter the motor parameteres

Required pulses for switching the IGBT transistors are produced by a PWM generator. PWM generator receives the reference alternating currents and converts them into pulses of width proportional to the amplitude of the alternating currents. The PWM switching procedure of the current controller in the system is represented with a hysterisis function in the model.

Sine wave generator block produces the reference alternating currents. In chapter four we understood that stator currents can be obtained by inverse Park's transformation matrix.

$$I_{abcs} = (K^{r}_{qdo})^{-1} (\Theta r) * I_{qdos} \tag{6.1}$$

$$\begin{bmatrix} i_{as} \\ i_{bs} \\ i_{cs} \end{bmatrix} = \begin{bmatrix} \cos\theta & \sin\theta & 1 \\ \cos(\theta-120) & \sin(\theta-120) & 1 \\ \cos(\theta+120) & \sin(\theta+120) & 1 \end{bmatrix} \begin{bmatrix} i_q \\ i_d \\ i_o \end{bmatrix} \tag{6.2}$$

Therefore, in the sine wave generator block the above equations should be considered.

If we look at inside the sine wave generator by double-clicking on the block in the model,

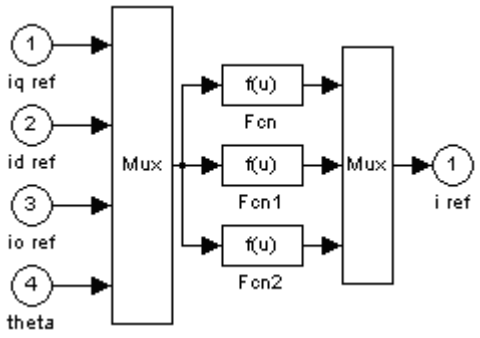

Figure 6.2 : Inside the sine wave generator block

We can see that i_q, i_d, i_o and Θ are the inputs of the block and after producing motor's stator currents i_{as}, i_{bs},i_{cs} according to the inverse park's transformation, in the output there are three alternating currents with 120 degree differences as the reference currents that provided into the PWM block. By double-clicking on each of the function blocks we can constitute the equation (6.2) in to the blocks.

By looking at the model, you can see that two control loops are used.

The inner loop regulates the motor's stator currents. The outer loops controls the motor position.

In the outer loop, the desired reference Θ_r^* and the Θ_r comes from the feedback compared and the error is sent to a PID controller for converting it to a maximum motor torque current demand as $i_{q\ ref}$ in the model.

$i_{d\ ref}$ and $i_{o\ ref}$ should be zero because in existing torque equation that said in equation (4.10) in chapter 4 we had the following equation

$$T_e = (3/2).p.[\ I_q.\Phi_m + (L_d - L_q).I_q.I_d\ ] \qquad (6.3)$$

In our PMSM parameteres $L_q = L_d =$ 0.01 H. Then the second term will be zero and the torque only deponds on I_q not on I_d and I_o. In addition to above equation usually because of the small inductance in PMSMs I_d and I_o is considered zero.

Machines measurement block near the PMSM block is for measuring the required information that we need from the motor. If you open the block by double-clicking on it you can choose any information of the motor's output that you want.

Angular position of the motor (Θ_r) is produced by some pulses that sent by an incremental encoder. These pulses should be agreement with the pole of thePMSMs.

PID, PD and PD+ gains that obtained by designing are entered by double-clicking on the PID blocks in the model.

Table 6.1 : Controller gains of the robot

Controllers	Gains of PMSM 1	Gains of PMSM 2
PID	$K_{p1} = 35$ $K_{i1} = 30$ $K_{d1} = 5$	$K_{p2} = 15$ $K_{i2} = 1.05$ $K_{d2} = 0.4$
PD	$K_{p1} = 35$ $K_{d1} = 5$	$K_{p2} = 15$ $K_{d2} = 0.4$
PD+	$K_{p1} = 35$ $K_{d1} = 5$	$K_{p1} = 15$ $K_{d1} = 0.4$

6.3 Running the system

Now the system is ready for running. Before running the system, the unknown variables should be determined for Matlab. M-file parameters is written for the purpose that is placed in Appendix-G. This M-file should be entered in the command window of Matlab.

The time step of the powergui block should also be entered.

Powergui block is a block that in each determined time step during the simulation the data values are transformed. Here proper time step of Ts = 3e- 5 s is considered. Then you can start the simulation and observe the results.

6.4 Results on loadless and load conditions

Two references $\theta_{r1}^{*} = \frac{\pi}{2}$ and $\theta_{r2}^{*} = \pi$ is considered for the 2DOF robot manipulator joints. Here we make the shoulder of the robot (joint 1) to rotate $\frac{\pi}{2}$ (rad) and the elbow of the robot (joint 2) to rotate π (rad). These two joints are driven by two PMSMs and accurate position of the robot joints deponds on controller performance that designed for the system.

Three controllers of PID, PD and PD+ are placed into the model respectively and simulation is started for 5 s.

When joints of the robot placed in desired positions the speed of the PMSMs is being zero as shown in appendices.

Results on loadless and load conditions by these three controllers (PID, PD, PD+) and performances of them are placed in appendices.

- Loadless conditions : $T_L = 0$, $m_2 = 1.285kg$ for step-type input.

When $\theta_{r1}* = \frac{\pi}{2} = 1.5708$ and $\theta_{r2}* = \pi = 3.1416$ are ordered as desired inputs to PMSM 1 and PMSM 2 in order to make the shoulder and elbow of the robot to rotate to desired positions the following results are observed after the simulation run for 5 s.

Table 6.2 : Position errors on loadless conditions

Controllers	Joints	Joints poistion (θ_r)		Steady-state errors ($\lvert E_{ss}\rvert = \theta_r* - \theta_r$)
PD	Joint 1	$\theta_{r1}* = \pi/2 = 1.5708$	$\theta_{r1} = 1.4$	$\lvert E_1\rvert = 0.1708$
	Joint 2	$\theta_{r2}* = \pi = 3.1416$	$\theta_{r2} = 3.1892$	$\lvert E_2\rvert = 0.0476$
PID	Joint 1	$\theta_{r1}* = \pi/2 = 1.5708$	$\theta_{r1} = 1.5710$	$\lvert E_1\rvert = 0.00020367$
	Joint 2	$\theta_{r2}* = \pi = 3.1416$	$\theta_{r2} = 3.1995$	$\lvert E_2\rvert = 0.0579$
PD+	Joint 1	$\theta_{r1}* = \pi/2 = 1.5708$	$\theta_{r1} = 1.5698$	$\lvert E_1\rvert = 0.00099633$
	Joint 2	$\theta_{r2}* = \pi = 3.1416$	$\theta_{r2} = 3.1433$	$\lvert E_2\rvert = 0.0017$

Table 6.3 : Overshoots on loadless conditions

Controllers	Joints	Maximum poistion ($\theta_{\max}$)	Maximum overshoot ($\theta_{\max} - \theta_r$)	Percent maximum overshoot ($\frac{\theta_{\max} - \theta_r}{\theta_r} \times 100\%$)
PD	Joint 1	$\theta_{\max 1} = 1.528$	0.128	9.14 %
	Joint 2	$\theta_{\max 2} = 4.192$	1.0028	31.44 %
PID	Joint 1	$\theta_{\max 1} = 1.822$	0.251	15.98 %
	Joint 2	$\theta_{\max 2} = 4.21$	1.0105	31.58 %
PD+	Joint 1	$\theta_{\max 1} = 1.683$	0.1132	7.21 %
	Joint 2	$\theta_{\max 2} = 4.35$	1.2067	38.39 %

- Load conditions : $m_{link2} = (m_2 + 4)kg$ for step-type input.

Now a load is installed on joint 2 and assume that this load makes the mass of link 2 to ($m_2 + 4$) kg.

Again after running the simulation following results are observed for 5 s.

Table 6.4 : Position errors on load conditions

Controllers	Joints	Joints poistion (θ_r)		Steady-state errors ($\lvert E_{ss} \rvert = \theta_r * - \theta_r$)
PD	Joint 1	$\theta_{r1}* = \pi/2 = 1.5708$	$\theta_{r1} = 1.4001$	$\lvert E_1 \rvert = 0.1707$
	Joint 2	$\theta_{r2}* = \pi = 3.1416$	$\theta_{r2} = 3.3341$	$\lvert E_2 \rvert = 0.1925$
PID	Joint 1	$\theta_{r1}* = \pi/2 = 1.5708$	$\theta_{r1} = 1.5729$	$\lvert E_1 \rvert = 0.0021$
	Joint 2	$\theta_{r2}* = \pi = 3.1416$	$\theta_{r2} = 3.3043$	$\lvert E_2 \rvert = 0.1627$
PD+	Joint 1	$\theta_{r1}* = \pi/2 = 1.5708$	$\theta_{r1} = 1.5697$	$\lvert E_1 \rvert = 0.0011$
	Joint 2	$\theta_{r2}* = \pi = 3.1416$	$\theta_{r2} = 3.1432$	$\lvert E_2 \rvert = 0.0016$

Table 6.5 : Overshoots on load conditions

Controllers	Joints	Maximum poistion ($\theta_{\max}$)	Maximum overshoot ($\theta_{\max} - \theta_r$)	Percent maximum overshoot ($\frac{\theta_{\max} - \theta_r}{\theta_r} \times 100\%$)
PD	Joint 1	$\theta_{\max 1} = 1.531$	0.1309	9.35 %
	Joint 2	$\theta_{\max 2} = 4.336$	1.0019	30.05 %
PID	Joint 1	$\theta_{\max 1} = 1.822$	0.2491	15.84 %
	Joint 2	$\theta_{\max 2} = 4.355$	1.0507	31.8 %
PD+	Joint 1	$\theta_{\max 1} = 1.683$	0.1133	7.22 %
	Joint 2	$\theta_{\max 2} = 4.356$	1.2128	38.58 %

6.5 Concluding remarks

In this study, the test of three control methods on a direct-drive robot arm has presented. All three methods are evaluated by simulations for step unit trajectories applied directly as joint references. The performance of PD+ controller was compared with the linear PID and PD controllers. As expected, from our experimental results we have observed that PD+ controller compensating in some way for the robot dynamics attained better tracking accuracy.

CHAPTER 7. CONCLUSION

Researchs about electrical motors and their drive systems have improved these years. Because of obvious advantages of brushless servomotors, using of these motors has increased at industry.

Brushless servomotors has gradually become widespread especially in robotic, aerospace industry, electric automobile and some computer control devices which require high performance in application.

In order to provide desirable work conditions in high performance applications servomotors should be controlled accurately. In PMSM drive system for doing a sensitive control, a controller should be added. Many control techniques have applicated at industry so far and successful results has obtained partly.

If you search about drive systems in the literature you are informed that in PMSM drive systems in addition to more adaptable and optimal control techniques, there are various techniques that used at industry. Almost these applicated techniques has designed by linear theory.

In this study an example of robotic configurations exposed to load uncertainties, a two degree of freedom (2DOF) planar robotic arm is considered. Three controllers are developed for the position and trajectory control of the arm; namely, PID and PD controllers as standard linear controllers and PD+ as a nonlinear model based controller.

In order to calculate the controller of the drive system, mathematical model of PMSMs model, linearizing the model and estimate parameters are required. There are many algorithms and different techniques for calculating the controllers.

The arm dynamics and load variations are seen by the controllers as disturbances. The PD and PID controllers are linear controllers and are still widely used in the robot industry due to their ease of application. PD control will result in a steady-state error under disturbance effects, while PID will make the steady-state error zero.

For more sophisticated applications, PD+ controllers appear to be more effective and attained better tracking accuracy.

Beyond the evaluation of control methods on direct-drive mechanisms, a number of experiments and simulations on robots have been presented in the literature.

This thesis mentions briefly a few of them on a 2DOF direct-drive robot arm.

The model-based control method (PD+ controller) appeared to be the best as compared to the independent joint PID and PD controllers.

APPENDIX - A : LOADLESS RESULTS OF 2DOF DIRECT DRIVE ROBOT WITH PD CONTROLLER

Step-type input

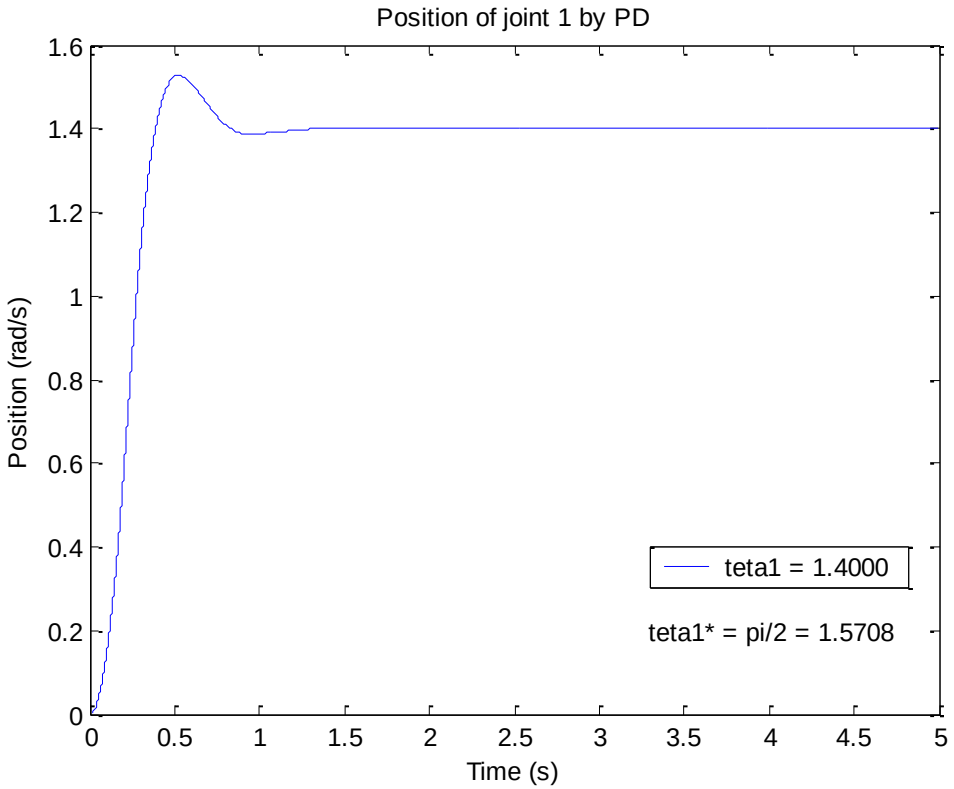

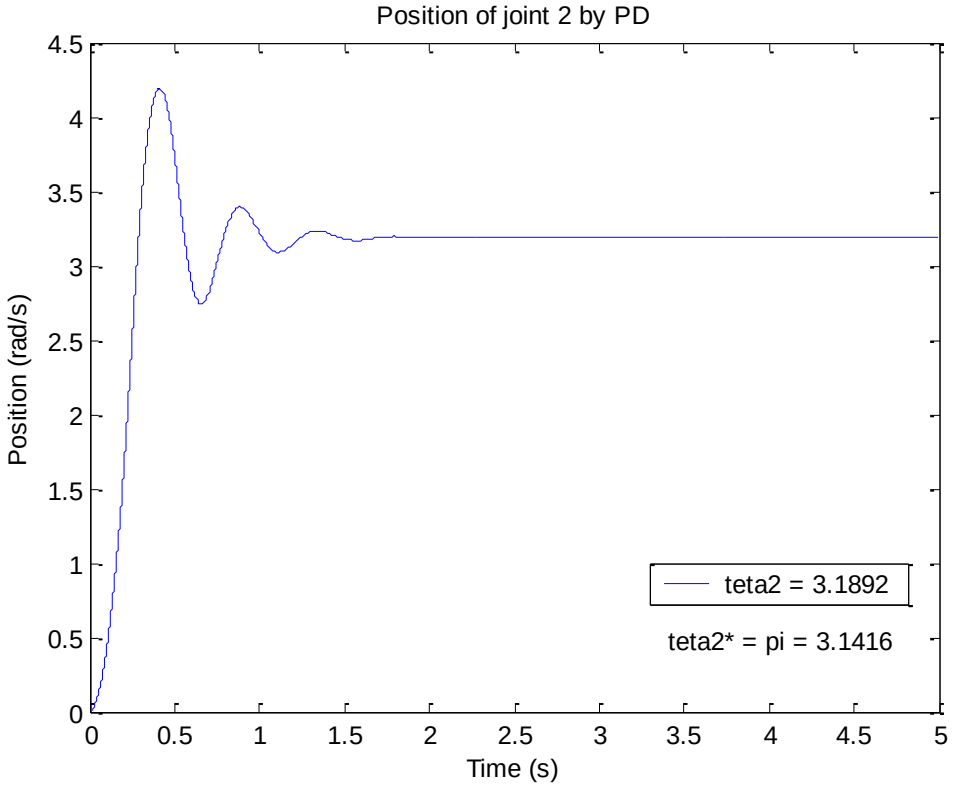

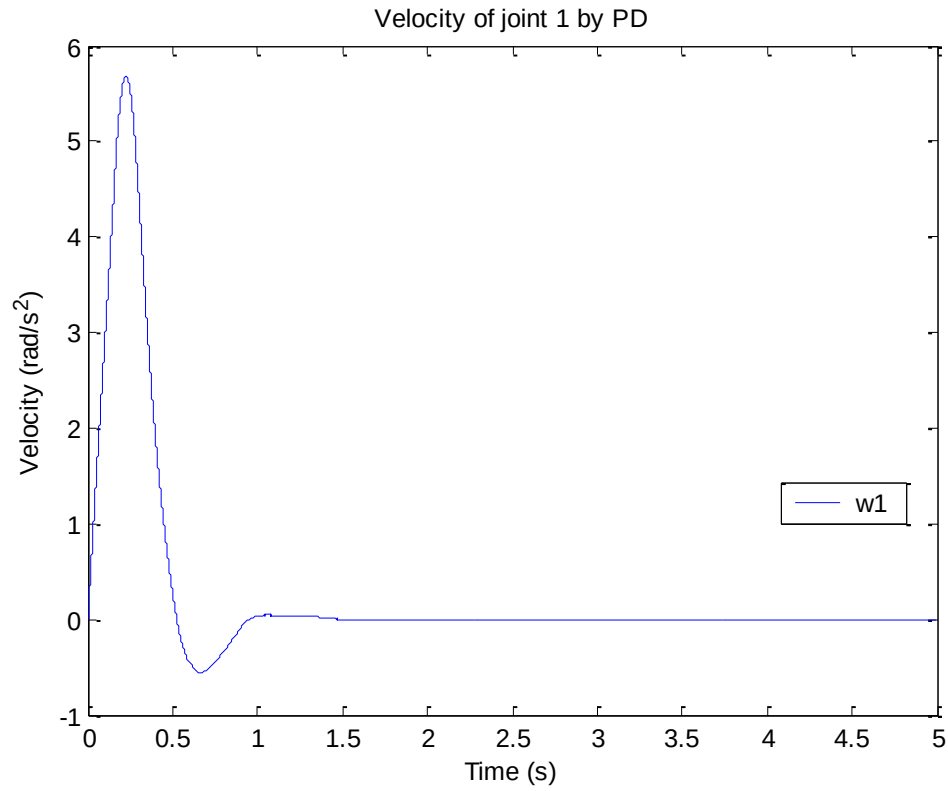
Velocity of joint 1 by PD
Velocity (rad/s2)
Time (s)
w1
6
5
4
3
2
1
0
-1
0
0.5
1
1.5
2
2.5
3
3.5
4
4.5
5

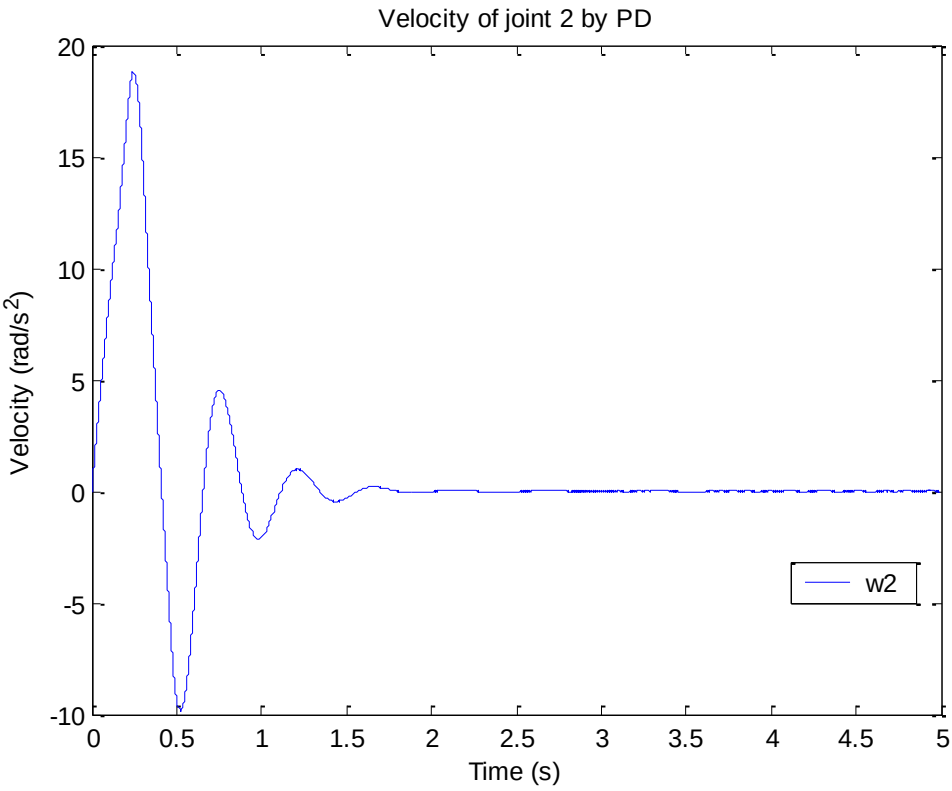
Velocity of joint 2 by PD
Velocity (rad/s2)
Time (s)
w2
20
15
10
5
0
-5
-10
0
0.5
1
1.5
2
2.5
3
3.5
4
4.5
5

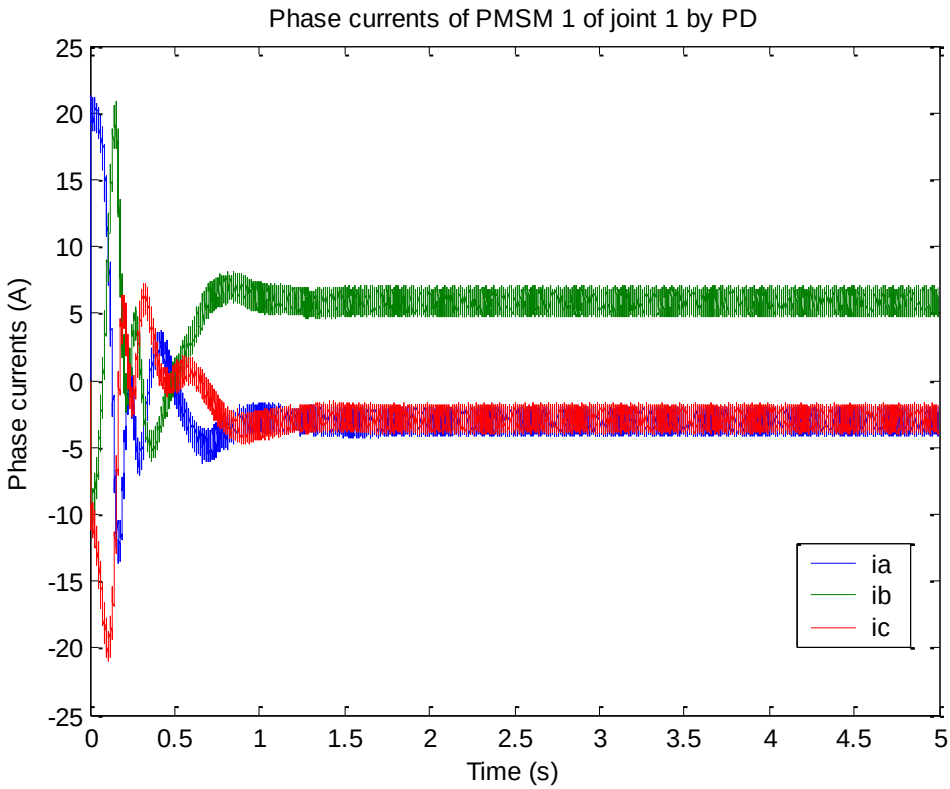
Phase currents of PMSM 1 of joint 1 by PD
Phase currents (A)
Time (s)
ia
ib
ic

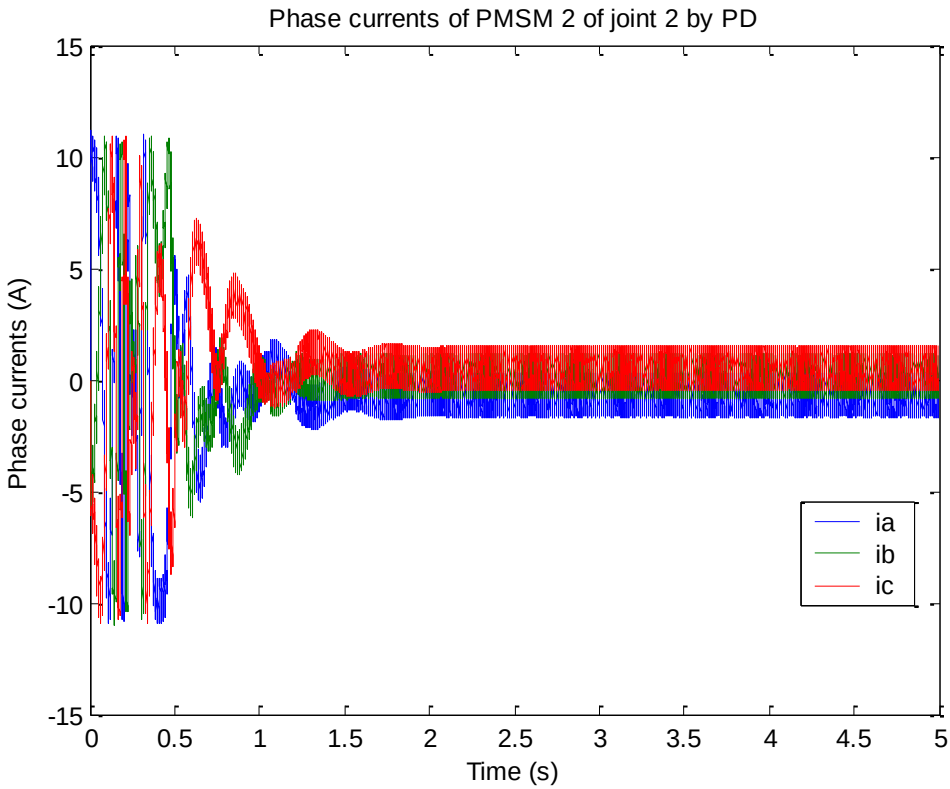
Phase currents of PMSM 2 of joint 2 by PD
Phase currents (A)
Time (s)
ia
ib
ic

APPENDIX - B : LOADLESS RESULTS OF 2DOF DIRECT DRIVE ROBOT WITH PID CONTROLLER

Step-type input

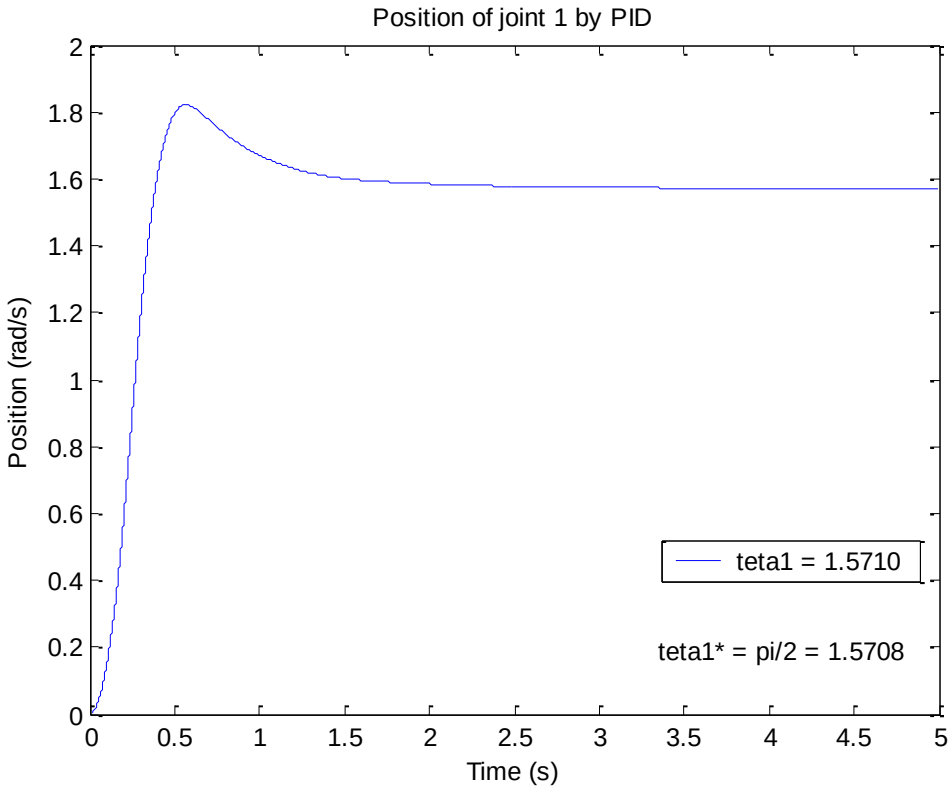

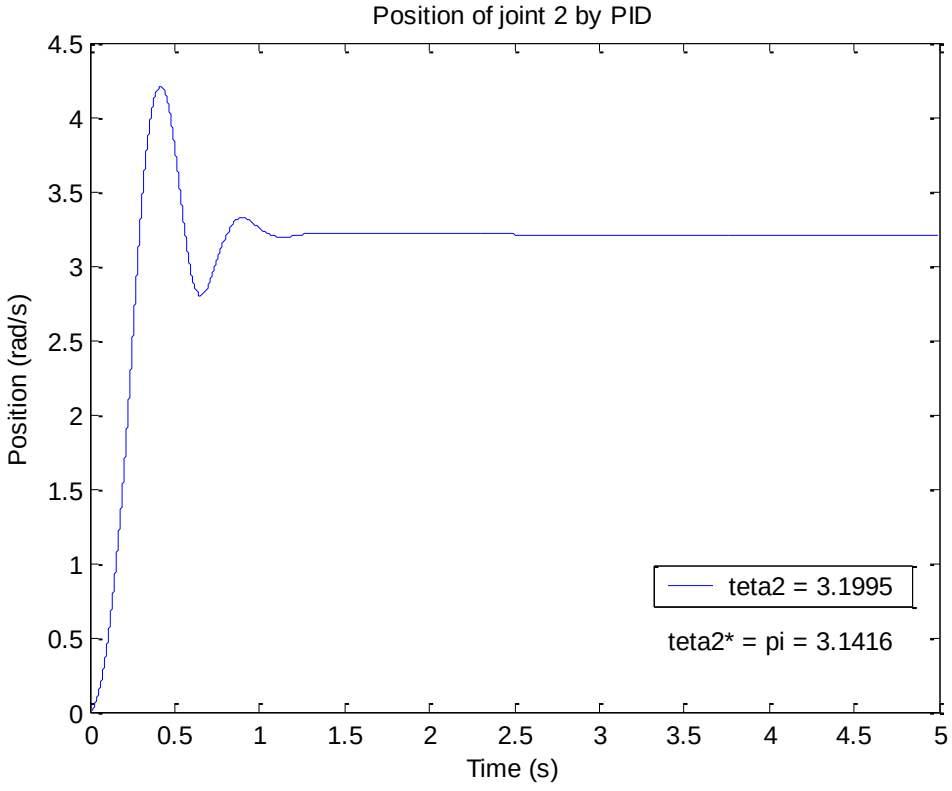

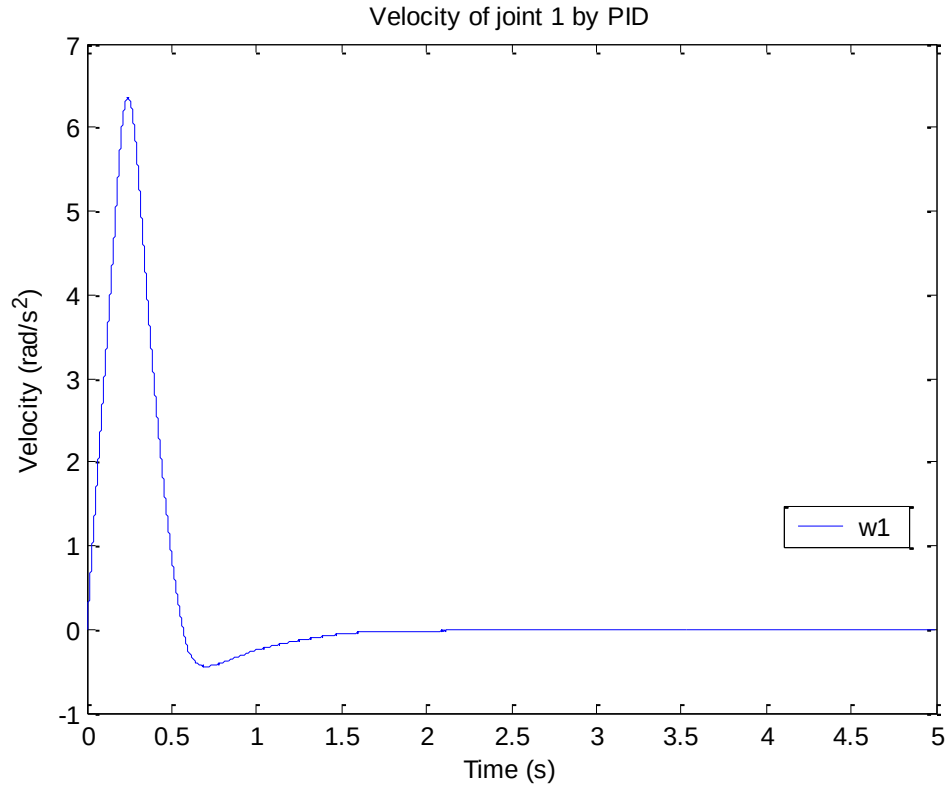
Velocity of joint 1 by PID
Velocity (rad/s2)
Time (s)
w1
7
6
5
4
3
2
1
0
-1
0
0.5
1
1.5
2
2.5
3
3.5
4
4.5
5

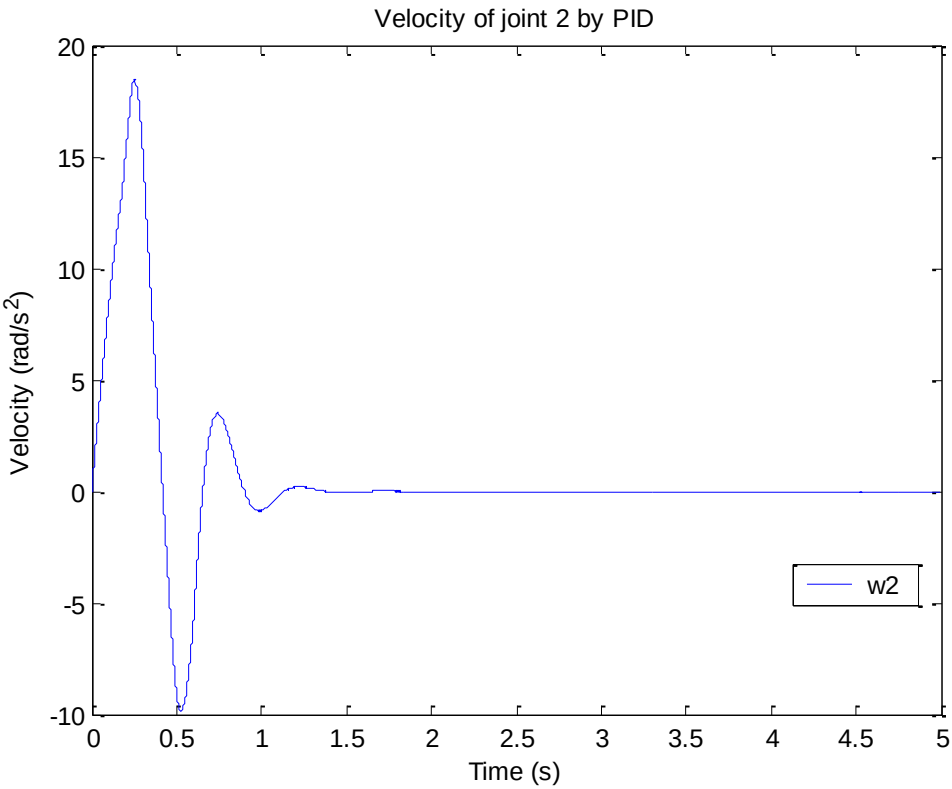
Velocity of joint 2 by PID
Velocity (rad/s2)
Time (s)
w2
20
15
10
5
0
-5
-10
0
0.5
1
1.5
2
2.5
3
3.5
4
4.5
5

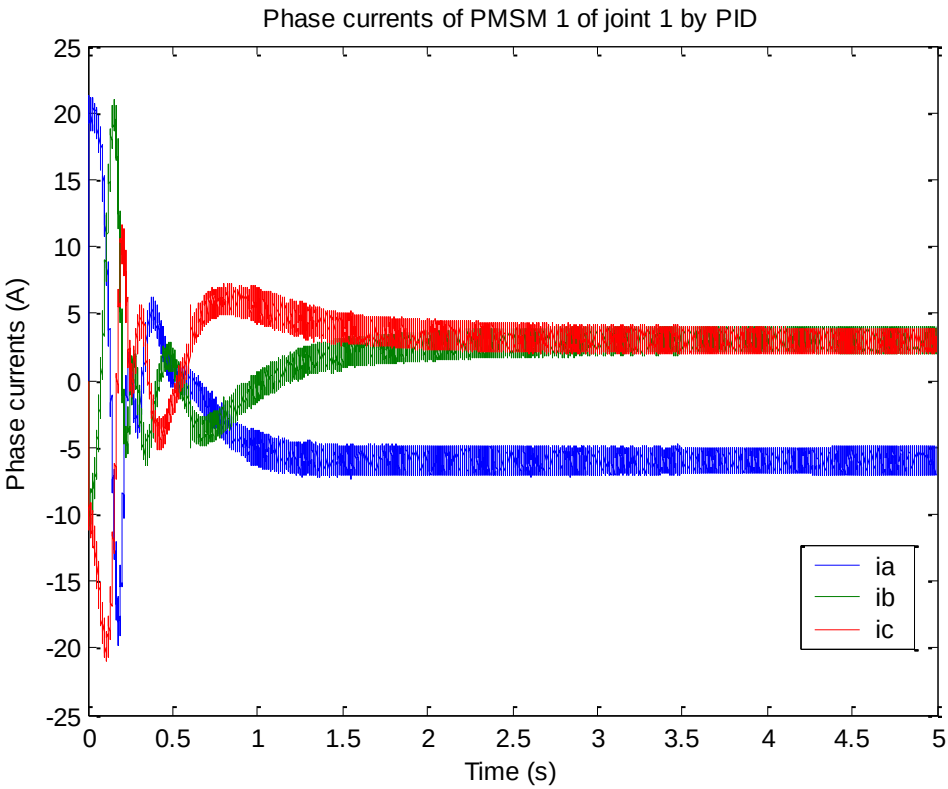
Phase currents of PMSM 1 of joint 1 by PID
Phase currents (A)
Time (s)
ia
ib
ic

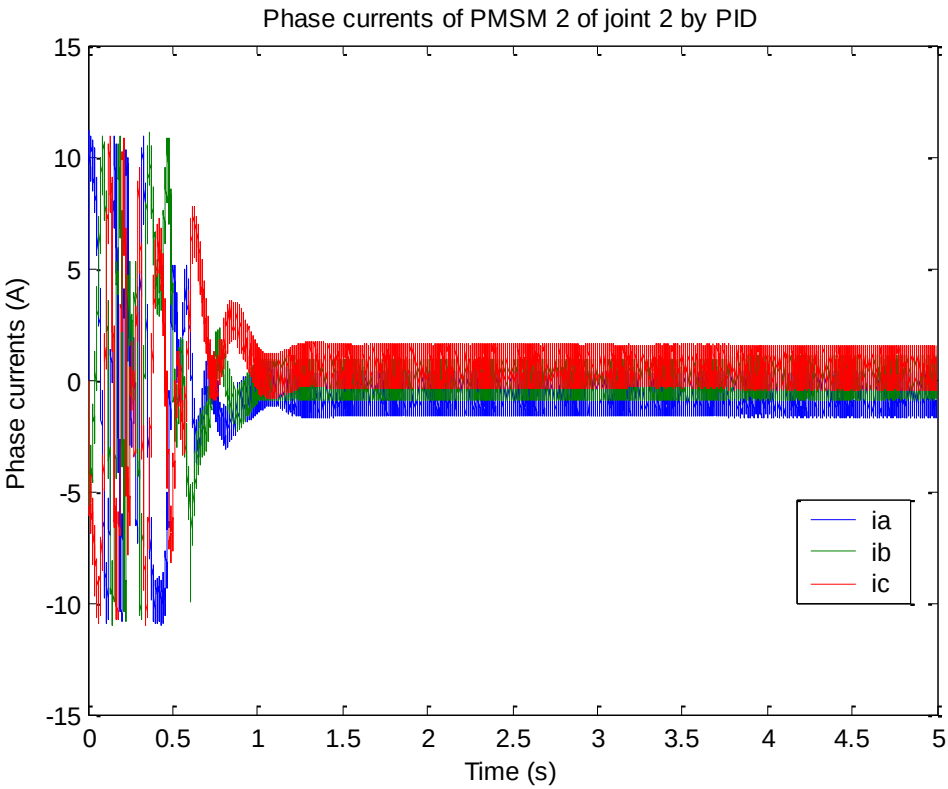
Phase currents of PMSM 2 of joint 2 by PID
Phase currents (A)
Time (s)
ia
ib
ic

APPENDIX - C : LOADLESS RESULTS OF 2DOF DIRECT DRIVE ROBOT WITH PD+ CONTROLLER

Step-type input

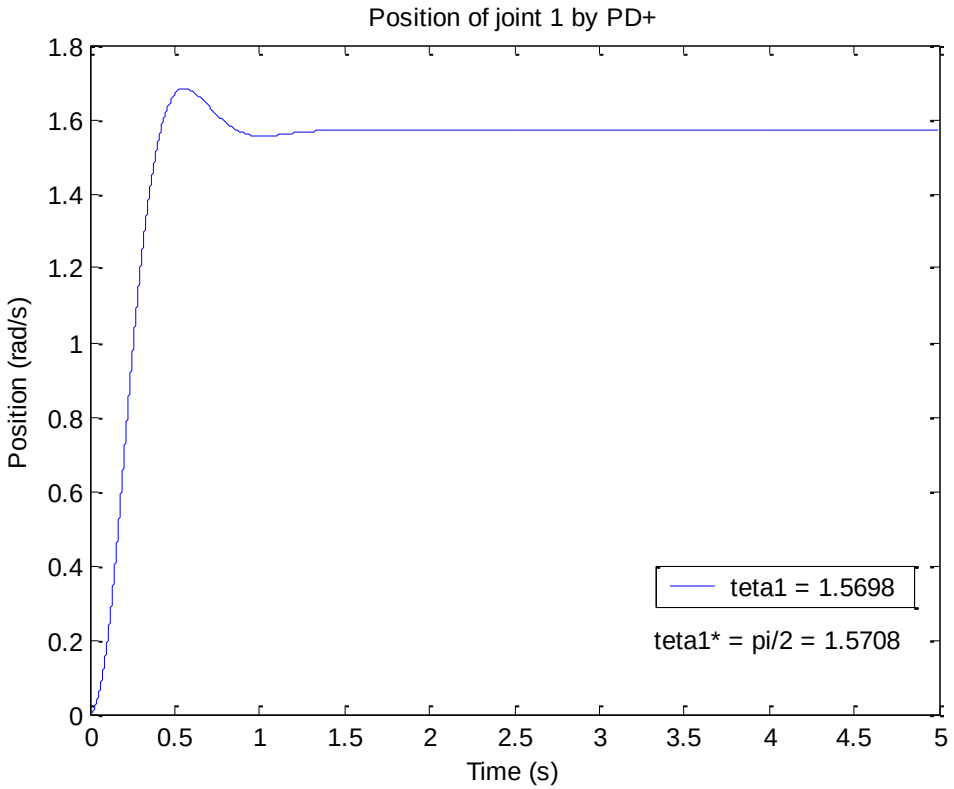

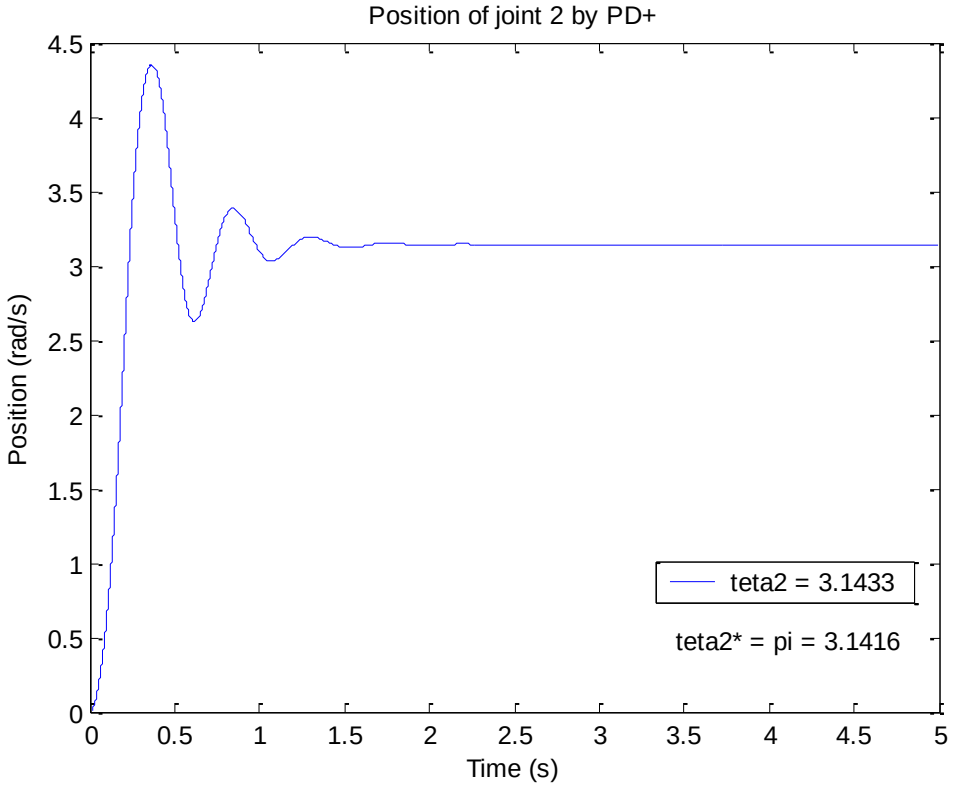

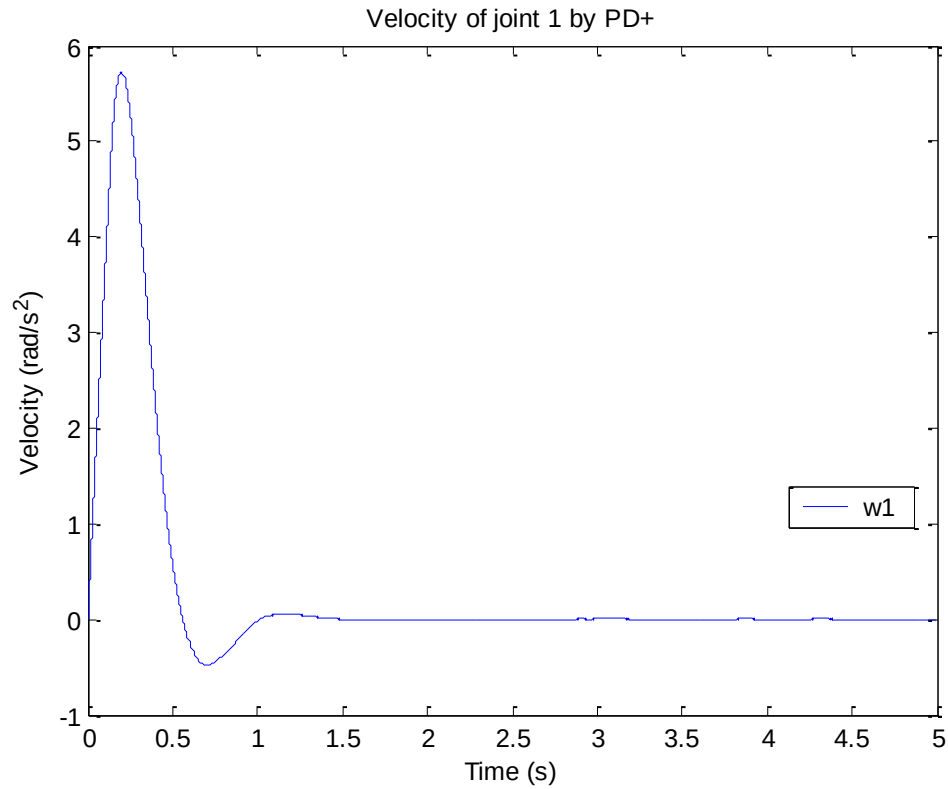
Velocity of joint 1 by PD+
Velocity (rad/s2)
Time (s)
w1
6
5
4
3
2
1
0
-1
0
0.5
1
1.5
2
2.5
3
3.5
4
4.5
5

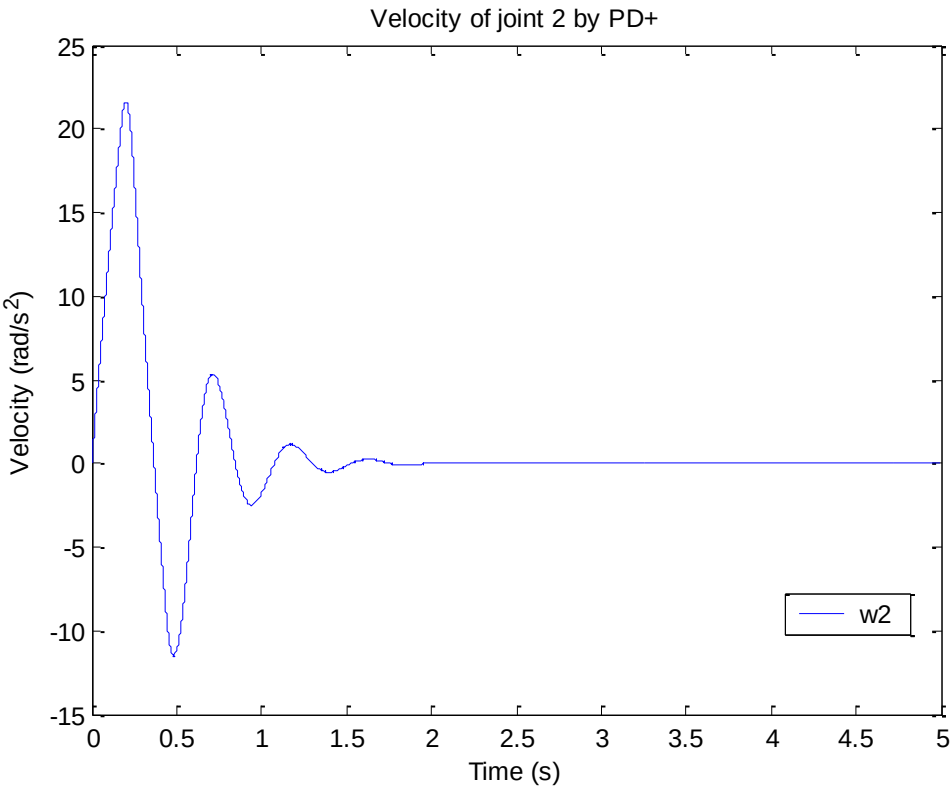
Velocity of joint 2 by PD+
Velocity (rad/s2)
Time (s)
w2
25
20
15
10
5
0
-5
-10
-15
0
0.5
1
1.5
2
2.5
3
3.5
4
4.5
5

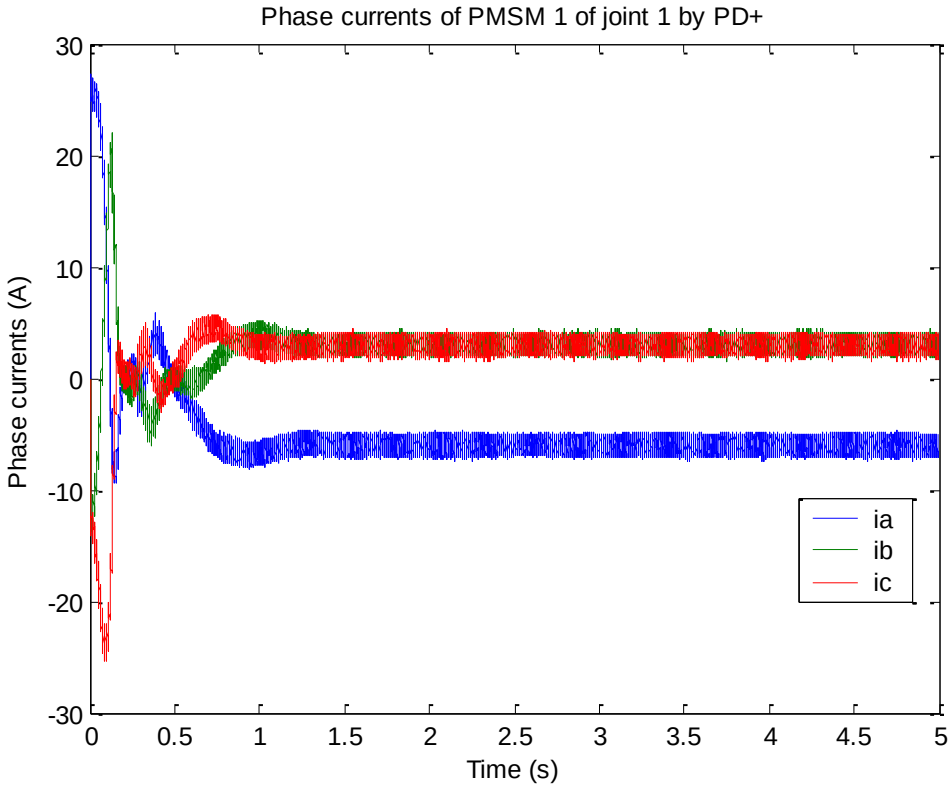
Phase currents of PMSM 1 of joint 1 by PD+
Phase currents (A)
Time (s)
ia
ib
ic

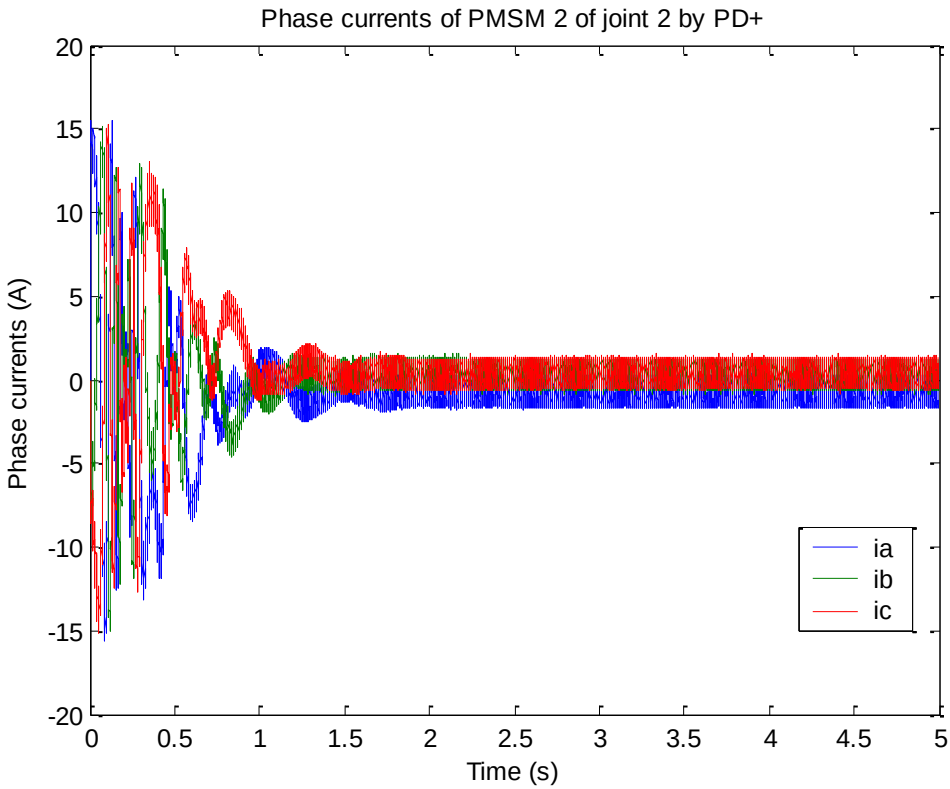
Phase currents of PMSM 2 of joint 2 by PD+
Phase currents (A)
Time (s)
ia
ib
ic

APPENDIX - D : LOAD RESULTS OF 2DOF DIRECT DRIVE ROBOT WITH PD CONTROLLER

$m_{link2} = (m_2 + 4)kg$ **,** Step-type input

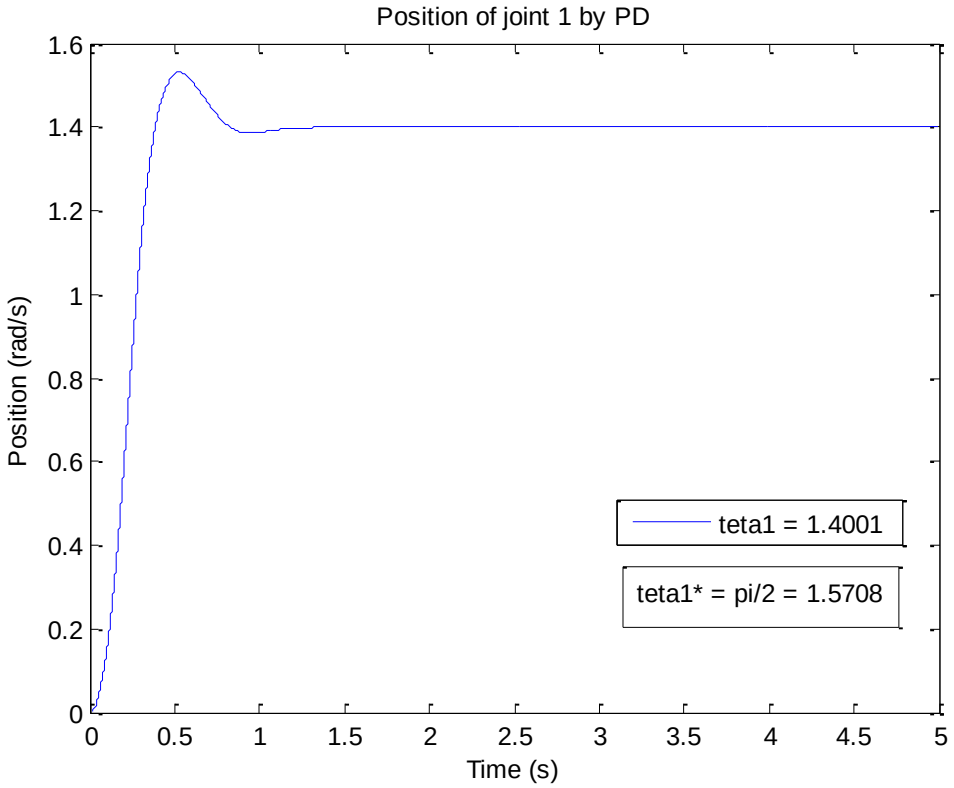

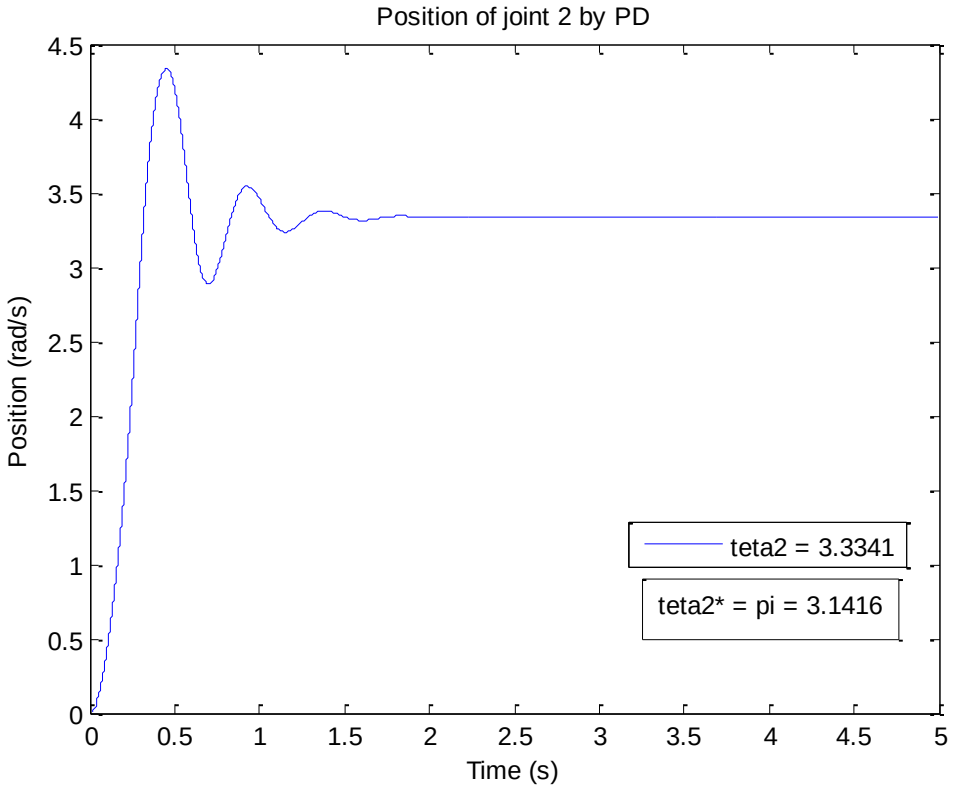

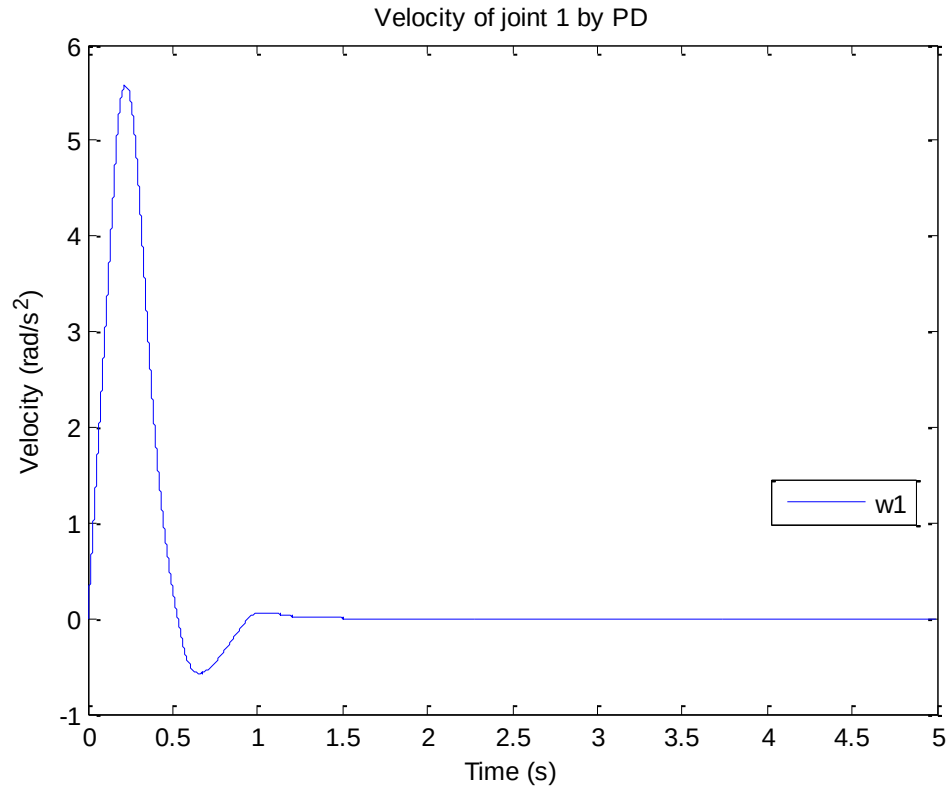
Velocity of joint 1 by PD
Velocity (rad/s2)
Time (s)
w1
6
5
4
3
2
1
0
-1
0
0.5
1
1.5
2
2.5
3
3.5
4
4.5
5

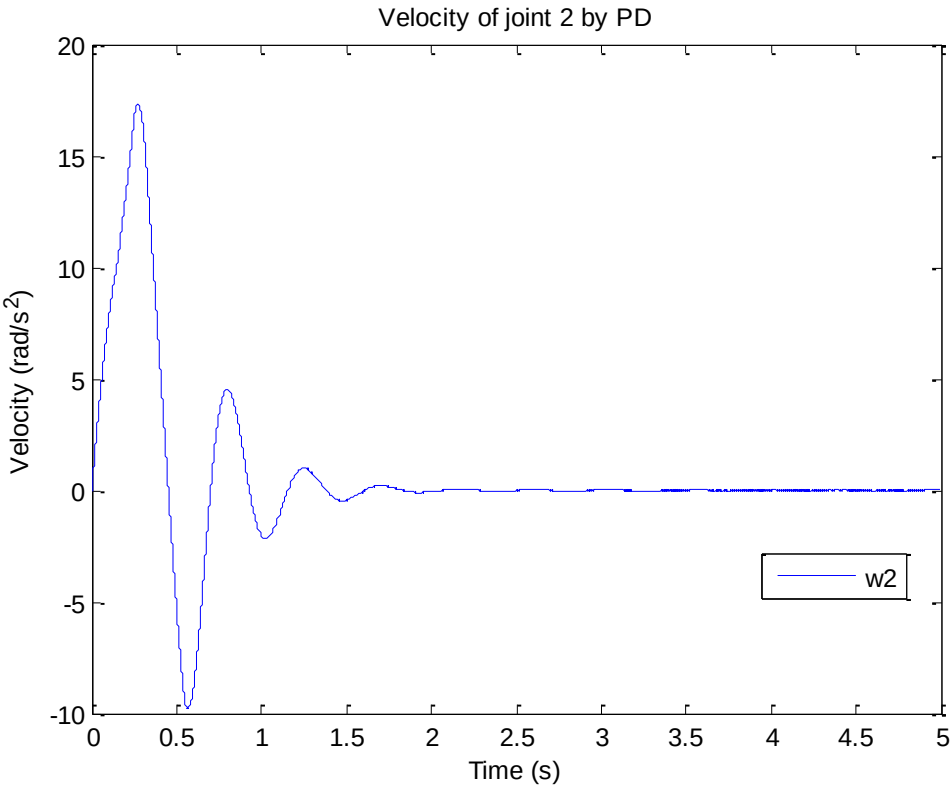
Velocity of joint 2 by PD
Velocity (rad/s2)
Time (s)
w2
20
15
10
5
0
-5
-10
0
0.5
1
1.5
2
2.5
3
3.5
4
4.5
5

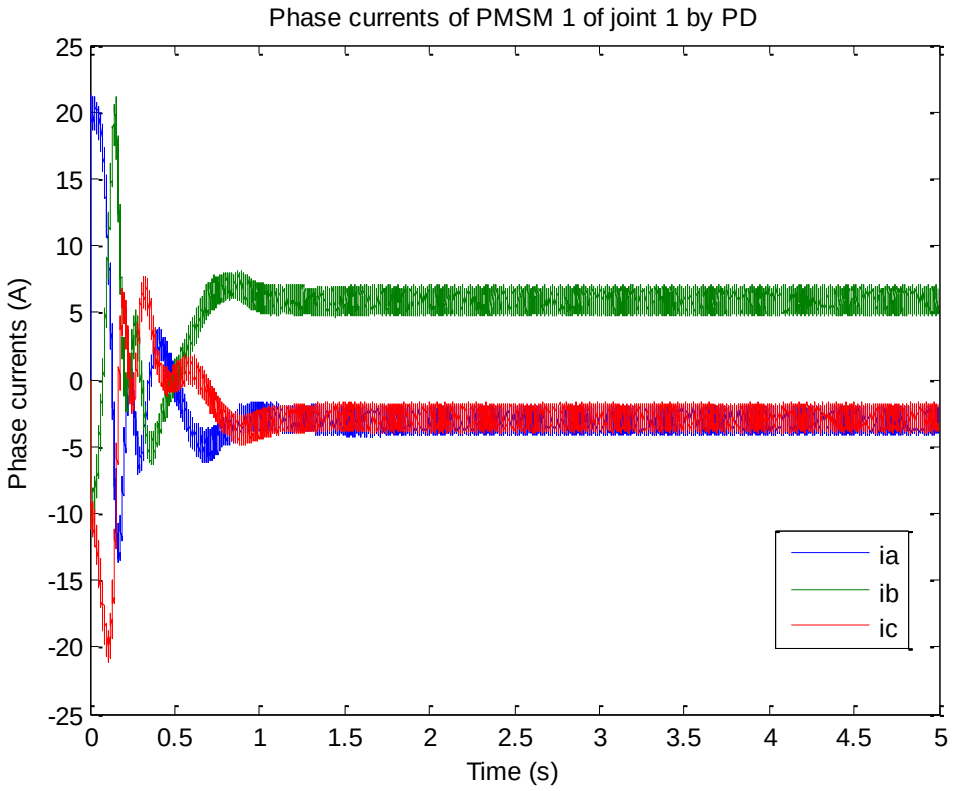
Phase currents of PMSM 1 of joint 1 by PD
Phase currents (A)
Time (s)
ia
ib
ic

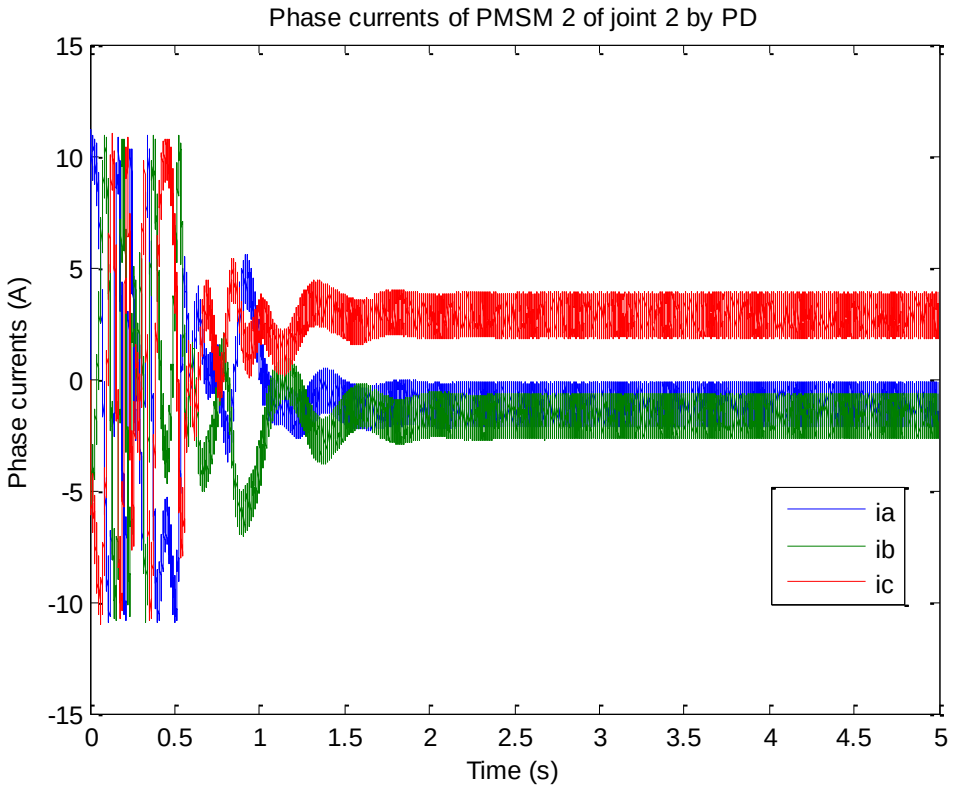
Phase currents of PMSM 2 of joint 2 by PD
Phase currents (A)
Time (s)
ia
ib
ic

APPENDIX - E : LOAD RESULTS OF 2DOF DIRECT DRIVE ROBOT WITH PID CONTROLLER

$m_{link2} = (m_2 + 4)kg$ **,** Step-type input

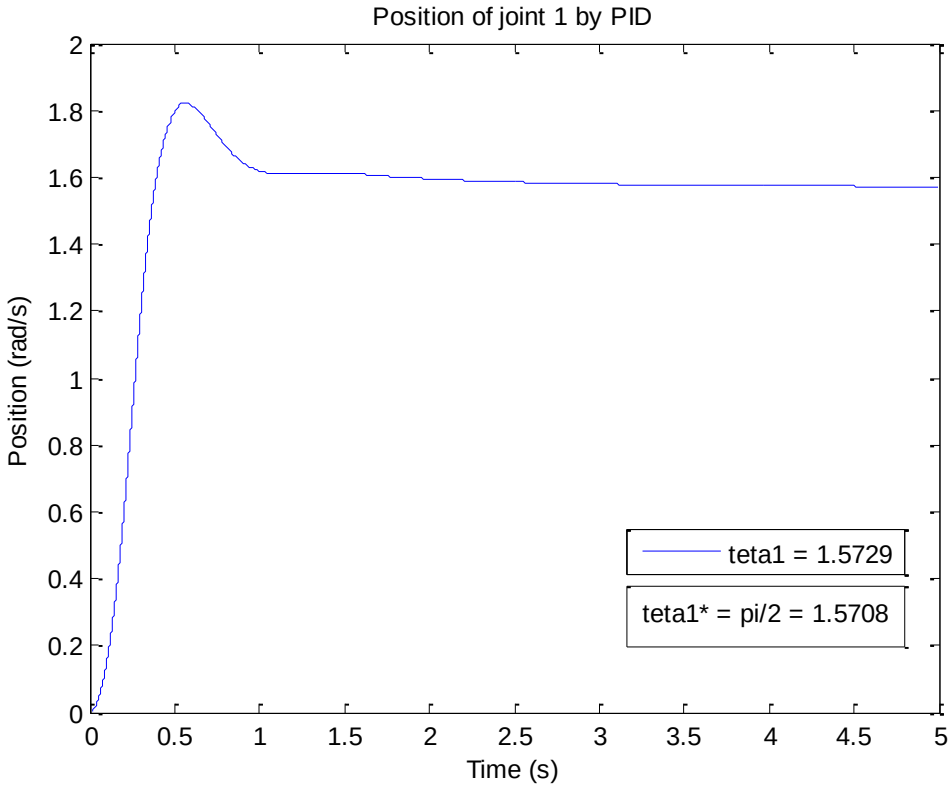

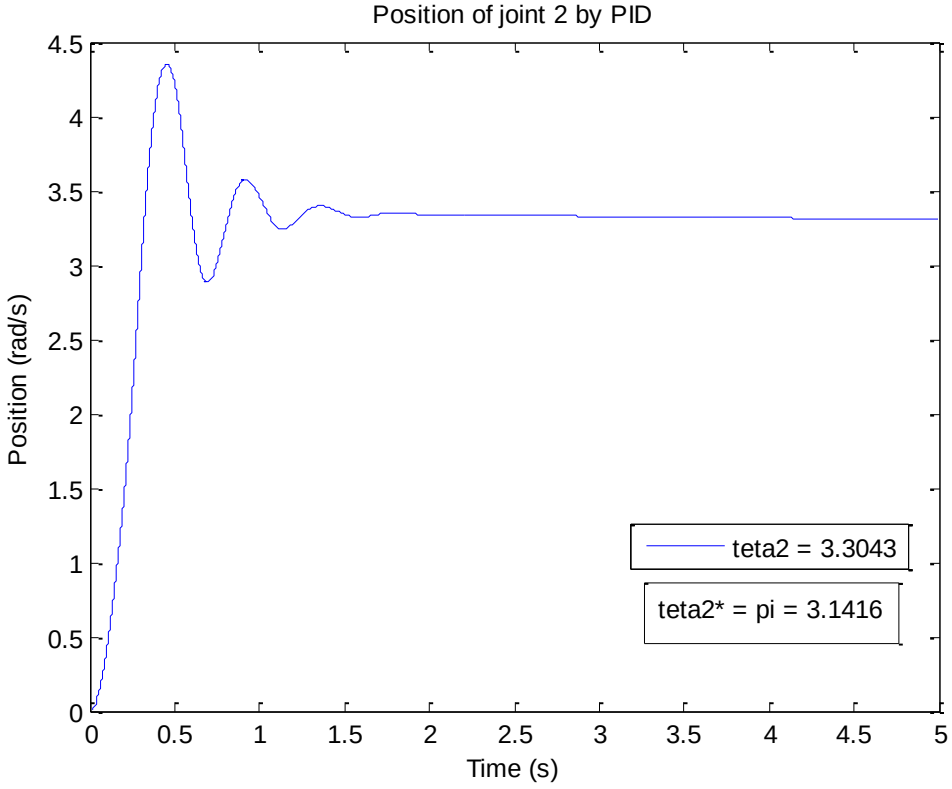

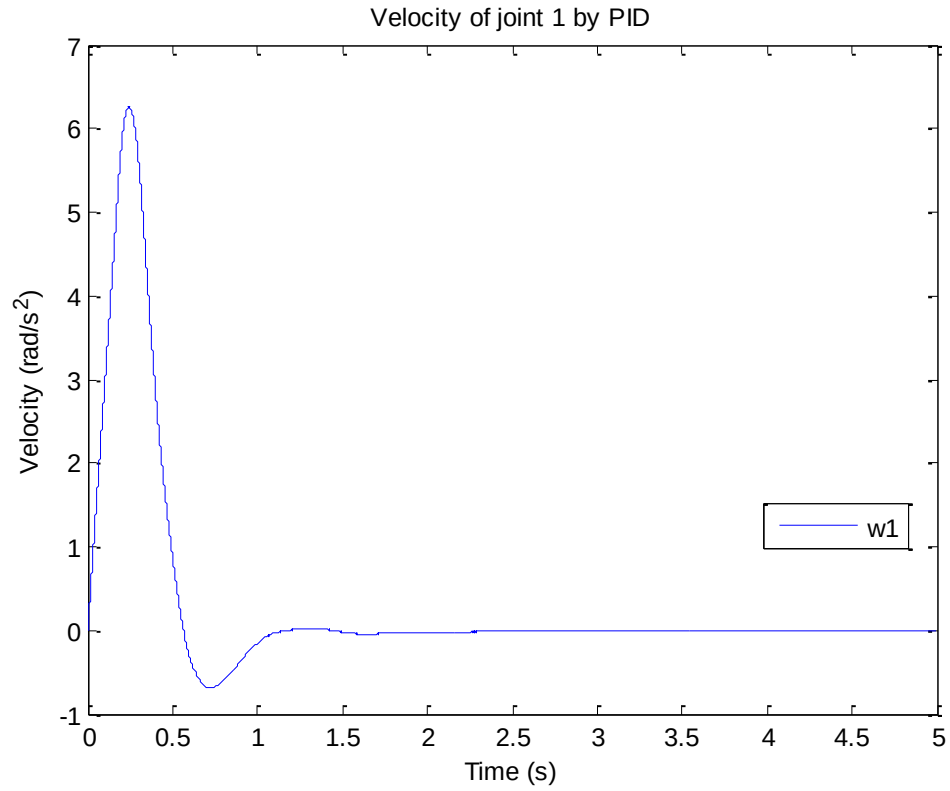
Velocity of joint 1 by PID
Velocity (rad/s2)
Time (s)
w1
7
6
5
4
3
2
1
0
-1
0
0.5
1
1.5
2
2.5
3
3.5
4
4.5
5

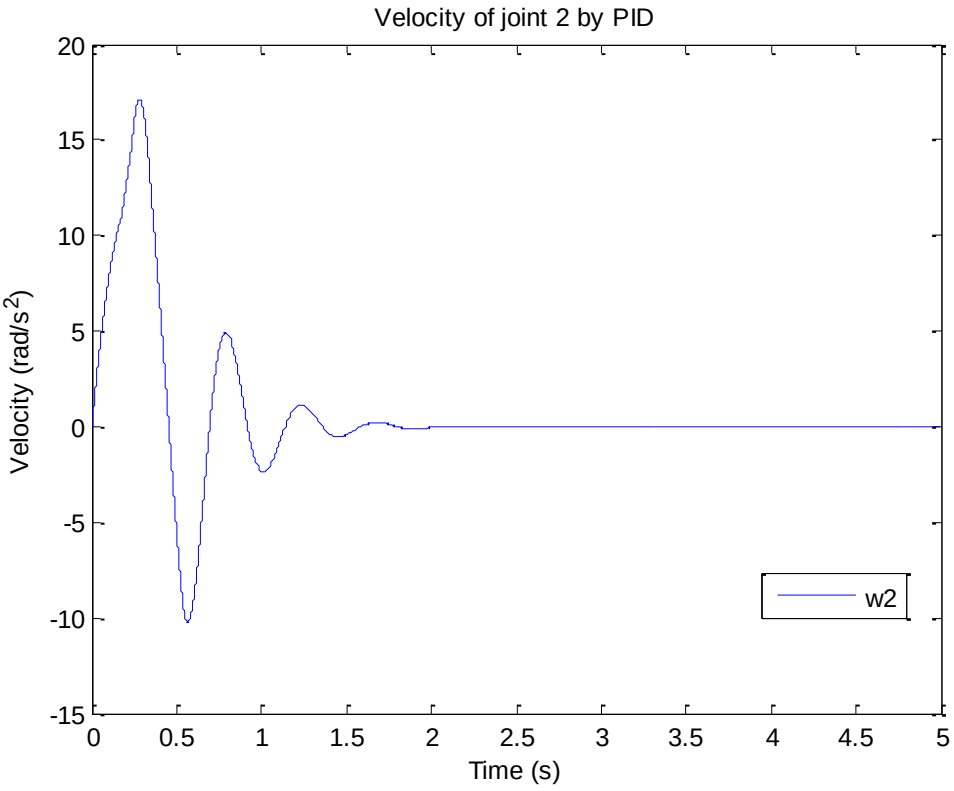
Velocity of joint 2 by PID
Velocity (rad/s2)
Time (s)
w2
20
15
10
5
0
-5
-10
-15
0
0.5
1
1.5
2
2.5
3
3.5
4
4.5
5

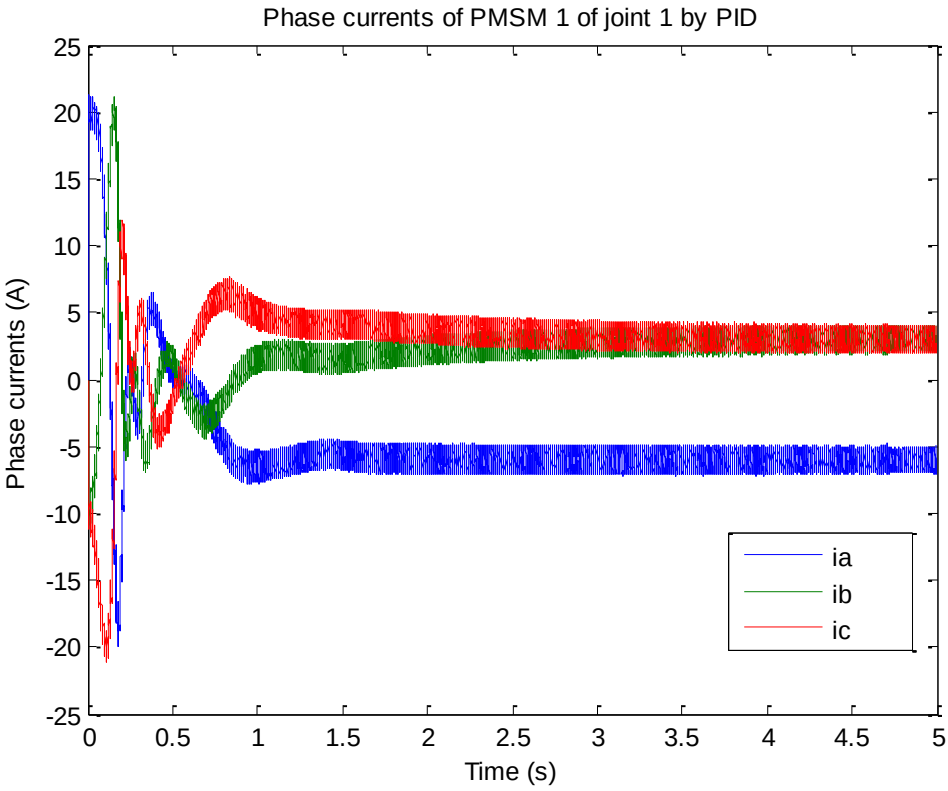
Phase currents of PMSM 1 of joint 1 by PID
Phase currents (A)
Time (s)
ia
ib
ic

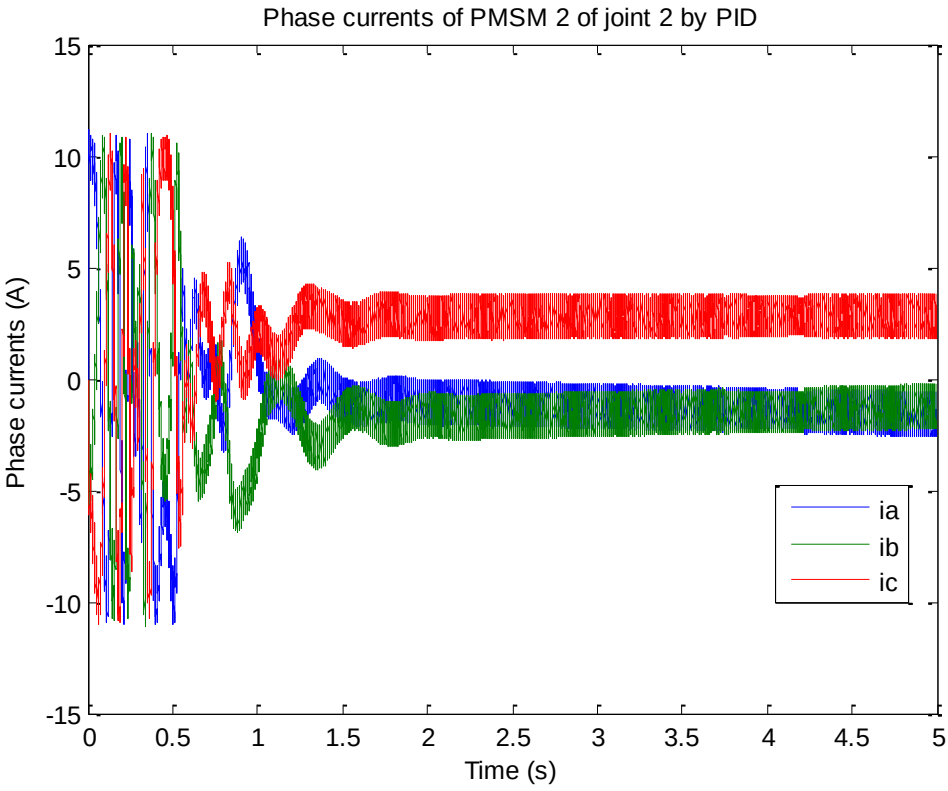
Phase currents of PMSM 2 of joint 2 by PID
Phase currents (A)
Time (s)
ia
ib
ic

APPENDIX - F : LOAD RESULTS OF 2DOF DIRECT DRIVE ROBOT WITH PD+ CONTROLLER

$m_{link2} = (m_2 + 4)kg$, Step-type input

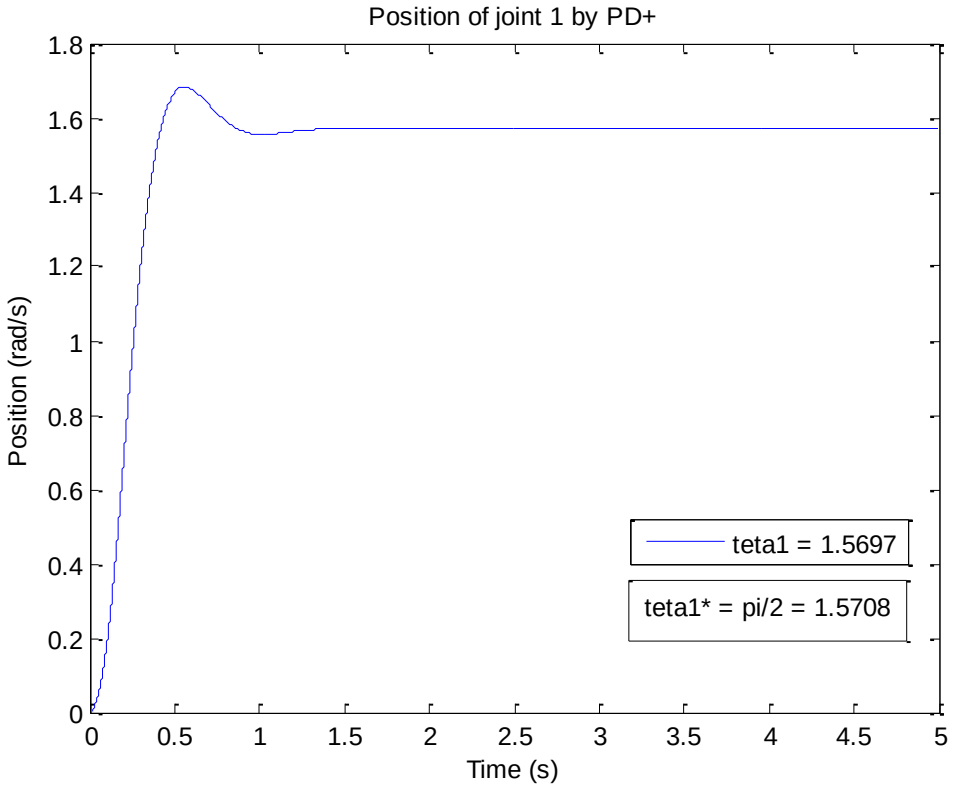

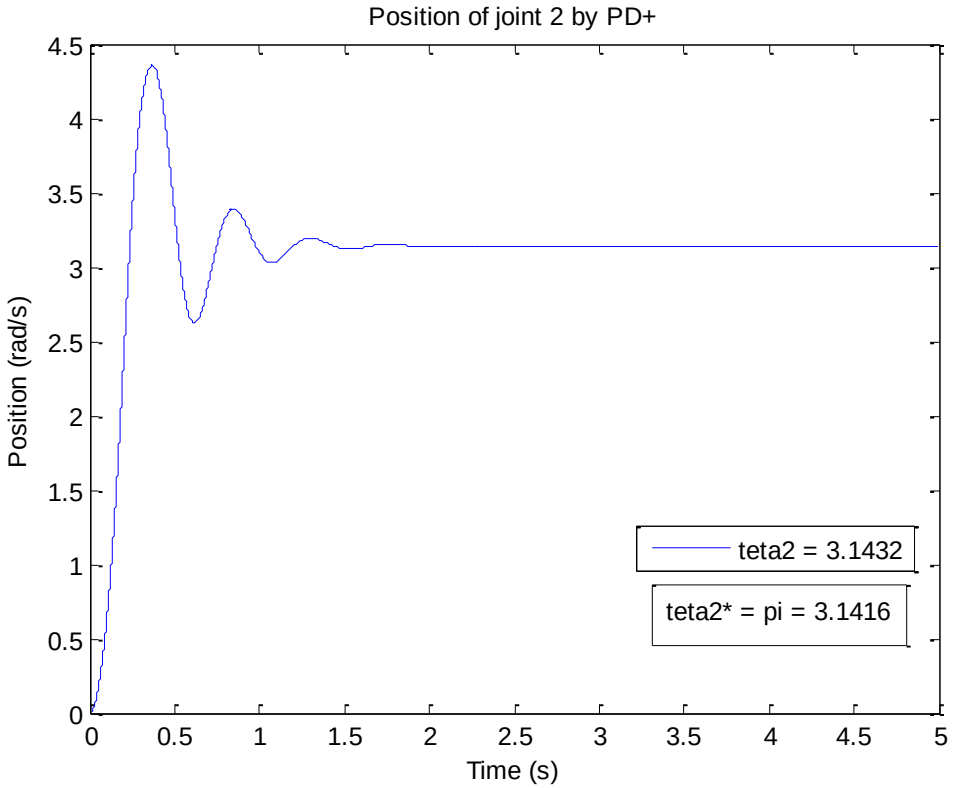

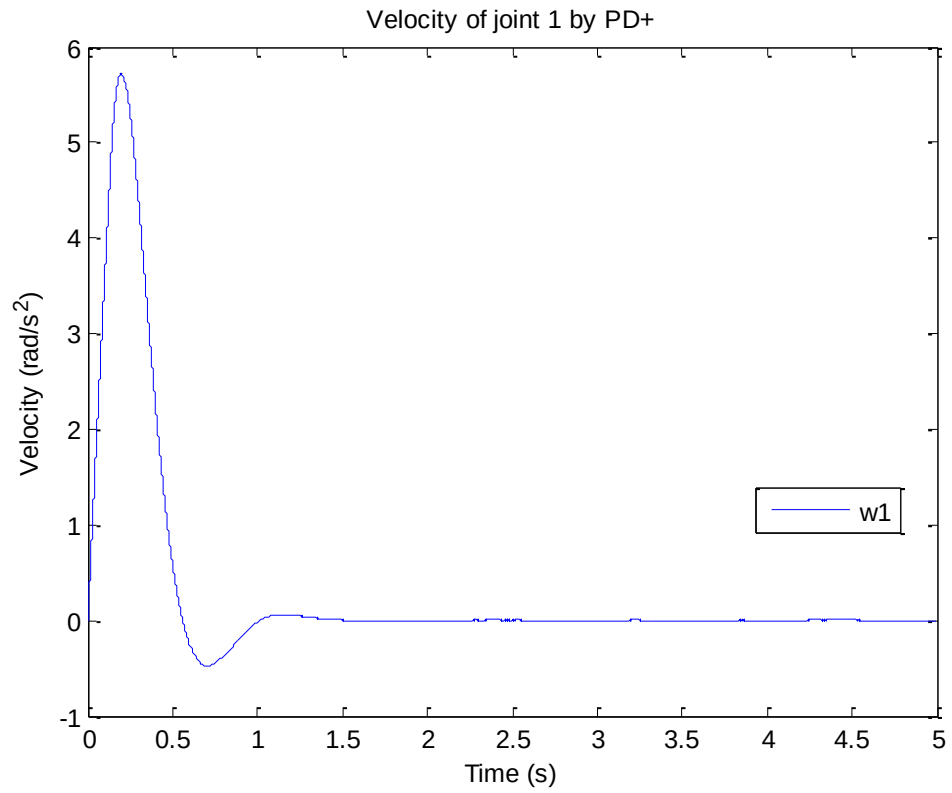
Velocity of joint 1 by PD+
Velocity (rad/s2)
Time (s)
w1
6
5
4
3
2
1
0
-1
0
0.5
1
1.5
2
2.5
3
3.5
4
4.5
5

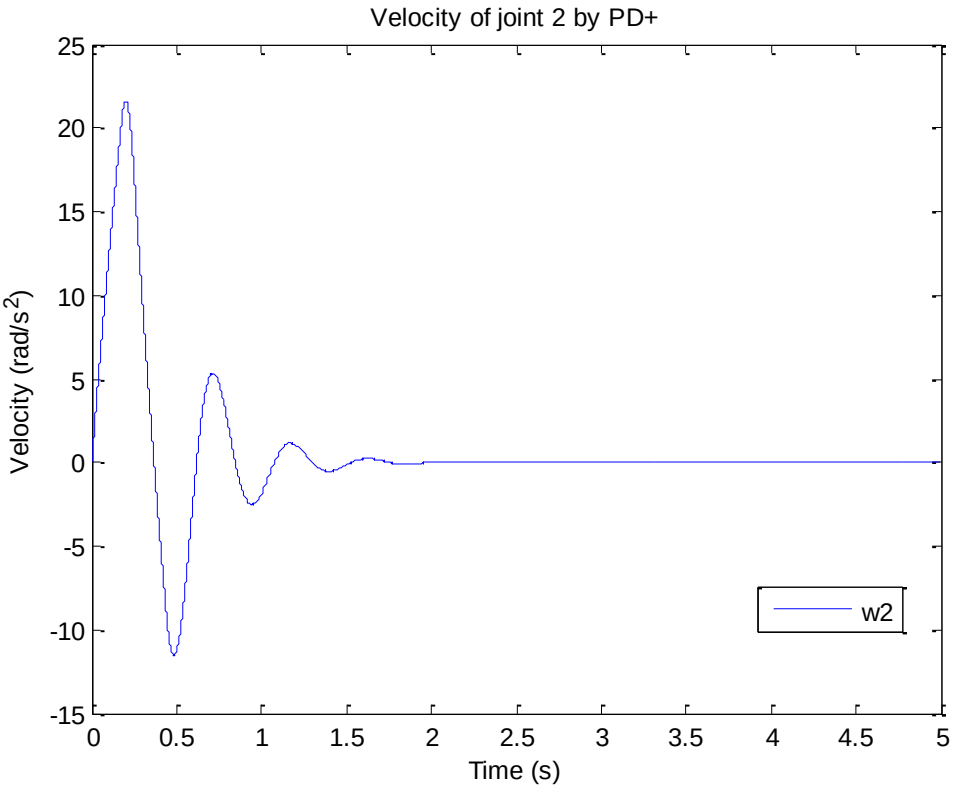
Velocity of joint 2 by PD+
Velocity (rad/s2)
Time (s)
w2
25
20
15
10
5
0
-5
-10
-15
0
0.5
1
1.5
2
2.5
3
3.5
4
4.5
5

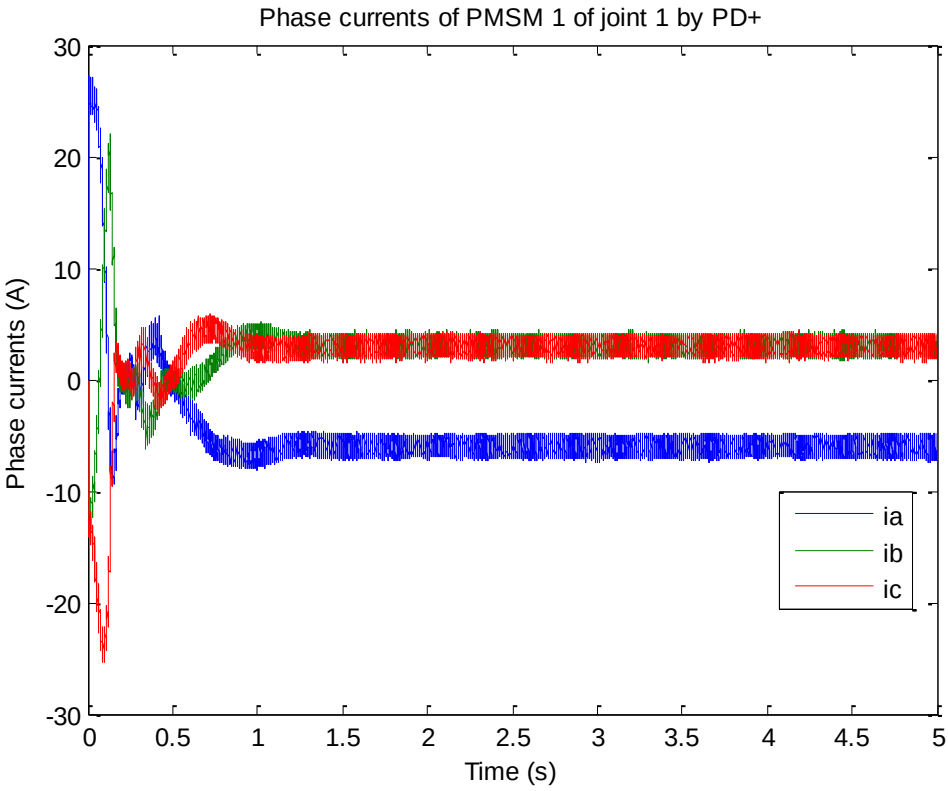
Phase currents of PMSM 1 of joint 1 by PD+
Phase currents (A)
Time (s)
ia
ib
ic

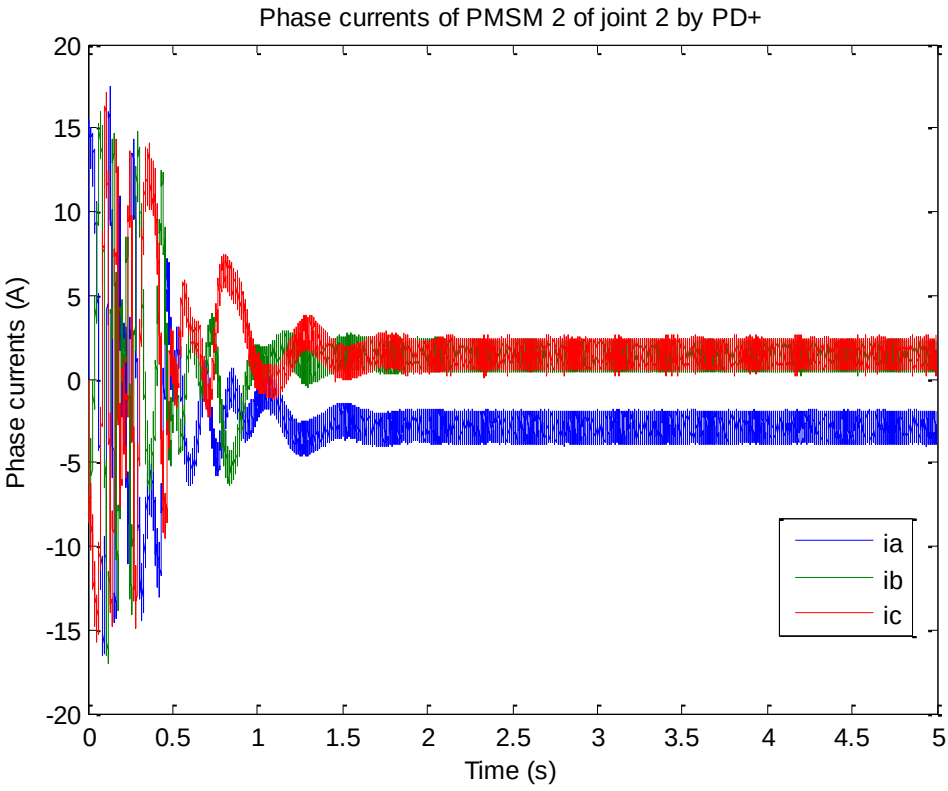
Phase currents of PMSM 2 of joint 2 by PD+
Phase currents (A)
Time (s)
ia
ib
ic

APPENDIX - J : PARAMETERS (M-FILE)

```
%2DOF SYSTEM PARAMETERS
m1=23.902;
m2=1.285;
l1=0.45;
lc1=0.091;
l2=0.45;
lc2=0.083;

%MOTOR1 parameters
R1=1;
L1=0.01;
Kt1=4.5;
n1=1
I1=1.266;
I2=0.093;
Im1=0.522;
Bm1=2.288;
g=9.81;

%MOTOR2 parameters
R2=1;
L2=0.01;
Kt2=1.5;
n2=1
Im2=0.01;
Bm2=0.175;
```

```
%Inertia
Je1=(m2*(l1+lc2)^2+m1*lc1^2)+Im1+I1;
Je2=(I2+m2*lc2^2)+Im2;


%Gravity coefficients
G11=(m1*lc1+m2*(l1+lc2))*g;
G12=m2*lc2*g;
G2=m2*lc2*g;
```

REFERENCES

[1] **Miller, T.J.E.,** 1989. Brushless Permanent Magnet and Reluctance Motor Drives. Oxford University Press. Wolton Street, Oxford OX 26 DP.

[2] **Yasuhiko, D. and Sakan K.,** 1990. Brushless Servomotors, Fundamentals and Applications. Oxford University Press.

[3] **Bose, B.K.,** 1988. Technology trends in microcomputer control of electrical machines, IEEE Trans. On Ind. Electron. Vol. 35.

[4] **Zimmermann, P.,** Electronically commutated DC feed drives for machine tools. Proceeding 3rd Int. Motorcon conference, Sept 82, pp.69-86.

[5] **Horner, G.R. and Lacy, L.J.,** High performance brushless PM motors for robotics and actuator applications. Proceeding 1st Europeon Conference On Electrical Drives/Motors/Controls 1982, pp. 91-99

[6] **Aengus, M. and Paul, K. and Fibarr, M.,** Advances in Brushless Motor Control. Analog Deviced Inc., Wilmington, MA 01887. aengus.**murray@analog.com**

[7] **Rubai, A. and Kotaru, R.,** Neural Net-Based Robust Controller Design for Brushless DC Motor Drives, IEEE Trans. On Systems, Man, and Cybernetics-part C: Applications and Reviews, Vol. 29, No 3, August 1999, pp. 460-473.

[8] **Low, R.S. and Chiun, K.Y. and Ling, K.V.,** Evaluating Generalized Predictive Control For A Brushless DC Drives, IEEE Trans. On Power Electronics, Vol 13, No. 6, November 1998, pp. 1191-1198.

[9] **Chen, H.C. and Huang, M.S. and Liaw, C.M. and Chang, Y.C. and YU, P.Y. and Huang, J.M.,** Robust Current Control For Brushless DC Motors, IEE Proc.-Electr. Power Appl., Vol. 147, No 6, November 2000, pp. 503-512.

[10] **Sciavicco, L. and Siciliano, B.,** 1999. Modeling and Control of Robot Manipulators. Springer-Verlag London, Great Britain.

[11] **Fernando, R. and Rafael, K.,** Experimental evaluation of model-based controllers on a direct-drive robot arm, accepted 4 January 2000, pp. 267-282.

[12] **Asada, H. and Kanade, T. and Takeyama, I.,** Control of a direct-drive arm. Trans of the ASME, Journal of Dynamic Systems, Measurement,and control 1983; 105:136-42.

[13] **Asada, H. and Toucef-Toumi, K.,** Direct-drive robots. Cambridge, MA: MIT press, 1987.

[14] **Paden, B. and Panja, R.,** Globally asymptotically stable PD+ controller for robot manipulators. International Journal of Control 1988;7(6):1697±712.

[15] **Koditscheck, D.E.,** Natural motion for robot arms. In: Proceedings of the 1984 IEEE Conference on Decision and Control, Las Vegas, NV, December. 1984. p. 733±5.

[16] **Lu, Z. and Shimoga, K.B., Goldenberg, A.A.,** Experimental determination of dynamic parameters of robotic arms. Journal of Robotic Systems 1993;10(8):1009±29.

[17] **Suravaram Reddy, P.,** Control of direct-drive robot manipulators under uncertainities. University of Alaska, Fairbanks, Dept. ECE, MS thesis, 2005

[18] **Zeki Bilgin, M.,** Permanent Magnet Synchronous Motor (PMSM), Artificial Neural Network (ANN), Position Control, Servodrive. PHD thesis, Kocaeli University, Kocaeli, Turkey

CURRICULUM VITAE

Ali AHMADI was born on 04.07.1975 of Mashhad in Iran. He graduated from Sajjad High School in 1993. He took his B.Sc. in Electronic engineering from Bojnourd Azad University of Iran in 1998. Currently he is a graduate student in Control and Automation engineering in Istanbul Technichal University.